Tyrphostin AG126 modulates Toll-like receptor (TLR) activation-induced functions in microglia by protein tyrosine kinase (PTK) -dependent and -independent mechanisms

Dissertation
for the award of the degree
"Doctor rerum naturalium" (Dr.rer.nat.)
Division of Mathematics and Natural Sciences
of the Georg August University Göttingen

submitted by
Christiane Menzfeld

from Cottbus

Göttingen, 2010

1st Member of the Thesis Committee:
Prof. Dr. Wolfgang Brück, Professor of Neuropathology,
Dept. of Neuropathology, University Medical Center Göttingen,
Georg August University, Göttingen

2nd Member of the Thesis Committee:
Prof. Dr. Dr. Hannelore Ehrenreich, Professor of Neurology and Psychiatry,
Dept. of Clinical Neurosciences,
Max Planck Institute for Experimental Medicine, Göttingen

3rd Member of the Thesis Committee:
Prof. Dr. Eberhard Fuchs, Professor of Neurobiology,
Clinical Neurobiology Laboratory,
German Primate Center, Göttingen

Supervisor:
Prof. Dr. Uwe-Karsten Hanisch, Professor for Experimental Neurobiology,
Dept. of Neuropathology, University Medical Center Göttingen,
Georg August University, Göttingen

Date of the oral examination: 24.08.2010

dedicated to my parents

Declaration

I hereby declare that I have written this thesis entitled "Tyrphostin AG126 modulates Toll-like receptor (TLR) activation-induced functions in microglia by Protein tyrosine kinase (PTK) -dependent and -independent mechanisms" independently and with no other sources and aids other than those quoted. This thesis has not been submitted elsewhere for any academic degree.

Göttingen, June 2010

Abstract

Tyrphostins comprise a class of synthetic protein tyrosine kinase (PTK) inhibitors structurally derived from tyrosine and aimed at the specific prevention of substrate phosphorylation. The tyrphostin AG126 revealed anti-inflammatory properties in numerous animal disease models, including septic shock induced by lipopolysaccharide (LPS) of gram-negative bacteria and bacterial meningitis induced by gram-positive cell walls. We now show beneficial effects in another CNS complication, in experimental autoimmune encephalomyelitis (EAE) as a model of multiple sclerosis, where AG126 treatment ameliorated clinical signs and myelin damage. At a cellular level, AG126 affected several functions of microglia, the CNS macrophages, as triggered by the activation of Toll-like receptors (TLR's). These innate immune receptors can sense microbial structures as well as factors generated by tissue injuries. For the first time, the present work addressed molecular targets and mechanisms of AG126 action, with a focus on microglia. AG126 interfered in particular with gene inductions depending on the adapter protein MyD88, one of the two TLR signaling pathways. Bruton's tyrosine kinase (BTK), a MyD88-associated PTK, was found to be inhibited in molecular and cell-based assays. Yet its inhibition could not explain the full spectrum of AG126 effects and, thus, alternative mechanisms which are even PTK-independent were considered based on structural relatedness and functional similarity to tyrosine-derived and/or microglia-active molecules. Such alternative mechanisms included principles based on antioxidants, adrenergic agonists, glucocorticoids or uncouplers of oxidative phosphorylation. It was found that AG126 undergoes degradation and that 3-hydroxy-4-nitrobenzaldehyde (BZ) and malononitirile (MN) are major breakdown products. MN was then demonstrated to mimic the microglia activity of AG126 and the similar behavior of other tyrphostins containing the essential structural motif, while BZ could not. Animal experiments finally showed that only AG126 as the parent structure, but not MN or BZ, could deliver the full protective action in EAE. Taken together, an ultimate identification of the AG126/MN-affected target may reveal a potent mechanism for developing anti-neuroinflammatory drugs.

Contents

List of Figures

List of Tables

Abbreviations

Aβ	amyloid β
APC	antigen presenting cell
APS	ammoniumpersulfate
ATP	adenosine-5'-triphosphate
BBB	blood-brain barrier
BCA	bicinchoninic acid
BCR	B cell receptor
BSA	bovine serum albumin
BTK	Bruton's tyrosine kinase
$[Ca^{2+}]_i$	intracellular calcium concentration
CFA	complete Freund's adjuvant
CNS	central nervous system
COX	cyclooxygenase
CSF	blood-cerebrospinal fluid
DAG	diacylglycerol
DAMP	danger-associated molecular pattern
DAPI	4'-6-diamidino-2-phenylindole
DC	dendritic cell
DMEM	Dulbecco's modified Eagles medium
DMSO	dimethyl sulfoxide
DMSO*aq*	DMSO with a residual water amount
DOSY	diffusion ordered spectroscopy
ds	double-stranded
ECL	enhanced chemiluminescence
ECM	extracellular matrix
ELISA	enzyme-linked immunosorbent assay
ERK	extracellular signal-regulated kinase
FACS	fluorescence activated cell sorting
FcR	Fc receptor
FCS	fetal calf serum
GC	glucocorticoid
GR	GC receptor

GROα	human growth regulated oncogen α
hsp	heat shock protein
HO-1	heme oxygenase 1
HRP	horseradish peroxidase
HMBC	heteronuclear multiple bond correlation
HSQC	heteronuclear single quantum coherence
IBA	ionized calcium binding adaptor molecule
IFN	interferon
IκB	inhibitor of NFκB
IKK	IκB kinase
iNOS	inducible nitric oxide synthase
IL	interleukin
IL-1R	IL-1 receptor
ILB4	isolectin B 4
IP_3	inositol-1,4,5-triphosphat
i.p.	intraperitoneal injection
IRAK	IL-1R associated kinase
JNK	c-Jun N-terminal kinase
KC	keratinocyte-derived chemokine, CXCL1, mouse equivalent of human GROα
ko	knockout [-/-] homozygote; [-/+] heterozygote
LPS	lipopolysaccharide
MAL	MyD88-adaptor-like protein
MAPK	mitogen-activated kinase
MC	mineralocorticoid receptor
MCP-1	monocyte chemoattractant protein-1, CCL2
MDA5	melanoma differentiation-associated gene 5
MDC	macrophage-derived chemokine, CCL22
MFI	mean fluorescent intensity
MHC	major histocompatibility complex
MIP-1α	macrophage inflammatory protein 1α, CCL3
MKK	MAPK kinase
MKKK	MKK kinase
MOG_{35-55}	myelin oligodendrocyte glycoprotein peptide 35-55
mRNA	messenger RNA
MyD88	myeloid differentiation factor 88
NEMO	NFκB essential modulator
NFκB	nuclear factor κB
NK	natural killer
NLR	NOD-like receptor

NMR	nuclear magnetic resonance
NOD	nucleotide-binding oligomerization domain
NO	nitric oxide
NSAID	non-steroid anti-inflammatory drugs
ODN	oligodesoxynucleotide
PAMP	pathogen-associated molecular pattern
PAMS	phentolamine methanesulfonate
PCR	polymerase chain reaction
PCW	pneumococcal cell wall
PFA	paraformaldehyde
PI3K	phosphatidylinositol-3-kinase
PIP_2	phosphatidylinositol-4,5-bisphosphat
PH	N-terminal plecktrin homology
PLC	phospholipase
PLL	poly-L-lysine
PR	propranolol
PTK	protein tyrosine kinase
RANTES	regulated upon activation normal T cell-expressed and presumably secreted, CCL5
RIG	retinoic acid-inducible gene
RLR	RIG-I like receptor
RNA	ribonucleic acid
ROS	reactive oxygen species
RT	room temperature
s.c.	subcutaneous
SDS	sodium dodecyl sulfate
SH	Src homology
ss	single-stranded
TAB	TAK binding protein
TAK	transforming-growth factor κ activated kinase
TASKIN	tyrphostin AG126 sensitive kinase
TEMED	Tetramethylethylenediamine
Th	T-helper
TIR	Toll/IL-1 receptor
TLR	Toll-like receptor
TMB	tetramethylbenzidine
TNFα	tumor necrosis factor α
TRAM	TIR domain containing adapter
WST	water soluble tetrazolium
wt	wild type

1. Introduction

This introductory chapter gives a short overview of the functional principles of the mammalian immune system and the important role of macrophages, especially microglia, the macrophage equivalent in the central nerve system (CNS). As a part of the innate immune system, microglia express pattern recognition receptors (PRR), such as Toll-like receptors (TLR). The key role of TLR signaling, especially for inflammatory processes, is briefly outlined. The involvement of TLR signaling in inflammatory disease processes led to the investigation of potential anti-inflammatory compounds. The tyrphostin AG126 revealed promising results in numerous animal disease models. A short introduction as to the known AG126 effects on TLR signaling, especially in microglia, is given. The elucidation of the anti-inflammatory properties and relevant target(s) of AG126 in the TLR signaling of microglia is the main focus of this study.

1.1. The mammalian immune system

Every day, mammals are exposed to a large amount of germs, such as bacteria, viruses and fungi. Most of them do not harm the mammalian organism. Some of the germs even live in symbiosis with the host, while a portion of them are potentially pathogenic. A finely regulated immune system has developed throughout evolution in order to discriminate between 'good' and 'bad' germs. The immune system provides mechanisms to detect potential pathogens as well as tools to fight off infections. It consists in higher vertebrates of two major components, the innate and the adaptive immunity. Both components are comprised of a humoral and a cellular part. The humoral components consist of immuno-active substances released by cells into the bodily fluids. Complement proteins and antibodies are major representatives of such soluble factors as they serve in the innate and the adaptive humoral components, respectively. In the innate immune system, monocytes, macrophages, dendritic cells (DCs), natural killer (NK) cells and granulocytes represent the major cellular carriers of defense activities. Adaptive immunity relies on the populations of T and B lymphocytes.

Adaptive immunity comes with the capacity to recognize and neutralize an enormous variety of different molecular structures as they are associated with soluble agents and toxins, particles or cells of foreign (*e.g.* bacteria) or even host origin (*e.g.* tumors). The molecular recognition diversity is achieved by highly variable complementary proteins either expressed as receptors by clones of T and B cells or being secreted by B cells as circulating antibodies. The gene-creation of such a recognition variety and expansion/selection of most appropriate clones guarantees a high degree of specificity and efficiency in covering virtually any structural motif (antigen) associating

with an infectious threat. In addition, the adaptive immunity invented the ability to memorize pathogenic structures. This unique feature enables the defense apparatus to react even more efficiently upon reencounter of a pathogen.

The innate immune system, evolutionary much older than the adaptive arm, has two major tasks to fulfill. It organizes for the first lines of defense. Epithelial barriers or the soluble components of the complement cascade are important, but innate immune cells are especially equipped to detect pathogens by virtue of germline-encoded receptors. Contact with infectious agents thereby triggers a range of gene inductions and functions, such as cytotoxic attacks, the phagocytotic clearance and intracellular killing of the invaders or the release of immunoregulatory messengers, such as cytokines and chemokines. Moreover, antigens can then be presented to T cells which trigger the specific mechanisms of adaptive immunity. Thus, innate immunity organizes for adaptive immune contributions. The molecules and cells of the innate immunity further participate in immune response by serving effector functions and, more recently acknowledged, also regulatory influences. Thus, only a close cooperation of the innate and adaptive immune system ensures the optimal defense strategies and unfolds their maximal potential. While the mammalian immune system thereby protects the body from daily attacks, insufficient responses, overreactions or a dysregulated decision on 'fight and don't fight' can cause life-threatening infectious diseases, cancer or severe self-damage by hyperinflammation and autoimmunity.

Interestingly, the last years brought a remarkable renaissance of interest in especially innate immunity. Its 'nonspecific' recognition features are seen in a new light based on a better understanding of the respective receptor repertoire and associated signaling options (Janeway and Medzhitov, 2002; Netea et al., 2004; O'Neill, 2004; Martinon and Tschopp, 2005; Akira et al., 2006; Beutler et al., 2006; Sansonetti, 2006). Moreover, uncovering of the versatility of cellular responses of innate immune cells, namely macrophages, completely changed the traditional concept of the 'stereotypic' response behavior (Mantovani et al., 2004; Gordon and Taylor, 2005; Gordon, 2007; Mosser and Edwards, 2008; Martinez et al., 2009; Pollard, 2009).

1.1.1. Functions of macrophages in the immune response

Exposure of macrophages to interferon (IFN) γ, tumor necrosis factor (TNF) α or bacterial cell wall components, such lipopolysaccharide (LPS), induces a complex expression of genes and functions, which together organize for a massive defense reaction. These macrophages support the Th1 type of adaptive immune responses with intensive inflammation — even at the cost of some tissue impairment. Already in the early 1990ies, another response was found when macrophage came under the influence of Th2 cytokines, such as interleukin-4 (IL 4) or IL 13. In contrast to the first type of 'classically' activated macrophages, such cells were described as 'alternatively' activated. Later, following the terminology of Th1 and Th2 cells, these two activation types were also named M1 and M2 macrophages (Gordon and Taylor, 2005; Gordon, 2007; Mosser and Edwards, 2008; Martinez et al., 2009). Soon, however, it became apparent that the dual differentiation would not satisfy the description of additional macrophage populations

as they present with distinct gene activation patterns and functional profiles. Influence of other cytokines, engagement with necrotic or apoptotic cells, contact with phagocytotic material of bacterial or endogenous origin, association with tumors and metabolic diseases, more and more tissues and situations revealed macrophages with discrete reactive phenotypes. While some 'markers' still serve to highlight M1- and M2-like reactions, such as the prominent induction of either IL 12 and IL 10, and while certain enzymes occur with almost reciprocal inductions, such as inducible nitric oxide synthase (iNOS) and arginase or cyclooxygenase (COX) 1 and 2, other cytokines, enzymes or receptors could be expressed by macrophage subsets which otherwise present with distinct phenotypes. In this regard, major histocompatibility complex (MHC) II structures can be found on both M1- and M2-like macrophages, suggesting that the polarized orientations come both with the ability to present antigens to T cells (Mantovani et al., 2004). Macrophages, indeed, serve as antigen presenting cells (APCs), but the actual outcome for the T cell response depends on further signals. In another example, the mannose receptor has been taken as an indicator of the M2 phenotype. Yet subdivisions as to the M2a, M2b and M2c distinction by the instructing signals, *i.e.* (i) IL 4/IL 13, (ii) co-exposure to immunoglobulin-antigen (immune) complexes (ICs) and a second signal, like LPS, or (iii) IL 10 show an uneven mannose receptor expression (Mantovani et al., 2004). Furthermore, the attempts to further define subtypes, especially among the M2-oriented macrophages, and to sort the phenotypes by a finite number are currently more and more replaced by a notion that macrophages come in major orientations, such as homeostatic maintenance, defense or repair but that individual reactive phenotypes are defined by variable assembly of actually induced genes and situation-controlled activities (Mantovani et al., 2004; Taylor et al., 2005; Mosser and Edwards, 2008; Gordon, 2007; Martinez et al., 2009).

Thus, macrophages can commit to rather diverse reactive phenotypes depending on the triggering events (activating signals) as well as the context of an activation. These cells can integrate a multitude of external signals — and their response profiles will largely depend on more than an isolated ligand-receptor signaling. Much of those signals is provided by the tissue environment, based on the special vascular properties, characteristic resident cells or the exchange of messengers among them. Conceivably, and also supported by a growing body of evidence, the macrophages in the various organs may also differ *a priori* by their individual response capacities, suggesting that phenotypes may vary by features for macrophages in the liver (*i.e.* Kupffer cells), the lung (alveolar macrophages), the epidermis (Langerhans cells), the bones (osteoclasts) and in the central nervous system (CNS), *i.e.* the microglia.

1.1.2. Microglia — tissue macrophages of the CNS

In comparison to other macrophages, microglia are embedded in a extremely vulnerable tissue with a limited capacity for regeneration. Inflammatory responses come with the five classical signs of redness, swelling, heat, pain and loss of function. While in the peripheral tissues a temporary swelling can be tolerated, it is detrimental and even a frequent cause of death in

infectious CNS complications, such as meningitis. Cell-mediated attacks on the surrounding healthy tissue can have equally severe consequences for neur(on)al structures and functions, exemplified by the devastating cause of demyelinating diseases, such as multiple sclerosis (MS), a disease thought to be driven by autoimmune reactions against white matter structures in the spinal cord and brain. Collateral damage of inflammatory processes and immune responses leads to disturbed CNS function and loss of neuronal connections and cells (van Rossum and Hanisch, 2004b). To protect itself from potential damage, the CNS needs to control immune responses. The blood-brain barrier (BBB) and the blood-cerebrospinal fluid (CSF) barrier are special formations which ensure not only a regulation of the transport of molecules between the periphery and the CNS, such as nutrients, metabolites or oxygen. These barriers also exert a control on the passage of immune cells across the compartments. The BBB is thereby based on capillary endothelial cells with specialized physical connections (tight junctions) and their cooperation with specialized processes (endfeets) of astrocytes to form complex shielding of the CNS milieu. Equipment with enzymes and transporters, the BBB organized molecular exchanges, while the expression of receptors and cell adhesion molecules can allow controlled penetration of immune cells. This tight border formation, a rare evidence for T cell patrolling and the reluctance to initiate and support experimentally induced immune reactions led to the description of the CNS (and associated structures, such as the eye) as an immune-privileged organ. While it has meanwhile been shown that immune responses can well be hosted by the CNS, the special regulations on such responses are being better understood. The CNS is thus not completely immune-isolated from the rest of the periphery, but rather immunocompetent and can interact with the peripheral immune system (van Rossum and Hanisch, 2004b; Carson et al., 2006). Microglia, as the CNS principal immunocompetent cells, play a central role in virtually all steps of neuroimmune processes — initiation of local inflammatory reactions, phagocytosis of infectious agents, dying cells and tissue debris, APC activities as well as the array of macrophage-associated effector functions (Hanisch and Kettenmann, 2007).

1.2. Microglia — the CNS innate immune sensor and effector cells

Microglial cells colonize the CNS in two waves. First, progenitors invade the embryonic and fetal CNS. Second, progenitors formed by bone marrow-derived monocytes settle again in the CNS around birth, for example in rodents during the early postnatal period (P0 to P5) or in humans before birth (Davoust et al., 2008). This cell type accounts for 5 to 20 % of the total glial population found in the gray and white matter (Barron, 1995). Microglia fulfil sentinel functions within the neural tissue. Therefore, they are in physical or indirect contact with the extracellular matrix (ECM), with neurons and other glial cell types. Microglia permanently monitor their environment. Moving their fine processes, they scan the environment as more recently discovered by two-photon microscopy of the living brain tissue in mice transgenic for enhanced

green fluorescent protein under the control of CX3CR 1, the receptor of the chemokine CX3CL 1, also known as fractalkine (Nimmerjahn et al., 2005). The territorially faithful cell body thereby moves the processes probably avoiding disturbance of the neuronal circuits, but in close contact to — and even nursing — synaptic structures (Wake et al., 2009). Even slight abnormalities can be detected, affecting the neural tissue homeostasis, including deviations from normal neuronal firing activities or unusual appearance, concentrations or formats of certain molecules, *e.g.* including infectious agents, neurotransmitters, cytokines, or malprocessed proteins (Hanisch and Kettenmann, 2007).

In the normal, healthy, adult CNS, the cells reveal a ramified morphology, unusual for macrophages, and thus being previously considered as 'resting', *i.e.* as functionally dormant. With the life imaging of their motile processes, the long-assumed surveillance functions got proven, thus also suggesting a constant interpretation of the sensory inputs through receptors. Indeed, upon activating signs, the processes rapidly re-orientate and a drastic morphological transformation to an amoeboid, more rounded and bushy or rod like cell shape can take place. Microglia can proliferate and become migratory to increase local densities at a site of infection or lesion. Cells unfold increased phagocytotic activity, express surface receptors and adhesion molecules, enzymes and releasable factors — similar to the peripheral macrophages and yet most likely distinct by regulation and profiles (van Rossum and Hanisch, 2004a). The repertoire of secreted factors ranges from NO and reactive oxygen species (ROS) to proteases and a plethora of cytokines and chemokines which affect neighboring CNS cells as well as recruit, guide and functionally instruct invading immune cells.

As is generally held to be the case with for macrophages, microglia also occur as different phenotypes, depending on the activation-triggering signals and the given microenvironment. The blend of insoluble cues (by ECM and cell contacts) and soluble messengers, like cytokines, contribute to this (Hanisch, 2002; Hanisch and Kettenmann, 2007). The changes in this environment during the course of activation likely associate with and instruct alterations in the microglial phenotype. Activated microglia may pass through shifts in the expressed gene patterns and adapt their functions as the response matures. Initial programs, such as for an antimicrobial defense, are then likely being followed by de-escalation, more repair-oriented profiles and eventually a return to the pre-activation state (Hanisch and Kettenmann, 2007).

Table 1.1 summarizes factors which can be sensed by microglia. All of these molecules can induce and/or modulate functions in microglia. Structures from bacteria and viruses, for example, alert to the invasion by foreign material. Certain plasma factors and ECM components are indicators for impaired BBB function, vascular injury or tissue trauma. Disruption of the ECM may also associate with extensive migratory events, *e.g.* by tumor cells. Microglia may also sense such processes. Detection of such indicators then activates microglia. They migrate to the site of an injury or infection along chemotactic gradients. This gradient can be caused by the foreign material or chemoattractive molecules released from resident as well as invading immune cells, including microglia themselves (Hanisch, 2002; van Rossum and Hanisch, 2004b). Depending on the activating signal and situational context, microglia will install a whole reper-

Table 1.1.: Indicator signals for disturbed homeostasis detectable for microglia (selection)[1]

Class of compound	Examples
Surface structures and DNA/ RNA of viral, bacterial or fungal origin	Agonists of members of the pattern recognition receptors, Toll-like receptors (TLR's), *e.g.*, peptidoglycan (TLR2), lipopolysaccharide (LPS; TLR4), retinoic acid-inducible gene I (RIG-I)-like receptors (RLRs)[2], *e.g.*, *ds*RNA and NOD-like receptors (NLRs)[3], *e.g.*, muramyl dipeptide (a substructure of peptidoglycane, NOD 2)[4],
complement	complement factor C1q, C5a
antibodies	immunoglobulins of various classes and isotypes (IgA, IgG, IgM)
cytokines	colony stimulation factor (M-CSF, GM-CSF), IL 6, IL10, IL12, IFNγ, TGFβ, TNFα
chemokines	ligands for chemokine receptors: CCR3, CCR5, CXCR2, CXCR1
neurotrophic factors	brain derived neurotrophic factor (BDNF)
plasma compounds	albumin, fibronectin, thrombin
neurotransmission-related compounds	ATP (and related purines), β-adrenergic agonists, glutamate
hormones	glucocorticoides

1 adapted from Hanisch and Kettenmann, 2007
2 receptor expression on microglia shown by Furr et al., 2008
3 receptor expression on microglia shown by Liu et al., 2010b
4 ligand for NOD 2 revealed by Girardin et al., 2003

toire of gene inductions (or suppressions) and functional adjustments, such as up-regulation of adhesion molecules or MHC structures for APC actions, up- or down-regulation of enzymes for the generation of messengers or ECM building blocks or altered phagocytotic performance.

Microglia cells express various receptors for the purpose of sensing these diverse molecules. Among them, microglial cells express germ line-encoded pattern recognition receptors (PRR). These receptors are specialized for binding a broad range of molecules which are described as pathogen associated molecular patters (PAMPs). There are three different known types of receptors: Toll-like receptors (TLR's), nucleotide-binding oligomerization domain (NOD)-like receptors (NLRs) and retinoic acid-inducible gene I (RIG-I)-like receptors (RLRs). These receptors do not detect individual pathogenic structures, such as antigenic epitops as they are specifically bound by antibodies. They are rather able to detect the characteristic structures of specific classes of pathogens (Creagh and O'Neill, 2006). Recognizing some invariant motifs, namely 'patterns', allows a still limited number of PRR's to cover nearly the entire range of pathogens. Indeed, the evolutionary conserved motifs cannot easily be altered by the germs, not without impaired vitality. Thus, PRR's extract structural essentials for detection. Members of these receptor families are also expressed by microglia (Olson and Miller, 2004; Liu et al., 2010a; Furr et al., 2008).

Today, it is known that microglia do not only serve the defence against pathogens, but that they can act neuroprotective and that they are thus very versatile cells in terms of their functions. In the past, however, microglia were frequently — if not mostly — described in the context of neurotoxicity. This prejudice resulted from the observation that neuropathological processes virtually always reveal with signs of microglial activation and that, in turn, standard procedures for the experimental activation of microglia employed mostly agents such as LPS — shifting the cells into an anti-microbial, defence-oriented, pro-inflammatory phenotype with a pronounced cytotoxic activity (Butovsky et al., 2005; Schwartz et al., 2006). Indeed, in neurotropic infections, autoimmune or neurodegenerative diseases, like bacterial meningitis, Parkinson's disease or MS, microglia may contribute to the tissue damage by excessive or chronic reactions, or by misinterpreting signals in their environment (Nau and Brück, 2002; Orr et al., 2002; Jack et al., 2005; Hanisch and Kettenmann, 2007). Since it became known that LPS, as a major bacterial cell wall component and standard tool in macrophage research, is a ligand of TLR4, investigations of TLR's in the context of health and disease have become a major topic in immunology, and thus also the microglial TLR's (Pais et al., 2008; Lehnardt, 2010 reviewed by Rivest, 2009).

1.3. Toll-like receptors (TLR) — key antennas for the activation of pro-inflammatory responses

Originally, the protein Toll was discovered for its essential role in the development of the dorsoventral pattern in embryos of *Drosophila melanogaster* (Hashimoto et al., 1988). Eight years later, Lemaitre et al. (1996) could show that mutations of the Toll gene led to a higher suscep-

Table 1.2.: Overview of TLR ligands (selection)[1]

TLR	ligand	origin
1	triacyl lipopeptides	bacteria and mycobacteria
2	peptidoglycan	gram-positive bacteria
	lipoteichoic acid	
	pneumococcal cell wall (PCW)	
	zymosan	fungi
	heat-shock protein	host
	$PamCS_3K_4$	synthetic ligand
3	*ds*RNA	viruses
	Poly(I:C)	synthetic ligand
	Poly(A:U)	
4	LPS	gram-negative bacteria
	fibrinogen	host
5	flagellin	bacteria
6	lipoteichonic acid	gram-positive bacteria
	Diacy lipopeptides	mycoplasma
	MALP2	synthetic ligand
7	*ss*RNA	viruses
	Poly(U)	synthetic ligand
8	single-stranded RNA	viruses
9	CpG-containing DNA	bacteria and viruses

adapted from Akira and Takeda (2004)
for experimental approaches synthetic analogous were used (see Material and Methods)

tibility to fungal infection in flies. Thereby it was demonstrated for the first time that Toll is an important protein within the immune defense of Drosphila. Medzhitov et al. (1997) discovered the Toll homologue in humans and named them Toll-like receptors. Further TLR's were identified and, today, more than 11 human and 13 mouse TLR's are known (Rock et al., 1998; Okun et al., 2009). TLR1 to TLR9 are currently the best characterized and the present study considered them in the context of microglia.

All these receptors bind a wide range of ligands that are usually absent in the mammalian host — or not accessible within a homeostatic environment. TLR's can recognize material of bacterial, viral, fungal or protozoic origins (PAMP). Table 1.2 gives an overview of the major ligands and their origin. Importantly, the recent years delivered also substantial insights into a principle by which PRR's, namely TLR's, would also detect endogenous factors as damage- or danger-associated molecular patterns (DAMPs). These molecules are usually serving a range of physiological functions within cells, the ECM or the blood plasma (Lotze et al., 2007; Kono and Rock, 2008; Milanski et al., 2009). The original concept of endogenously derived molecules which can elicit an immune response was suggested by Matzinger in her 'danger model' (Matzinger, 2002; Seong and Matzinger, 2004; Matzinger, 2007). In contrast — or extension — of the classical 'stranger model' of immune activation by non-self molecules, as proposed by Medzhitov and Janeway (2002), the idea of danger signals considers DAMPs as endogenous signs of dis-

turbed homeostasis or injury which initiate a protective reaction. DAMPs are diverse molecules, often yet not exclusively proteins, and acquire a DAMP role when they are presented in an unphysiological compartment or format, for example, when they are released by dying cells or appear in parenchymal compartments upon vascular leakage, when they are cleaved off from the ECM upon tissue damage or when they are modified by changed conformation, aggregation, glyosylation or oxidization (Lotze et al., 2007; Pineau and Lacroix, 2009).

TLR's are expressed on a wide range of immune and non-immune cells (Hanisch et al., 2008). As to major immune cell populations, macrophages, monocytes and DCs (Kaisho and Akira, 2006), but also B cells (Gerondakis et al., 2007), were found to express TLR's. Endothelial cells are an example of non-immune cells expressing TLR's (Gibson et al., 2008). TLR's are also present in the CNS parenchyma, with microglia (Olson and Miller, 2004), astrocytes (Bowman et al., 2003) and oligodendrocytes as the cellular carriers (Bsibsi et al., 2002). Tang et al. (2007) could even show that neurons express some TLR's.

TLR's are type I integral membrane glycoproteins. Due to the considerable homology in the cytoplasmatic Toll/interleukin-1 receptor (TIR) domain, TLR's are members of a larger superfamily that includes also the interleukin-1 receptors (IL-1R). The extracellular region of TLR's and IL-1Rs are, on the other hand, markedly different. TLR's consist of multiple leucine-rich repeats forming a horseshoe structure. Despite the conservation among the extracellular domains, several different and even unrelated structures can activate the TLR pathways (Tab. 1.2). While TLR1, 2, 4, 5 and 6 are expressed on the cell surface and get activated predominantly by bacterial and fungal molecules, TLR3, 7, 8 and 9 are localized endosomally and exclusively recognize nucleic acids (Akira and Takeda, 2004). For TLR7/8, a species-specific expression and signaling is still under debate (Gorden et al., 2006; Liu et al., 2010a). Additional members have been described as well, but little is still known about their agonists and functional implications.

1.3.1. The TLR signaling cascade

Binding of a TLR ligand leads to a dimerization of the receptors. While most of the TLR's homodimerize, TLR2 dimerizes with either TLR1 or TLR6 to generate receptors with distinct ligand specificity but substantial similarities in signaling (Okun et al., 2009). More recently, also a TLR4/6 heterodimer got identified (Stewart et al., 2010). Some TLR's complex with further coreceptors, *e.g.* with MD-2 and CD14. Both participate, for example, in the activation of TLR4 by LPS (Beutler, 2009). The principle of complex formation between certain TLR members and non-TLR receptors may, indeed, be important to allow a given TLR to accept so different agonists. Especially for TLR4, several surface molecules got suggested as partners, including Fc receptors (FcRs) for immunoglobulins G (IgG) and integrins (Triantafilou and Triantafilou, 2002). Switching the association with the complex may thereby enable the TLR to not only bind different PAMPs and DAMPs but to also transduce agonist-adapted signaling consequences. Such partner switch has been described for TLR4 and its responses to amyloid β and oxidized low-density lipoprotein in contrast to LPS, with CD36 acting as the DAMP-

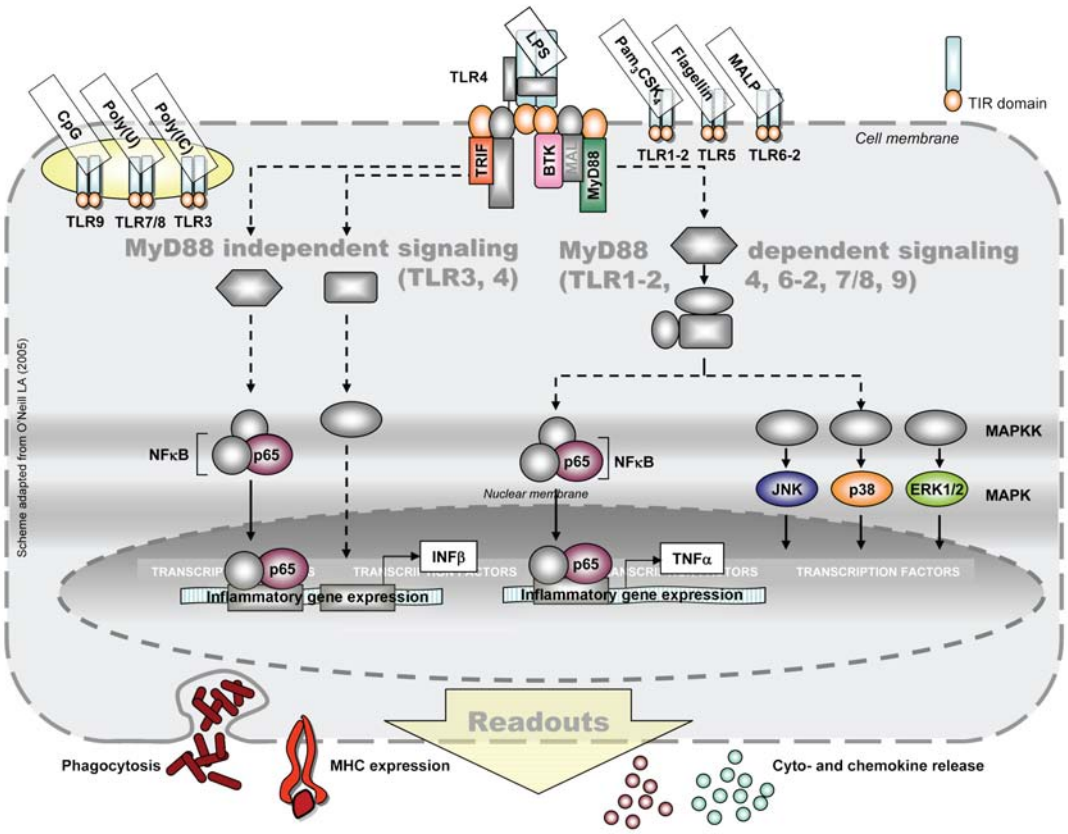

Figure 1.1.: Overview of TLR signaling. The signaling cascade is shown for TLR4 as a representative member of the TLR family and since both of the major pathways are used by it. Briefly, binding of LPS to TLR4 leads to its dimerization, with the involvement of CD14 and MD-2 as co-receptor elements, followed by the recruitment of sorting and signaling adapter proteins. Using the signaling adapter protein MyD88, this MyD88-dependent pathway gets activated and organizes further downstream events. This pathway is known to be used also by TLR1-2, 6-2, 7/8 and 9. Subsequently, MAPK and the NFκB system are activated, which leads finally to a transcription of genes for pro-inflammatory factors, including cytokines and chemokines, like TNFα. In parallel, the MyD88-independent pathway gets induced by activation of the signaling adapter protein TRIF. This pathway typically leads to INFβ transcription and can be induced by TLR4 and TLR3 stimulation. Under TLR4, MyD88 and TRIF routes may actually be subsequently activated with the first being triggered from the plasma membrane, while the second requires receptor internalization and signaling events from inside the cell. The elements relevant for the thesis are represented in colour. Important contributors to the signaling cascade are represented in gray. Details of the cascades are described in the text. Scheme adapted from O'Neill LA (2005).

associating coreceptor (Stewart et al., 2010).

Fig. 1.1 shows a simplified scheme of the signaling cascade for the example of TLR4. Here, signaling elements are shown which are especially considered in our study. Generally, TLR dimerization leads to the recruitment of adapter proteins to the cytoplasm membrane by binding to the TIR domain of the TLR's. The adapter protein myeloid differentiation factor 88 (MyD88) activates the MyD88-dependent signaling cascade, known for the TLR1-2, 4, 6-2, 7/8 and 9 signaling. Subsequently, MyD88 facilitates the connection of the interleukin 1 (IL1) receptor-associated kinase 4 (IRAK4). Phosphorylation of the associated IRAK1 by IRAK4 induces IRAK1 kinase activity. N-terminal autophosphorylation of IRAK1 enables TNF receptor-associated factor 6 (TRAF6) binding to this complex. The IRAK1-TRAF6 complex dissociates from the receptor and interacts at the plasma membrane with transforming-growth factor β-activated kinase 1 (TAK1), TAK binding protein 1 (TAB1) and TAB2.

TAK1 is a member of the mitogen-activated protein kinase kinase kinase (MAPKKK) family and phosphorylates mitogen-activated kinases (MAPK) kinase (MKK). MKK3 can activate $p38^{MAPK}$ and MKK7 activates the c-Jun N-terminal kinase (JNK). TLR4 and TLR7 stimulation can also lead to the activation of extracellular signal regulated kinase (ERK)1/2 (also known as $p44/p42^{MAPK}$) via the MAPKKK TPL2 (Loniewski et al., 2007). Additionally, phosphorylation, ubiquitylation and subsequent degradation of the inhibitor of NFκB (IκB) allows NFκB to translocate to the nucleus and to induce the expression of its target genes, like TNFα (Akira and Takeda, 2004). These downstream routes thus organize for a large number of genes to be activated upon TLR(4)-driven MyD88 recruitment.

Next to the MyD88-dependent pathway a MyD88-independent signaling route is used by TLR4 and TLR3 as these receptors interact with another signaling adapter protein, *i.e.* the TIR-domain-containing adapter protein inducing IFN β (TRIF). TLR3 exclusively signals *via* TRIF and TLR4 signals *via* both MyD88 and TRIF while all other TLR's signal through MyD88. The TRIF-dependent signaling pathway is known for the interferon (IFN) β production. Activation of TRIF leads to its association with TRAF3. TRAF3 binds to TBK1 (TRAF family member-associated NFκB-activated binding kinase 1) and IκB kinase (IKKϵ) . The resulting phosphorylation of the transcription factor IFN regulation factor 3 (IRF3) leads to its dimerization, translocation into the nucleus and the regulation of transcription. Alternatively, TRIF also interacts with TRAF6, leading to NFκB activation. Furthermore, TRIF activation may also result in IRF2 translocation by the phosphatidylinositol-3-kinase (PI3K)-Akt signaling cascade (Okun et al., 2009).

Additional sorting adapters, like the MyD88 adapter protein (MAL) and the TIR domain containing adapter (TRAM), are involved in the MyD88-dependent and MyD88-independent signaling pathways, respectively (Oshiumi et al., 2003b; Gray et al., 2006). The mediate TLR links to MyD88 and TRIF, probably allowing for more regulation and adaptation of signaling flows. Especially TLR4 enjoys the use of both sorting and both signaling adapters. Yet many more factors have been added to the TLR signaling options, and links to classical pathways of signaling are also becoming more apparent. Among the kinases with association to TLR's, some

are still not understood as to their impact. The Bruton's tyrosine kinase (BTK) was found to associate with the TIR domain of TLR 4, 6, 8 and 9 and seems to be further linked to MyD88, MAL and IRAK1 (Jefferies et al., 2003; Doyle et al., 2005).

In general, a wide range of ligands can activate the different TLR pathways, with an induction and release of diverse cyto- and chemokines and further immunoactive molecules. Analysis of individual TLR's and members of their signaling pathways continue revealing a complex signaling network — also with cooperations of the TRIF- and MyD88-dependent pathways as well as their cooperation with other signaling systems (Akira and Takeda, 2004; Brodsky and Medzhitov, 2009).

1.3.2. Positive and negative regulation of TLR signaling

The investigation of TLR cooperation revealed a huge amount of both positive and negative regulators of the TLR signaling system as well as crosstalk to other PRR's as well as more classical signaling systems. For example, enhancing activity and synergistic effects could be shown for certain TLR's regarding NOD1 and NOD2. These interactions suggest that a PAMP challenge may naturally not only recruit a single PRR or TLR, but that surface and DNA/RNA structures of a given germ would more or less simultaneously trigger multiple TLR's. The ensemble of activated receptors may then integrate a signaling consequence. In addition, the MyD88 and TRIF routes are certainly the most prominent, TLR-characteristic limbs, but their complexity is still not fully revealed as more and more factors are identified to influence TLR signaling. For example, certain protein tyrosine kinases (PTK), namely the Tec family member BTK, seem to influence (*e.g.* enhance) the TLR signaling (Liew et al., 2005).

Negative feedback mechanisms are mediated by soluble decoy receptors, like TLR2 or TLR4, a shortened form of MyD88 or IRAK-M. Corresponding knockout (*ko*) studies revealed increased pro-inflammatory cytokine levels upon TLR stimulation (Liew et al., 2005). Here too, the list of regulatory factors is still growing. Additionally, activation of anti-inflammatory pathways *via* glucocorticoids (GC) can also down-regulate TLR-induced pro-inflammatory cytokine responses (Ogawa et al., 2005; O'Neill, 2008).

Furthermore Kizaki et al. (2009) demonstrated that activation of the adrenergic signaling pathway induced a negative feedback on activated TLR signaling. Actually, the analysis of enhancing and inhibitory feedback mechanisms as well as the crosstalk among TLR's and with other pathways is important for understanding the conditions which provoke or dampen inflammatory responses and for defining new targets of their manipulation in treating diseases (Liew et al., 2005). Dysregulation of the TLR pathways seems to be involved in the pathogenesis of chronic inflammation and infectious diseases, in sepsis and asthma, or in autoimmune diseases, like multiple sclerosis (Poltorak et al., 1998; Dabbagh et al., 2002; Kerfoot et al., 2004). The present work aimed at the characterization of a TLR signaling-interfering and -modulating compound, its mechanism(s) and target(s) — based on experiments *in vitro* and *in vivo* and, indeed, suggesting it as a mean for dampening overshooting pro-inflammatory reactions.

1.3.3. AG126 a potent inhibitor of TLR signaling

In many pathogenic situations, overshooting inflammatory responses have detrimental effects, ranging from tissue impairment and functional failure to even lethal outcome. Strategies have been developed to fight — or at least moderate — such excessive immune responses and hyper-inflammation, giving raise to a range of anti-inflammatory drugs. While GCs and non-steroid anti-inflammatory drugs (NSAID) have found broad applications, search for alternatives has been continuing in order to tailor applications with less undesired side effects (McGeer and McGeer, 2007). The small compound AG126 revealed beneficial effects in many disease models of diseases with an inflammatory component. In 1994, Novogrodsky and colleagues could show that septic shock induced by LPS and provoking profound toxic effects as well as leading to death in mice could be modified by AG126, including the prevention of lethal outcome. Today it is known that the overshooting immune response involves TLR4, as the receptor of the bacterial PAMP (Poltorak et al., 1998).

Afterwards, AG126 was tested on several inflammatory disease models, also in acute and chronic settings, such as carrageenan-induced pleurisy and collagen-induced arthritis in rats, respectively, where AG126 exhibited potent anti-inflammatory effects (Cuzzocrea et al., 2000a). Furthermore, AG126 modulated pro-inflammatory factors in the mouse model of acute pancreatitis and zymosan-induced multiorgan failure in rats, thereby reducing the disease symptoms (Balachandra et al., 2005; Dugo et al., 2002). In CNS-associated diseases, AG126 reduced the inflammatory parameters in bacterial meningitis, as experimentally triggered in rodents by the administration of pneumococcal cell walls (PCW) prepared from *Streptococcus pneumoniae* (Hanisch et al., 2001; Angstwurm et al., 2004). Both disease inducing agents, zymosan and PCW activate the TLR2 signaling pathway.

1.4. Tyrphostin AG126 — member of a PTK inhibitor class

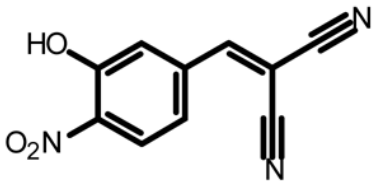

Figure 1.2.: Structure of AG126

AG126 or α-cyano-(3-hydroxy-4-nitro)cinnamonitrile belongs to the substance class of tyrphostins, as it stands for descriptive name protein-TYRosine PHOSphorlyation INhibitors (Fig. 1.2). By its inference with a still unknown PTK, it prevented the activation of ERK1/2 ($p44/42^{MAPK}$) in microglia and suppressed the PCW-induced release of TNFα (Hanisch et al., 2001). AG126 also affected the expression of iNOS and COX2 (Cuzzocrea et al., 2000a). Nevertheless, these few observations could not identify a direct PTK target nor narrow down on the pathways affected by AG126. Actually, the assumption of a PTK-dependent effect was deduced more from the chemical structure rather than from experimental proof.

1.4.1. Properties of tyrphostins

Tyrphostins were originally designed by Levitzki (1992) as anti-cancer drugs. These compounds are structurally related to the amino acid tyrosine. It can hinder the binding of the appropriate target protein by its occupation of the substrate pocket of PTK's. Therefore, the PTK can not phosphorylate the respective tyrosine residue. This process blocks the respective cellular signaling cascade. Alternatively, the binding site for the phosphate donor, meaning the ATP binding site, can be blocked. Generally, tyrphostins can be classified into compounds which compete with substrates and are noncompetitive with ATP, compounds which are ATP competitive and compounds which are bisubstrate competitive or mixed competitive (Levitzki and Mishani, 2006).

While many ATP-related inhibitors are used, substrate competing tyrphostins revealed key benefits. They act more specifically because the substrate-binding domain is less conserved than the ATP binding site. Due to a high abundance of ATP within the cell, huge amounts of ATP competing inhibitors are needed for an appropriate execution. Furthermore, substrate specific inhibitors can be used in a diminished dosage because they do not have to compete with the high intracellular ATP concentration. This reduces the risk of toxic site effects by the compound.

Despite the straightforward concept and a design of a large number of tyrphostin, only a few structures got thus far assigned to an identified PTK. AG1296 is a potent and specific inhibitor of the platelet-derived growth factor receptor tyrosine kinase (Kovalenko et al., 1997). AG490, also known as B42, inhibits the JAK2 in an acute lymphoblastic leukaemia (Meydan et al., 1996). Interestingly, it was also reported to interfere with the TLR-mediated cytokine induction in microglia, thus suggesting contributions of JAK2 (Hanisch et al., 2001). Nevertheless, various tyrphostins were tested for pharmacological effects in diverse disease models also without a molecularly defined target action. While in the beginning the focus of tyrphostin applications was on cancer treatment, over the years it became clear that beneficial effects could also be obtained in other disease contexts, such as inflammatory processes. AG126, in particular, represents an example of a tyrphostin with many beneficial effects in disease models although the mode of action remained unknown.

1.4.2. AG126 has modulatory effects on microglial cells

The promising results from applications in inflammatory disease models increased the interest in understanding the molecular mechanisms of the inhibitory or modulator effects of AG126. However, both the direct target and mode of action remained enigmatic. During the last years, more detailed analysis of AG126 actions were performed. Studies in our lab on microglia cell cultures revealed a repression of the activation of ERK1/2 in TLR-activated cells. These data suggested an AG126-sensitive PTK upstream of ERK and even MEK1/2, the ERK-activating MAPKK. ERK1/2 activation is known to be involved in cellular responses to stress, like oxidative stress, and or increased intracellular calcium $[Ca^{2+}]_i$ levels (Prinz et al., 1999; Hanisch et al., 2001; Koistinaho and Koistinaho, 2002).

Indeed, Kann et al., 2004, showed that AG126 prevented the chronic rise of $[Ca^{2+}]_i$ in microglia which had been observed before with exposures to PCW and LPS (Hoffmann et al., 2003). An elevated $[Ca^{2+}]_i$ appeared to be needed — although by itself not being sufficient — for the proper induction and release of certain cyto- and chemokines in microglia (Hoffmann et al., 2003). Inhibition of cytokine, such as TNFα and IL6, release by AG126 in PCW- or LPS- treated microglia was shown by Hanisch et al. (2001) and the interference with the required $[Ca^{2+}]_i$ could thus play a role. In addition to preventing a chronic elevation of $[Ca^{2+}]_i$ upon TLR2 and TLR4 stimulation in microglia, AG126 also affected the basal $[Ca^{2+}]_i$ level in unstimulated cells. This was taken as an evidence that AG126 has general calcium-regulating effects. Actually, many kinases are regulated by $[Ca^{2+}]_i$, however, only very few kinases are known to be a regulator of the calcium level. Thus, the putative AG126-sensitive PTK seemed to be a global regulator of $[Ca^{2+}]_i$, at least in microglia. Furthermore, consistent with the *in vivo* data, modulation of this kinase, *i.e.* treatment with AG126, did not reveal overt toxicity on the cells (Hanisch et al., 2001).

Virtually nothing was previously known about the nature of such an AG126-sensitive PTK or its involvement in signaling pathways — not for microglial TLR's and further aspects. Yet its upstream triggers, hierarchical position, intracellular partners and consequences are of great interest. On the other hand, AG126 may not necessarily and exclusively affect a single PTK entity, as other kinase inhibitors also reveal broader specificities. Finally, effects in cells and *in vivo* may depend on non-PTK mechanisms — an alternative which we kept in mind when designing the experimental approaches.

2. Aim of the study

The tyrphostin AG126 was originally designed as a PTK inhibitor and has been successfully applied in several animal models of inflammation-associated diseases. However, the cellular mechanisms and molecular targets of action remained enigmatic. In the present project, we focused on its interference with microglial functions, namely pro-inflammatory responses as they can be triggered by TLR activation. We aimed at identifying a potential PTK target and at unraveling the related — or alternative — modulations affecting TLR signaling pathways. Moreover, we also raised the question of whether AG126 could serve as a pharmacological tool for the treatment of a CNS-afflicting autoimmune disorder — by ameliorating the course of an experimental autoimmune encephalomyelitis (EAE) in mice, as a model of multiple sclerosis. These aims translated into the following specific questions:

- Can AG126 block or modulate microglial reactions upon stimulation of different TLR members? Is there a general or more TLR-specific effect and are microglial responses globally suppressed or selectively altered?
- Can an AG126-sensitive PTK be identified which plays a role for TLR signaling?
- How does AG126 affect signaling pathways and elements downstream of TLR's?
- Are there additional or alternative mechanisms involved which contribute to or carry the actions of AG126?
- Is AG126 protective *in vivo* by alleviating the clinical symptoms and reducing tissue damage in EAE?

To address these tasks, a range of cell-based experiments, bio/chemical and pharmacological assays and molecular analysis were performed and complemented by *in vivo* approaches. The project thereby also considered five alternative modes of action based on PTK-dependent and -independent mechanisms (Fig. 2.1). Considering the broad applications and the beneficial outcomes of AG126 in diverse inflammatory disease settings *in vivo*, the present work aimed at the underlying molecular and cellular principles, which could have implications also for other related tyrphostins. With microglia as the innate immune cells of the CNS being more and more acknowledged for beneficial functions as well as understood for detrimental actions findings from the present study could offer structures, mechanisms and targets of therapeutic intervention.

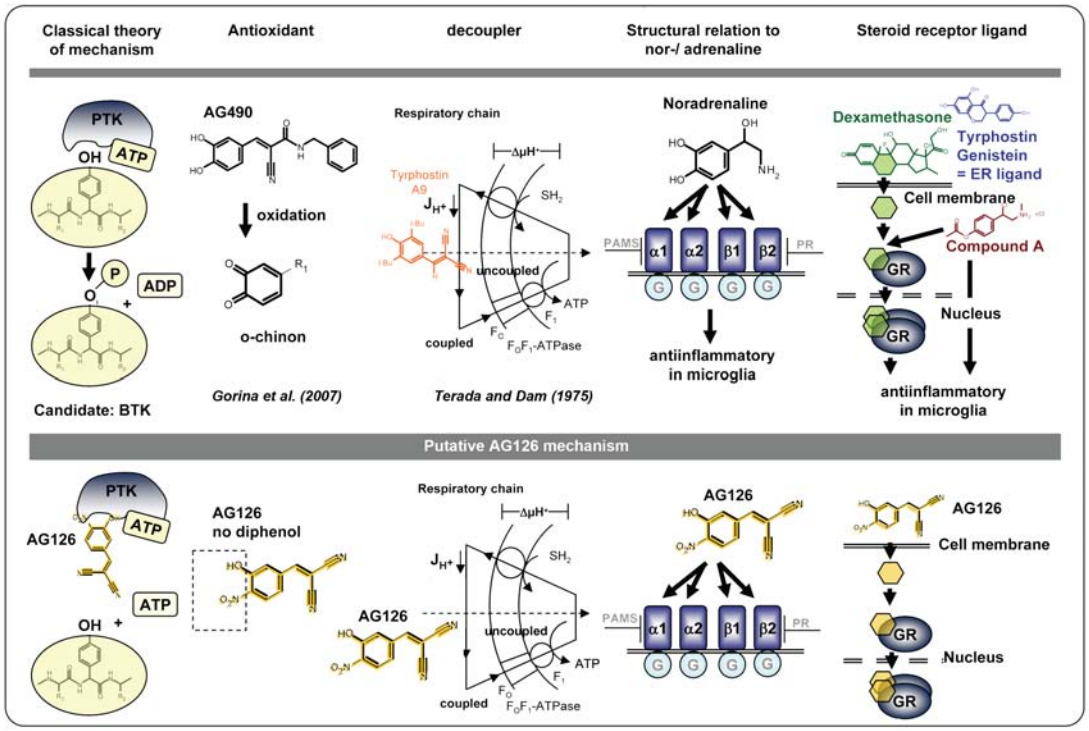

Figure 2.1.: Overview of possible mechanisms for AG126.

3. Materials and Methods

Materials were purchased from companies listed in Tab. 3.1. Use of the products is described in the method section and their origin of the material is indicated with the abbreviation of the respective company.

3.1. Animals

C57BL/6 mice used for EAE induction were purchased from Charles River. For primary cell culture NMRI and C57BL/6 wild type (*wt*) new born mice were obtained from the Central Animal Facility of the University Medical Center Göttingen (UMG). Heterozygous glucocorticoid receptor ($GR^{+/-}$) knockout(*ko*) mice for primary cell culture were kindly provided by Dr. Fred Luehder, Institute for Multiple Sclerosis Research (IMSF) Göttingen and described elsewhere (Wang et al., 2006; Finotto et al., 1999). TLR $4^{-/-}$ were obtained from Jackson Laboratories and described by Poltorak et al. (1998). $MyD88^{+/-}$, $MyD88^{-/-}$ and $TRIF^{-/-}$ mice (all C57BL/6) were kindly provided by Prof. Dr. Marco Prinz, currently at the Department of Neuropathology, University of Freiburg, Germany and described elsewhere (Adachi et al., 1998; Yamamoto et al., 2003). All animals were housed under standard laboratory conditions at the animal facility of the UMG or IMSF Göttingen, Germany and had access to food and water *ad libitum*. All animals were treated according to the guidelines for animal care of the University of Göttingen.

3.2. EAE induction and therapy

Myelin oligodendrocyte glycoprotein peptide 35-55 (MOG_{35-55})-induced EAE is a classical animal disease model for MS. This model was used to analyze anti-inflammatory properties of AG126 and its breakdown products malononitrile and 3-hydroxy-4-nitrobenzaldehyde. C57BL/6 female *wt* mice were immunized with MOG_{35-55}/ Complete Freund's Adjuvant (CFA) emulsion (1:1 50 µg of MOG_{35-55} peptide (PanaTecs) in PBS. CFA consisted of Incomplete Freund's Adjuvant (Sigma) and *Mycobacterium tuberculosis* H37RA (Difco; 1 mg/ml at final concentration) which were given subcutaneously (*s.c.*) into the flanks.

Injections of 200 ng/mouse/day pertussis toxin (List; diluted in 9 % NaCl) were given immediately and on day two after immunization. The induction of EAE was previously described by Linker et al. (2002).

Animals were weighed and scored daily for clinical signs of disease on a scale from 0 to 10 (IMSF score) or 1 to 4 (ZTE score) depending on severity. IMSF scores were as followed 0 = normal,

Table 3.1.: Overview of companies

Abbreviation	Company	Address
Amersham	Amersham/GE Healthcare Europe GmbH	Freiburg, Germany
Apotech	Apotech, Alexis Corporation	Lausen, Switzerland
Bandelin	Bandelin Electronics	Berlin, Germany
BD	BD Biosciences	San Jose, USA
Biochrom	Biochrom AG	Berlin, Germany
Biolegend	Biolegend/Biozol Diagnostica Vertrieb GmbH	München, Germany
BioRad	BioRad Laboratories Inc.	Hercules, CA, USA
CST	Cell Signaling Technology Inc.	Danvers, MA, USA
Roth	Carl Roth GmbH & CO. KG	Karlsruhe, Germany
Dako	DakoCytomation	Glostrup, Denmark
Difco	Difco/BD Biosciences	San Jose, CA, USA
eBioscience	eBioscience Inc.	San Diego, CA, USA
Imgenex	Imgenex Corporation	San Diego, CA, USA
Intas	Intas, Science Imaging Instruments GmbH	Göttingen, Germany
Invitrogen	Invitrogen GmbH	Karlsruhe, Germany
Jackson ImmunoResearch	Jackson ImmunoResearch Europe Ltd.	Newmarket, UK
The Jackson Laboratory	The Jackson Laboratory	Bar Harbor, ME, USA
Leica	Leica Mikrosysteme Vertrieb GmbH	Wetzlar, Germany
List	List Biological Laboratories Inc.	Campbell, CA, USA
Merck	Merck KGaA	Darmstadt, Germany
MWG	MWG-Biotech AG	Ebersberg, Germany
Nunc	Thermo Fisher Scientific (Nunc GmbH & Co. KG)	Langenselbold, Germany
Olympus	Olympus Deutschland GmbH	Hamburg, Germany
Olympus Soft	Olympus Soft Imaging Solutions GmbH	Münster, Germany
PBL	PBL Biomedical Laboratories	Piscataway, USA
PeqLab	PeqLab Biotechnologie GmbH	Erlangen, Germany
Qiagen	Qiagen GmbH	Hilden, Germany
Roche	Roche Diagnostics	Mannheim, Germany
R&D	R&D Systems	Wiesbaden, Germany
Sarstedt	Sarstedt AG & Co.	Nümbrecht, Germany
Serva	Serva Electrophoresis GmbH	Heidelberg, Germany
Sigma	Sigma-Aldrich	Steinheim, Germany
Moss	Moss Inc.	Pasadena, MD, USA
PanaTecs	PanaTecs GmbH	Tübingen, Germany
Pierce	Pierce/Thermo Fisher Scientific	Rockford, IL, USA
Promega	Promega GmbH	Mannheim, Germany
Santa Cruz	Santa Cruz Biotechnology Inc.	Santa Cruz, CA, USA
Tetenal	Tetenal AG & CoKG	Norderstedt, Germany
Vector	Vector Laboratories	Burlingame, USA
Worthington	Worthington Biochemical Corporation	Lakewood, NJ, USA

1 = reduced tone of tail, 2 = limp tail, impaired righting, 3 = absent righting, 4 = gait ataxia, 5 = mild paraparesis of hind limbs, 6 = moderate paraparesis, 7 = severe paraparesis or paraplegia, 8 = tetraparesis, 9 = moribund and 10 = death. ZTE scores were as followed: 0 = normal, 0.5 = reduced tone of tail, 1.0 = limp tail, mouse can not be rotated, 1.5 = mouse can be rotated, turns back on its own, 2.0 = mouse can not rotate back alone, 2.5 = paraparesis of one hind limbs, 3.0 = paraparesis of both hind limbs 3.5 = paraparesis of both hind limbs and one

forelimb 4.0 = tetraparesis (abort criterion). Disease score was previously described by (Wüst et al., 2008)

Mice were treated as indicated with 10 mg/ml/day/animal AG126 (Calbiochem), malononitrile or 3-hydroxy-4-nitrobenzaldehyde (both Sigma) diluted in DMSO *vs.* DMSO-CTL or PBS-CTL on three consecutive days or on five days (three consecutive days, day 5 and 7) by intraperitoneal injection (*i.p.*).

3.3. Animal perfusion, tissue sectioning and fixation

Mice were anesthetized with 150 µl of 14 % chloral hydrate (Merck) *i.p.* Loss of consciousness was tested by eyelid reflex and experience of pain. The thorax was then opened and transcardial perfusion was performed through the left cardial ventricle with PBS followed by 4 % paraformaldehyde (4 % PFA, Merck, 1.0 µM sodium hydroxide, 10 % 10 x PBS in $dd\mathrm{H_2O}$, pH 7.3).

Vertebral canal, head, an specimens of liver and spleen were postfixed for one more day in 4 % PFA at 4°C. Subsequently PFA was exchanged for one day with PBS at 4°C. Spinal cord and brain were dissected from vertebral canal and head, respectively. Spinal cord was cut into 4 mm-long pieces, brain, liver and spleen into 4 mm slices. Whole tissue was dehydrated and paraffined in the Leica TP 1020 Tissue Processor according to standard procedure. All were then embedded into a paraffin block. The embedded tissue was sliced into 1-µm slices and coated onto object slides (Leica SM 2000 R sliding microtome, Superfrost Plus microscope slides, Thermo Scientific). Slides were dried and stored at *RT* until further staining procedure (see following sections).

3.4. Histological staining

References and staining methods described in detail were published by (Romais, 1989).

3.4.1. Deparaffinization

For histological staining, the paraffin from tissue sections has to be dissolved in xylene. Therefore, slides were placed consecutively in three containers of xylene for 5 min each. Afterwards, the tissue was transferred into m-xylene for 1 min. The alcohol series was performed for tissue rehydration.

3.4.2. Alcohol series

For many staining procedures, a specific hydrophilic or hydrophobic environment was required. For tissue dehydration, slides were consecutively transferred from a more hydrophobic to a more hydrophilic solution, *i.e.*, 2 x 100 % isopropyl alcohol, 4 min each, 90 %, 70 %, 50 % isopropyl

alcohol, 3 min each and rinsed in distilled water ($d\mathrm{H_2O}$). For tissue dehydration the procedure was performed *vice versa*.

3.4.3. Haematoxylin-Eosin (H&E) staining

H&E staining was performed to obtain a general morphological overview of the tissue. Sections were deparaffinized (see section 3.4.1) and hydrated stepwise by alcohol series to $d\mathrm{H_2O}$ as described in section 3.4.2, washed in $d\mathrm{H_2O}$ and incubated in Mayer's hemalun solution (Merck) for 5 min. Afterwards, sections were washed with $d\mathrm{H_2O}$ and differentiated by short dip into 1 % HCl-alcohol (1 % HCl in 90 % isopropyl alcohol). Tissue was blued by rinsing slides under tap water for 10 min. The tissue was then incubated in 1 % eosin solution (1 % eosin G, Merck, in 70 % isopropyl alcohol, stirred and filtered, 10 drops glacial acetic acid was added before use) for 5 min. Afterwards, slides were rinsed in $d\mathrm{H_2O}$ and fast dehydrated by alcohol series until 100 % alcohol to avoid excessive elution of eosin. Next, slides were incubated for 2 x 3 min in 100 % isopropyl alcohol (two containers), 3 min m-xylene and 3 x 3 min xylene (three containers). Slides were mounted using DePex mounting medium (Serva).

3.4.4. Luxol Fast Blue/ Periodic Acid Schiff (LFB/PAS) staining

LFB/PAS staining is used to detect demyelinized areas in EAE animals. Paraffin embedded tissue sections were deparaffinized until 90 % of alcohol (section 3.4.1 and 3.4.2). Afterwards, sections were incubated in LFB solution (0.1 % w/v LFB in 96 % ethanol, 0.05 % acetic acid) overnight at 60 °C. Sections were washed shortly in 90 % ethanol, and afterwards dipped in 0.05 % lithium carbonate (diluted in $d\mathrm{H_2O}$, Roth), 70 % alcohol for differentiation and rinsed in $d\mathrm{H_2O}$. For the PAS staining, sections were incubated for 5 min in 1 % periodic acid (in $d\mathrm{H_2O}$, Merck), then rinsed for 5 min under tap water and shortly washed in $d\mathrm{H_2O}$. Tissue was incubated for 20 min in Schiff reagent (Sigma), rinsed under tap water for 5 min, hemalun solution (Merck) for 2 min and rinsed again under $d\mathrm{H_2O}$. For differentiation, sections were incubated in 1 % HCl alcohol (see above) and blued under tap water. The sections were dehydrated in increasing alcohol series and incubated in xylene (see section 3.4.1 and 3.4.2) and embedded in synthetic mounting medium (DePeX, Serva).

3.4.5. Bielschowsky silver staining

Bielschowsky silver staining was performed to determine axonal density. Sections were deparaffinized as described earlier (section 3.4.1 and 3.4.2) and washed with $d\mathrm{H_2O}$. Next, sections were incubated in 20 % silver nitrate solution (in $dd\mathrm{H_2O}$, Roth) for 20 min and stored in $d\mathrm{H_2O}$. Meanwhile 32 % ammonium hydroxide (Merck) was added dropwise to the already used 20 % silver nitrate solution while stirring, until the formed precipitate disappeared. A further two drops were then added. In this solution, slides were incubated in the dark for 15 min. Subsequently,

slides were stored in $dd\mathrm{H_2O}$ containing a few drops of ammonium hydroxide. Ten drops of developer (6 % formalin in $d\mathrm{H_2O}$, 0.4 % citric acid, 0.05 % nitric acid) were stirred into the already used silver nitrate/ammonium hydroxide solution. By adding this solution quickly to the slides, a fast developing process took place. The reaction was stopped by $d\mathrm{H_2O}$. Afterwards, slides were incubated in 2 % sodium thiosulfate (diluted in $d\mathrm{H_2O}$) for 2 min and rinsed shortly under tap water. The sections were dehydrated in alcohol series until xylene (see section 3.4.1 and 3.4.2) and then embedded in synthetic mounting medium (DePeX, Serva). In the stained tissue, nuclei become brown and axons black.

3.4.6. IBA1 staining

Macrophages and microglia were detected in EAE tissue by staining cell against microglia/ macrophage-specific calcium-binding protein, the ionized calcium binding adaptor molecule 1 (IBA1). For this, tissue sections were deparaffinized according to section 3.4.1 and completely rehydrated (see section 3.4.2). Slides were pretreated with citrate buffer (10 mM citric acid, adjusted to pH 6.0 with NaOH, both Merck) 6 x for 3 min. Afterwards, the sections were cooled to room temperature (*RT*) and transferred into PBS. Endogous peroxidase was blocked with 3 % $\mathrm{H_2O_2}$ in PBS for 20 min. Slides were rinsed in PBS and blocked in normal serum solution (5% serum, 5% skimmed milk powder) for one hour at *RT*. Normal serum origin from the same animal species as the origin of the secondary antibody, *i.e.*, donkey serum. Afterwards, sections were incubated in primary antibody solution (1:400 α-IBA1 rabbit antibody (Amersham) diluted in 50 % blocking solution in PBS) overnight at 4 °C. Sections were washed 3 x 5 min with PBS and then incubated in secondary antibody solution (1:100 α-rabbit donkey antibody (Amersham) in 50 % blocking solution in PBS) for one hour at *RT*. Sections were again washed in PBS for 3 x 5 min and incubated in peroxidase-complex solution (1:1000 in 50 % blocking solution in PBS, Sigma) at *RT* for one hour. Sections were washed yet again 3 x with PBS. Afterwards, staining was developed with diaminobenzidin (DAB, Sigma) within 10 min and rinsed in $d\mathrm{H_2O}$.

Tissues were incubated for 3 min with Mayer's hemalum solution (Merck) for counterstaining. Bluing of nuclei was performed by rinsing sections in tap water for 10 min. Finally, sections were rinsed in $d\mathrm{H_2O}$, dehydrated until xylene (see section 3.4.2) and embedded as H&E stained tissue (see section 3.4.3).

3.4.7. CD3 staining

Staining of CD3, a T cell co-receptor, allows T cells to be detected in the EAE tissue. This staining procedure equals the IBA1 staining (see section 3.4.6). Here, goat-normal serum, 1:400 α-CD3 rat primary antibody (Amersham) and 1:100 goat α-rat secondary antibody (Amersham) were used.

Table 3.2.: Overview of seeded cells depending on analysis

Purpose	Culture dish	Cell amount/well	Volume of culture medium
ELISA	96 well plate	1.5×10^4	100 µl
Cellular staining	4 well plate containing PLL coated glas slide	5×10^4	500 µl
Lumox® slides	4 wells PLL coated	5×10^4	500 µl
FACS	12 well plate	2×10^5	1 ml
Cell lysates	3 ø cm Petri dish	1×10^6	2 ml
	6 ø cm Petri dish	3×10^6	4 ml

3.5. Histological analysis of EAE tissue - detection of demyelination

To determine the extent of demyelination in the white matter of spinal cord sections, tissue slides were stained according to section 3.4.4. Photos were taken from 7 to 12 spinal cord sections per animal at 4 x magnification with an Olympus microscope equipped with a DP71 camera and Olympus Cell F software (2006, Olympus Soft). Ratio of white matter lesion area (appears pink) to white matter total size (appears blue) was determined by Analysis Software (analySIS, Olympus Soft). Lesion detection was supported by the use of IBA1 stained sections. The mean ratio of every animal and subsequently of every group determined.

3.6. Cell cultures

3.6.1. Primary microglial cultures - P0 wild type cells

The routine NMRI *wt* microglia served in previous studies as a standard model (Hanisch et al., 2004). The response and cultivation properties of NMRI *vs.* C57BL/6 *wt* mice were compared because the background of several homo/heterozygous *ko* mouse systems used in the actual studies were C57BL/6. A similar responsiveness to stimuli, like LPS and other TLR ligands, could be demonstrated. Cell preparation was previously described by (Draheim et al., 1999; Kann et al., 2004)

Before preparation of primary cells, T_{75} polystyrol culture flasks (Sarstedt) were coated with 100 µg/ml poly-L-lysine (PLL, Sigma) in distilled and de-ionized (dd)H_2O for 30 min at RT and under sterile conditions. Preparation of microglia was performed on ice in Hank's balanced salt solution (HBSS, Biochrom). The primary cells were obtained from newborn to 2-day-old mice. The animals were sacrificed by decapitation, brains were excised and the meninges removed. The

tissue was washed in HBSS and incubated with 2.5 % trypsin (Biochrom) for 10 min at 37 °C. The reaction was stopped with culture medium supplemented by 0.4 mg/ml DNase (Worthington). Culture medium contained 10 % fetal calf serum (FCS, heat inactivated for 30 min at 56 °C, Invitrogen/Gibco), 100 U/ml penicillin and 100 µg/ml streptomycin (both Biochrom) in Dulbecco's Modified Eagle Medium (DMEM, Invitrogen/Gibco). Cells were mechanically separated and centrifuged at 129 *g* for 10 min at 4 °C. The pellet was resuspended in culture medium and the equivalent of two brains per one PLL-coated T_{75} flask was cultivated for 24 h at 37 °C and 5 % CO_2. On day one of primary culture, the cells were washed three times with Dulbecco's phosphate-buffered saline (D-PBS, Invitrogen/Gibco) and fresh medium was added. On day four, the primary cells were stimulated with fresh medium containing 30% culture supernatant of the mouse fibroblast cell line L929 (routinely cultured in DMEM and split once a week; L929 culture supernatant was removed before the medium change and stored at -20 °C until use). On day 7, microglial cells were harvested for experiments. The primary culture was shaken at 120 *rpm* for 30 min at 37 °C to separate microglial cells from other cerebral cells. The supernatant containing the microglia culture was collected and the remaining primary culture (still containing microglia) was again stimulated with fresh medium supplemented with 30 % L929 culture supernatant. With this procedure it was possible to harvest microglia up to four times more on days 9, 13, 15 and day 20.

For *in vitro* experiments, the harvested microglia were transferred into a 50 ml conical tube and centrifuged at 129 *g* for 10 min at 4 °C. After resuspension in culture medium the cell number was determined and the cells were plated depending on the experimental setting (see Tab. 3.2) for 24 h without any stimulation.

3.6.2. Microglia cells deficient for TLR 4, MyD88 and TRIF

The primary culture obtained from the $TRIF^{-/-}$, $MyD88^{+/-}$ and $MyD88^{-/-}$ mice were prepared like the *wt* cells. An individual culture was prepared from each animal. The *ko* cells were seeded on one half of a 96-well plate together with *wt* cells on the other half and treated in the same way for comparison.

3.6.3. Microglia cells deficient for the Glucocorticoid receptor (GR)

Pregnant animals were sacrificed by cervical dislocation. Skin was disinfected by 70% EtOH and removed on ventral side. Uteri were opened and embryos separated from placentas; both embryos and placentas were transferred separately to Petri dishes filled with HANK'S solution. Brains were removed according standard procedure (see section 3.6.1). Arms were taken for genotyping (performed by AG Reichardt, Department of Cellular and Molecular Immunology, University of Göttingen, Göttingen, Germany). All animals were separately cultivated in T_{75} culture flasks. Mice, which showed no GR*ko* phenotype, were used as *wt* control.

3.6.4. B cell lines

The mouse K46 B cell strain, positive for IgG, and human Ramos B cell strain, positive for IgM were kindly provided by the research group of Prof. Jürgen Wienands, Institute of Cellular and Molecular Immunology, University of Göttingen, Göttingen. This suspension cells were cultivated to a density of 2×10^5 to 2×10^6 cells/ml at 37°C, 5 % CO_2 in RPMI 1640 medium supplemented with 10 % FCS. Cells were centrifuged at 1350 *rpm* at 4°C. Pellets were washed in PBS. Centrifuged cells were concentrated to 6×10^6 cells/ml in serum-free medium. 500 µl of cell suspension was transferred into a 1.5 ml reaction tube. Cell stimulation is described in section 3.8.

3.7. Stimulation of microglial cells

Until stimulation. the microglia monoculture rested for 24 h as described in the previous section. Afterwards, medium was removed and medium containing stimuli was added. The *ko* cells were always treated together with the respective *wt* cells. All substances were diluted to their working concentration in DMEM containing FCS.

3.7.1. TLR ligands

For stimulation experiments, highly purified TLR agonists were purchased (TLR-Ligands Set I from Apotech):

- Pam_3CSK_4 ((S)-[2,3-bis(palmitoyloxy)-2(2-RS)-propyl]-N-palmitoyl-(R)-Cys-(S)-Ser-(S) - Lys_4-OH_3HCl) activates TLR 1 complexed with TLR 2
- Poly(I:C) (polyinosinic-polycytidylic acid), a synthetic analogue of *ds*RNA activates TLR 3
- Poly(A:U) (polyadenylic acid-polyuridylic acid, a synthetic analogue of *ds*RNA activated TLR 3 was purchased from Sigma
- LPS *E.coli R515* (LPS from *Escherichia coli*, serotype R515) stimulates TLR 4
- Flagellin (isolated from *Salmonella typimurium* strain 14028) activates TLR 5
- MALP-2 (S-[2,3-bis(palmityloxy)-(2R)-propyl–cysteiny - GNNDESNISFKEK]) activates TLR 6 complexed with TLR 2
- Poly(U) (polyuridylic acid.potassium salt), a synthetic analogue of *ss*RNA activates TLR 7 and 8
- CpG ODN 2395 (synthetic oligodesoxynucleotide (ODN) (TCG TCG TTT TCG GCG CGC GCC G) activates TLR 9

All ligands were diluted to stock solutions according to the manufacture's instructions and stored in aliquots at -20°C. For microglia stimulation, TLR ligands were freshly diluted in

culture medium and added to the cells in physiologically relevant ranges as indicated. Cells were cultivated in a total volume of 100 µl/well for 18 h at 37°C and 5 % CO_2. Subsequently, supernatant was taken and stored at -20 °C until analyzed.

For further experiments, fixed TLR ligand concentrations were used: 10 ng/ml Pam_3CSK_4, 50 µg/ml poly(I:C) and poly(A:U), 10 ng/ml LPS, 10 ng/ml MALP, 5 µg/ml CpG ODN.

3.7.2. Tyrphostins and tyrphostin-related compounds

The tyrphostin AG126 (α-cyano-[3-hydroxy-4nitro]cinnamonitrile) was purchased from Calbiochem/Merck. Light-sensitive AG126 was stored as 50 mM stock solution in dimethyl sulfoxide (DMSO, Sigma) in aliquots at -20°C and always kept in the dark. All AG126 experiments were performed under minimal lighting. Medium solution containing AG126 was filtered with a 0.2 µm syringe filter.

To analyze the effect of AG126 on TLR-stimulated microglia, AG126 was added to cells as indicated (5 to 100 µM) together with fixed TLR ligand concentrations (see section 3.7.1). Cells which received TLR ligands and AG126 for stimulation were pre-treated with the respective AG126 concentration without the ligand for one hour at 37 °C, 5 % CO_2. Subsequently, the supernatant was removed and cells were stimulated with the respective TLR ligand and AG126 for 18 h or as indicated at 37 °C, 5 % CO_2. Control groups received culture medium during pre-treatment and for the stimulation period or the respective TLR ligand without AG126, respectively. Depending on the subsequent assay, supernantant was taken and stored at -20 °C until use. Alternatively supernatant was removed and cells were prepared for further analysis.

To analyze the phosphorylation status of NFκB p65, $p38^{MAPK}$, ERK1/2 or JNK, cells were stimulated for 5, 15, 30, 60 or 240 min with or without AG126 containing TLR solution. Medium control and AG126 without TLR ligand were stimulated for 15 min.

For the analysis of MHC molecule expression on TLR-stimulated microglia in the presence or absence of AG126, cells were cultivated in 12-well plates as described above. Cells were stimulated with 10 ng/ml of Pam_3CSK_4, LPS and MALP, respectively, with and without 10 or 100 µM AG126 for 48 h. Cells which received AG126 were pre-incubated for one hour with culture medium containing the appropriate AG126 concentration. Unstimulated microglia served as control and received 10 or 100 µM AG126 without a TLR ligand. Flow cytometry analysis was performed as described later.

For dose response analysis, TLR-stimulated microglia were treated with further tyrphostins and related structures by the same procedure as AG126.

The tyrphostins used were AG9, AG17, AG18, AG43, AG82, AG1288 (Calbiochem/Merck). All compounds were diluted in DMSO to a 50 mM stock solution and stored at -20°C and always kept in the dark. For dose response analysis cells, were treated with 1, 5, 10, 50 and 100 µM.

Tyrphostin-related structures ABD509, ABD517, ABD521, ABD571, ABD593, ABD604 and ABD642 were synthesised and provided by Dr. Ian Greig (Institute of Medical Sciences, University of Aberdeen, Foresterhill, Aberdeen, UK). Compounds were diluted in DMSO to a 10 mM

stock solution, stored at -20°C and kept in the dark. Cells were treated with 10, 50 and 100 µM.

Malononitrile (MN) and 3-hydroxy-4-nitrobenzaldehyde (BZ, both Sigma) were used and diluted as AG126.

3.7.3. Agonists and antagonist

BTK analysis For inhibition of the BTK the inhibitor LFM-A13 (Calbiochem/Merck) was diluted to a 50 mM stock solution and used in 1, 5, 10, 50 and 100 µM working concentrations.

Glucocorticoid receptor analysis

Dexamethasone (Sigma) was used as the synthetic ligand for the glucocorticoid receptor, diluted to a 100 µM stock in PBS and stored at -80°C. Cells were treated in 0.1, 1, 10, 100 and 100 nM concentrations.

Compound A (Cpd A; (2-((4-Acetoxyphenyl)-2-chloro-N-methyl) ethylammonium chloride, Merck) is a tyrosine related compound with binding capacity to the glucocorticoid receptor. The compound was diluted to a 10 mM stock solution in ethanol, stored at -80°C and used in working concentrations of 0.5, 1, 10, 50 µM.

Adrenergic receptors

Noradrenalin (DL-noradrenaline hydrochloride, Sigma) was diluted to an 8.2 mM stock solution and stored at -20°C. Cells were treated with 8.2 µM.

Phentolamine methanesulfonate (PAMS) and propranolol (PR) were purchased from Sigma. The compounds were used as selective antagonists for the α_1/α_2 or β_1/β_2 adrenergic receptors, respectively. They were diluted to a 10 mM stock in PBS. PAMS was used in working concentrations of 0.1, 1 and 10 µM and PR in 1, 10 and 100 µM. AG126, TLR ligand and antagonists were added to the cells without pre-incubation.

Analysis of the major histocompatibility complex (MHC)

Recombinant mouse IFNγ 485-MI7CF was purchased from R & D and diluted to a 50 µg/ml stock solution in PBS and stored at -20°C. Cells were treated with 10 ng/ml. IFNγ was used as positive control for the up-regulation of MHC class I.

3.8. Stimulation of B cells

Prepared cells, described in section 3.6.4, generally, starved for one hour or were preincubated with appropriate inhibitor before stimuli were added.

In our case, before B cell receptor (BCR) or TLR stimulation, AG126 or LFM-A13 (see section 3.7.2, 3.7.2 and 3.7.3) were added to the cells in working concentrations of 50 or 300 µM for one hour at 37°C (Thermomixer comfort, Eppendorf). Controls remained meanwhile untreated. To activate the BCR signaling, K46 cells were stimulated with 10 µg/ml $F(ab')_2$ fragment goat-α-mouse IgG+IgM (H+L) and Ramos cells with 10 µg/ml $F(ab')_2$ fragment goat-α-human IgM Fc fragment specific (H+L) (both Jackson Immunoresearch) for 1 to 3 min at 37°C. Afterwards, clear cellular lysates were prepared. Therefore, cell suspension was centrifuged at 1000 *g* for 2 min at 4°C. Medium was removed and cells were lysed in 100 µl lysis buffer (150 mM NaCl, 50 mM Tris, 5 mM NaF, 0.5 % NP-40, 1 mM protease inhibitor Na_3VO_4). Lysates were centrifuged at 20000 *g* for 10 min. Supernatant was heated for 5 min at 95°C and stored at -20°C until Western blot analysis (see section 3.18).

3.9. Cell viability

The WST-1 cell assay was used to determine cell viability. This colorimetric method is based on the cleavage of the tetrazolium salt WST-1 (Roche) by the mitochondrial succinyltetrazolium reductase (part of the respiratory chain) of viable cells which forms a soluble dye (formazan). Cells were plated on a 96-well plate as described in section 3.6. After microglial stimulation (see section 3.7) cells received fresh medium with WST-1 reagent and were incubated at 37°C for 3 h. The color reaction was measured in a microplate reader (Model 680, BioRad) at 450 nm with 655 nm as reference.

3.10. Cyto- and chemokine release

Cyto- and chemokine release was determined by enzyme-linked immunosorbent assay (ELISA). Interleukin (IL)6, IL10, IL12p70, keratinocyte-derived chemokine (KC, mouse equivalent of growth-related oncogene α, CXCL1), monocyte chemoattractant protein 1 (MCP1, CCL2), macrophage-derived chemokine (MDC, CCL22), macrophage inflammatory protein 1α (MIP-1α, CCL3), RANTES (regulated upon activation of normal T cell-expressed and presumably secreted, CCL5) were measured by the respective mouse-specific DuoSet ELISA development system (R&D). Tumor necrosis factor α (TNFα) was measured by the ELISA provided from R&D or Biolegend and the total IL12/23 p40 total ELISA from eBioscience. The assays were performed according to the manufacture's instructions. Before probing, the immunoabsorbent plates (Maxisorb, Nunc) were blocked with 1% bovine serum albumin (BSA), 5 % sucrose and 0.05 % NaN_3 in PBS (50 mM Na_2HPO_4/NaH_2PO_4, 150 mM NaCl, pH 7.3). The TNFα ELISA from Biolegend

was blocked with 1 % BSA in PBS pH 7.0. For the development of the ELISA, an ultrasensitive tetramethylbenzidine product (Moss) was used as substrate for the color reaction. Interferon (IFN) β release was determined using the Mouse Interferon Beta ELISA Kit (PBL). The assay was performed according to manufacturer's instructions.

All ELISA color reactions were measured in a microplate reader (Model 680, BioRad) at 540 nm with 450 nm as reference. Generally, cell culture supernatant was diluted 1 : 10. For the KC ELISA, samples were diluted 1 : 20.

3.11. Analyses of NFκB, p38^{MAPK}, ERK and JNK activation

The phosphorylation status of diverse signaling molecules in TLR-stimulated microglia (see section 3.7.2) was analyzed by the PathScan® phospho-NFκB p65 (Ser 536), phospho-p38α^{MAPK} (Thr 180/Tyr 182), phospho-p44/42^{MAPK} (ERK 1/2, Thr 202/Tyr 204) and phospho-JNK^{MAPK} (Thr 183/Tyr 185) Sandwich ELISA Kits from CST according to the manual. To obtain cleared cell lysates, TLR-stimulated microglia were washed with ice-cold PBS and incubated with cell lysis buffer containing 1 mM phenylmethylsulfonylfluoride for 5 min. Scraped cells were transferred into 1.5 ml reaction tubes, sonificated for 5 s at ~ 65 % (Sonicator sonoplus HD 2070 MS72, Bandelin) and centrifuged at 10 000 *g* for 10 min. Supernatant was taken and cleared cellular lysates were stored at -80°C until performance of ELISA. The whole procedure was carried out on ice. ELISA colour reaction was measured in a microplate reader (Model 680, BioRad). To ensure an equal protein amout in all samples, GAPDH Western blot analysis and protein determination was performed (see section 3.18 and 3.13). Dually phosphorylated Thr/Pro/Tyr region (pTPpY) was derived from the catalytic core of the active form of JNK kinase, which corresponds to Thr183 and Tyr185 of the mammalian JNK2 enzyme.

3.12. MAPK antibody array

To analyze the relative level of phosphorylation of MAPKs and further serine/threonine kinases the Human Phospho-MAPK Proteome Profiler Array™ was purchased from R&D. For this, microglial cells were plated in a 6 ø cm Petri dish according to section 3.6.1 and stimulated with TLR's with or without AG126 for 15 min (see section 3.7). The array was performed according to the manufacturer's instructions.

3.13. Protein quantification

The amount of total protein was determined by bicinchoninic acid (BCA) protein assay provided from Pierce according to the manual. Generally, cell lysates were diluted 1:20 - 1:500 depending on the expected protein content. Proteins in lysis buffer were diluted in *dd*H_2O. For the standard

curve, BSA was diluted in $dd H_2O$ containing the same amount of lysis buffer as the diluted samples. Color reaction was measured at 540 nm in a microplate reader (Model 680, BioRad).

3.14. Protein tyrosine kinase assay

The PTK assay used in this study allows the measurement of phosphorylated tyrosine residues in random tyrosine-containing peptides coated on a 96-well plate. The phosphorylation reaction is initiated by the addition of the PTK and the reaction buffer containing adenosine-5'-triphosphate (ATP), Mg^{2+} and Mn^{2+}. A monoclonal anti-phospho-tyrosine antibody conjugated with HRP allowed conversion of a chromogenic substrate. The developed color reflects the amount of phosphorylated tyrosine residues. The *pan*-PTK assay (Sigma) was performed according to the manufacturer's instructions. The phosphorylation activity of recombinant Bruton's agammaglobulinemia tyrosine kinase (BTK) PV3363 (Invitrogen) was determined with 10 ng/ml and 100 ng/ml of BTK for 15, 30 and 60 min reaction time. The BTK was diluted to appropriate concentrations in enzyme dilution buffer (20 mM Tris [pH 7.5], 0.05 % Triton® X-100, 10 % glycerol, 0.1 mg/ml BSA, 2 mM dithiothreitol, 0.5 mM Na_3VO_4). Based on the results, the *pan*-PTK assay conditions and BTK concentrations were optimized for further analyzes. The modulatory effect of 50 to 500 µM of AG126 on the phosphorylation of the random peptides by 50 ng/ml BTK was then determined during a 30 min reaction time.

3.15. Flow cytometry analysis

3.15.1. Analysis of whole blood

For fluorescence-activated cell sorting (FACS), in particular flow cytometry analysis, blood was collected from a horizontal cut in the tail blood vessel. Three to four drops of whole blood were collected into an excess volume (1-2 ml) of FACS buffer (2 % FCS, 0.01 mM EDTA pH 8.0, 0.1 % NaN_3 in PBS) and mix immediately by shaking. Samples were centrifuged for 10 min at 200 *g*, 4°C and supernatant discarded. Cells were resuspended by vortexing and 100 µl FACS buffer containing the appropriate fluorescence-coupled antibodies was added (see Tab. 3.3). Samples were again vortexed and incubated at 4°C in the dark for 30 min. After staining, samples were vortexed and 1 ml of lysis buffer was directly added to the cells. Samples were again vortexed and incubated for 5 - 10 min at *RT* in the dark. Afterwards, the tubes were filled with FACS buffer, centrifuged as above and the supernatant discarded. Washing was repeated once with FACS buffer. Cells were finally resuspended in 300 µl FACS buffer. Samples were stored at 4°C in the dark and analyzed within 48 h.

Table 3.3.: Overview of antibodies used for FACS analysis

Purpose	Antibody	Clone	Company
Cell markers			
B cells	α-mouse-CD45R/B220-PerCP	RA3-6B2	BD
Inflammatory monocytes Granulocytes	α-mouse-Ly6C-PE high expression normal expression	AL-21	BD
Granulocytes	α-mouse-Ly6G-PE	1A8	BD
T cells	α-mouse-CD3e-FITC	145-2C11	eBioscience
Microglia	α-mouse-isolectin B4 (ILB4)-FITC	-	Vector Laboratories
	α-mouse-CD11b-APC	M1/70	eBioscience
Blocking FcγR III/II	α-mouse-CD16/CD32 (Mouse BD Fc Block®)	2.4G2	BD
MHC analysis	α-mouse-MHC class I AlexaFluor®	KH114	BioLegend
	α-mouse MHC class II AlexaFluor®	KH116	BioLegend
Secondary Antibody	α-rabbit-FITC labeled		Sigma

all antibodies were used in a 1:100 working concentration

3.15.2. Analysis of primary microglia cell culture

For FACS analysis, plated microglia (see Tab. 3.2) cells were stimulated with the respective TLR ligands with or without AG126 for 24 h for myelin phagocytosis analysis or for 48 h for MHC class I and II measurements. In AG126-treated groups, cells were pre-incubated with AG126 for one hour when combined with another ligand. The stimulation was stopped by washing the cells twice with 1 ml DMEM and once with PBS. Microglial cells were detached from the culture dish upon addition of 300 µl 0.05 % trypsin, 0.02 % EDTA (w/v) (all Biochrom) in PBS, for 3 min at 37 °C, 5 % CO_2. The reaction was stopped by adding 600 µl culture medium. Cells were scratched off, transferred to 2 ml reaction tubes, washed in DMEM and centrifuged at 800 g for 12 min at 4°C. Supernatant was discarded and cells were washed in PBS or FACS buffer.

To measure MHC class I or -II expression, the CD 16/32 antibody was first added (5 min, RT) to the harvested and washed microglial cells followed by the addition of either the MHC class I or class II-APC antibody (20 min,ice). Cells were washed with FACS buffer and resuspended in 100 µl FACS buffer with ILB4-FITC, for 30 min. Cells were again washed in FACS buffer, resuspended and analyzed as described above. As positive control for the MHC class II expression, a recombinant mouse IFNγ (R&D)-treated microglia group was included.

For extracellular staining, cells were washed in FACS buffer instead of PBS. FcR were directly blocked and antibody for MHC class I or II-APC labeled were incubated for 20 min on

ice. Washed cells were incubated with microglia marker ILB4-FITC labeled for 30 min in the dark. Cells were washed in FACS buffer and analyzed.All samples were measured with a FACS Calibur (BD) and the data acquisition was performed with Cell Quest™ software (BD). Data are analyzed using WinMDI 2.8® (1993-1998, Joseph Trotter). Single color controls and unlabeled cells were used for the acquisition and analysis settings. For MHC class II analyzed cells, microglia were stimulated with recombinant mouse IFNγ, carrier free, R&D).

To quantify the myelin phagocytosis by microglial cells, myelin was purified from freshly isolated brains, as described by Norton and Poduslo (1973). Purified myelin was then labeled with FITC with the use of an EZ-Label protein labeling kit (Pierce). FITC-labeled myelin (10 µg/ml) was added to the treated cultures for 30 or 120 min. Excess myelin was removed with 2 x 1 ml DMEM and 1 ml PBS washes. Harvested cells were then stained with CD11b-APC, washed, resuspended in FACS buffer and analyzed as described above.

3.16. Polymerase chain reaction analysis

The polymerase chain reaction (PCR) was performed to analyze the messenger (m)RNA expression of TLR 1 to 9 in unstimulated microglia. RNA was isolated from 8×10^6 microglial cells by the RNA purification kit (RNeasy mini kit, Qiagen). 1 µg RNA samples were treated with 1 µl DNaseI (Roche), 1 µl RNase Inhibitor (Promega) in 14 µl RNase free $dd\mathrm{H_2O}$ for 30 min at 37°C and for another 10 min at 70°C. Thereafter, 14 µl RNA mixture was transcribed into cDNA using 8 µl oligo-dT primers (Roche), 8 µl 5 x buffer, 4 µl0.1 M DTT, 4 µl SuperScript II Reverse Transkriptase (Kit from Invitrogen) and 4 µl *d*NTP's (PeqLab) for 60 min at 37°C. The reverse transcriptase was inactivated at 95°C for 15 min. PCR was performed with a final concentration of 1 x PCR buffer, 1.5 mM $MgCl_2$, 0.25 mM dNTP's, 1 pmol/µl forward and reverse primer and 1 U/Taq polymerase (Kit from Promega). The following PCR program was used: 94°C: 5 min; followed by 28 or 30 cycles 94°C: 30 s; 55.5°C: 45 s; 72°C: 45 s and finally 5 min at 74°C. The following forward (*fw*) and reverse, (*rv*) primers were used and obtained from MWG.

TLR 1	*fw* 5' CAA ACG CAA ACC TTA CCA GAG TG,	*rv* 3' GAG ATT CGG GGT CTT CTT TTT CC,
TLR 2	*fw* 5' AAA ATG TCG TTC AAG GAG,	*rv* 3' TTG CTG AAG AGG ACT GTT,
TLR 3	*fw* 5' ACT TGC TAT CTT GGA TGC,	*rv* 3' AGT TCT TCA CTT CGC AAC,
TLR 4	*fw* 5' TCC CTG ATG ACA TTC CTT CTT,	*rv* 3' TGA GCC ACA TTG AGT TTC TTT A,
TLR 5	*fw* 5' CGC CTC CAT TCT TCA TTC CG,	*rv* 3' CCT TCA GTG TCC CAA ACA GTC G,
TLR 6	*fw* 5' CTT ACT CGG AGA CAG CAC TGA AGTC,	*rv* 3' GCA GGT GGG TGA CAT CTT TAG G,
TLR 7	*fw* 5' TGA CTC TCT TCT CCT CCA,	*rv* 3' GCT TCC AGG TCT AAT CTG,
TLR 8	*fw* 5' CTG TCC AAG GTG TTA CAA TGC TCC,	*rv* 3' TTG AGA GAG GTT TCC GAA GAC G
TLR 9	*fw* 5' GGT GTG GAA CAT CAT TCT,	*rv* 3' ATA CGG TTG GAG ATC AAG.

PCR products were separated in a 1.5 % agarose gel and stained with ethidium bromide.

3.17. Immunohistochemistry

Translocation of phospho-NFκB p65 to the nucleus was analyzed to detect activated NFκB pathways in stimulated microglia. Therefore, TLR-stimulated microglia cells seeded on a cover slip (see section 3.7) were washed with PBS and fixed for 15 min with PFA (4 % in PBS). The procedure was performed at *RT*. Modifications are indicated. After washing three times with PBS, cells were incubated in permeabilization and blocking solution (0.1 % Triton, 10 % FCS in PBS). Rabbit-α-phospho-NFκB p65 (Ser536) antibody (CST) was diluted 1:500 in 10 % FCS in PBS overnight at 4°C. The cells were washed three times with PBS and then incuabated with the secondary antibody α-rabbit-Cy3 (1:400 in 10 % FCS in PBS) for 30 min in the dark. Cells were washed again three times and counterstained with the microglia marker ILB4-FITC (1:200 in 10 % FCS in PBS, Vector) for 2 h. For nuclear staining, washed cells were incubated with 4'-6-diamidino-2-phenylindole (DAPI, 1:1000 in PBS, Roche) for 10 min. Cells were washed once, dipped in $dd\mathrm{H_2O}$ and mounted with and mounted with fluorescence mounting medium (Dako) on an slide. Slides were dried overnight and were stored until analysis in the dark at 4°C. Fluorescence photos were taken with a BX51 Olympus microscope equipped with a DP71 camera, a mercury lamp device (Olympus U-RFL-T) and Olympus Cell F software (2006, Olympus Soft).

3.18. Western blot analysis

Western blot analysis was performed to detect GAPDH, JNK and PLCγ2 in microglia and PLCγ2 in B cells. JNK Western blot analysis was performed in collaboration with Vicki Wätzig, Research group of Prof. Herdegen, Institute of Pharmacology, Kiel University Medical Center, Germany. PLCγ2 analysis on B cells was performed in collaboration with Dr. Konstantin Neumann and Vanessa Bremes, Research Group of Prof. Wienands, Institute of Cellular and Molecular Immunology, University of Göttingen, Germany.

3.18.1. SDS-PAGE

Cellular lysates were analyzed by sodium dodecylsulfate polyacrylamide gel electrophoresis (SDS-PAGE) under reducing conditions using 12 % resolving gels (acrylamide/bis-acrylamide solution ratio 37.5:1, Roth, 25 % resolving buffer, 1 % sodium dodecyl sulfate (SDS) in $dd\mathrm{H_2O}$, with the aid of 0.1 % tetramethylethylenediamine (TEMED), and 1 % ammonumpersulfat (APS) solidified for 30 min) with 4 % stacking gels containing loading pockets (4 % acrylamide/bis-acrylamide solution ratio 37.5:1, 25 % stacking buffer, 1 % SDS in $dd\mathrm{H_2O}$, solidified for 30 min by the help of 0.12 % TEMED, 1.2 % APS). Four times resolving buffer contained 1.5 M Tris pH adjusted

to 8.8 with HCl. Four times stacking buffer contained 0.5 M Tris pH adjusted to 6.8 with HCl. Cleared microglia cell lysates were diluted in 4 x sample buffer (500 mM Tris pH to 6.8 with HCl, 6 % SDS, 10 % β-mercaptoethanol, 30 % glycerol and 0.02 % bromophenol blue). Samples were heated to 99°C for 5 min. An appropriate sized sample was loaded onto the gel together with 'Pre stained Protein plus standard', broad range, from BioRad. Electrophoresis was performed in 1 x SDS-PAGE-running buffer containing 1 % SDS. Ten times running buffer comprised 0.25 M Tris 1.92 M glycine in $dd\mathrm{H_2O}$ pH 8.3. Samples were run by 200 V for 50 min with the Mini-PROTEAN® 3 Mini Vertical Electrophoresis System from BioRad.

3.18.2. Transfer of protein to membrane

After SDS-PAGE, sandwich semidry Western blot was performed. For this, proteins were transferred from the gel to a polyvinylidene fluoride membrane (BioRad) using the Trans-Blot® Semi-Dry electrophoretic transfer cell from BioRad. Priorly used, membrane was dipped in pure methanol and equilibrated in 1 x transfer buffer consisting of 1 x running buffer which contains 10 % methanol (10 x running buffer is described in section 3.18.1). Transferbuffer soaked filter paper, membrane and gel were assembled according to the manual. The blot was run at 10 V for 30 min. To check the protein load, still wet, standard and side labelled membrane was covered with Ponceau S solution (Sigma) for 3 min. The solution was removed and pink membrane destained with $dd\mathrm{H_2O}$. The occurence of pink protein bands showed that a proper protein transfer had taken place.

3.18.3. Immunodetection

Whole incubation procedures were performed at *RT* on a shaker. Modifications are indicated. An overview of the specific antibodies used and therefore the conditions for the experiments are summarized in Tab. 3.4.

Protein-loaded PVDF membrane was blocked in milk or BSA blocking buffer, depending on the target protein for at least 30 min at *RT* or overnight at 4°C. Afterwards, membrane was washed three times for 5 min each in PBS-T (PBS containing 0.5% Tween) and incubated in primary antibody solution for one hour or overnight at 4°C. Again, membrane was washed tree times in PBS-T and then incubated in secondary peroxidase (POD)-labeled antibody solution for one hour. Membrane was washed under standard procedures and once in addition in $dd\mathrm{H_2O}$. For the development, the following steps were performed in the dark room. Membrane was covered equally with 900 µl chemiluminescence peroxidase substrate (Sigma) for 5 min, removed from solution and wrapped in a plastic sheet. Membrane was exposed to X-ray film (Lumi-Film Chemiluminescent detection film, Roche) in exposure box for the required time. The film was then placed in silver nitrate developing solution (X-ray developer $1 + 3.5$ $\mathrm{H_2O}$, Tentenal) until bands were detectable under the red light. Subsequently, the film was transferred in fixing solution (X-ray fixing solution $1 + 4$ $\mathrm{H_2O}$, Tetenal) and incubated until it was transparent.

Table 3.4.: Overview of antibodies used for Western blot analysis

Antibody	kD	Company	Working conc. diluted
Primary Antibody			
Rabbit-α-mouse BTK	77 kDa	CST	1:1000 [1]
Mouse-α-GAPDH	36-40 kDa	Imgenex	1:3500
Rabbit-α-phospho-JNK	46, 54 kDa	Promega	1:2500
Rabbit-α-phospho-mouse-PLCγ2 Y759	150 kDa	CST	1:2000[2]
Rabbit-α-mouse-PLCγ2	150 kDa	CST	1:1000[2]
Mouse-α-phospho tyrosine clone 4G10®		Upstate	0.5µg/ml
Secondary Antibody			
Goat-α-rabbit IgG-POD (whole molecule)	-	Sigma	1:20000
Goat-α-rabbit IgG-POD	-	Pierce	1:10000
Goat-α-mouse IgG-POD (whole molecule)	-	Sigma	1:20000

[1] TBS, 0.1 % Tween-20 with 5 %BSA
[2] TBS-T, 5 % BSA
[3] PBS-T, 0.5 % BSA

Finally, the film was rinse with H_2O and scanned for documentation. PVDV membrane was stored in PBS at 4°C if needed.

Immunodetection, with primary antibodies purchased from CST, was performed according to manufacturer's instructions.

3.18.4. Membrane stripping

For membrane stripping, ECL-developed membrane was washed twice in TBS-T and incubated for 30 min at 50°C in stripping buffer (68.5 mM Tris pH 6.8, 2 % SDS, 100 mM β-mercaptoethanol). Afterwards, membrane was washed over the whole day in PBS-T.

3.18.5. Western blot analysis of B cell lysates

For the analysis of PLCγ2 of B cell lysates a 10 % resolving gel was used. Proteins were blotted on a nitrocellulose membrane. Immunodetection was performed according to the manual from CST of PLCγ2. For the detection of protein bands ECL detection system (Amersham) and digital imaging system ChemiLux Imager (Intas) was used.

3.19. Analysis of inner-membrane electrochemical gradient in mitochondria

Changes in the mitochondrial electrochemical potential gradient ($\Delta\psi$) was analyzed using a mitochondria staining kit (Sigma). Microglia seeded in 96-well plate were stimulated with TLR ligands of standard concentrations in the presence or absence of AG12 for 18 h. JC-1 staining was performed according to the manufacturer's instruction. Mitochondria with an intact membrane potential concentrates the JC-1 dye in the mitochondrial matrix in the form of red fluorescent aggregates. Disrupted membrane potential prevents the dye from accumulation in the mitochondria and disperses it throughout the cell as green fluorescent JC-1 monomers. The antibiotic valinomycin was used according to the manual as a negative control.

3.20. Spectral analysis

Tyrphostins AG126, AG18 and AG82 (50 mM in DMSO diluted to 100 µM in medium) were incubated in 96-well plates with or without microglia at 37 °C, 5% CO_2 for different time periods. Afterwards, absorbance spectra (230 to 500 nm all 2 nm) of tyrphostin solution was measured in a 384-well, flat bottom transparent UV permeable plate (Greiner), using Safire spectrometer (Tecan) together with x-Fluor 4 Software at *RT*. Spectra were normalised to an absorbtion peak of medium containing phenol red at 560 nm. Characteristic absorbance maximum (AG18 449 nm, AG82 470 nm, AG126 435 nm) was plotted against time.

3.21. NMR spectroscopy

NMR analysis was performed in cooperation with Dr. Michael John, Institute for Inorganic Chemistry, University of Göttingen, Germany.

3.21.1. ^{1}H NMR

For nuclear magnetic resonance (NMR) spectroscopy, samples of 1 or 5 mg of AG126 were prepared in 600 µl absolute DMSO-d_6, 600 µl commercially available DMSO-d_6 containing H_2O and 500 µl DMSO-d_6 + 100 µl D_2O. The solutions were transferred to 5 mm NMR tubes. All NMR spectra were recorded on a Bruker (Rheinstetten, Germany) Avance 500 MHz NMR spectrometer at 25°C. The samples were monitored over a period of 21 days. ^{1}H NMR spectra were recorded using 20 scans and 2.75 s acquisition; the solvent HDO peak was calibrated to 4.70 ppm.

3.21.2. ^{13}C NMR, HSQC and HMBC

Due to its low intrinsic sensitivity ^{13}C NMR spectra were run on the 5 mg samples with 2048 scans in typically 1.5 h. The ^{13}C resonances were calibrated indirectly using $\Xi(\mathrm{TMS}) = 0.25145020$ and assigned using the 2D heteronuclear single quantum correlation (HSQC) and heteronuclear multiple bond correlation (HMQC) experiments, optimized for $^{1}J_{CH} = 145$ Hz and $^{2/3}J_{CH} = 7$ Hz, respectively. The 2D spectra were recorded using spectral widths of 11 ppm (^{1}H) and 110 ppm (^{13}C), 16 or 32 scans and 1024 (^{1}H) $\times$ 256 (^{13}C) complex time domain data points in typically 4 or 8 h.

3.21.3. Diffusion-ordered spectroscopy (DOSY)

2D Diffusion-ordered (DOSY) spectra were recorded using the *ledbpgp2s* sequence with ($\delta/2 =$ 2 ms) bipolar z gradients ramped from 1 to 50 G/cm, a diffusion delay (Δ) of 100 ms and a longitudinal eddy current delay of 10 ms. The data matrix had a size of 8k (^{1}H, 0.68 s acquisition) $\times$ 64 (diffusion dimension) and was recorded with 8 scans in typically one hour.

4. Results

This chapter summarizes first the data of AG126 effects in experimental autoimmune encephalomyelitis (EAE). Afterwards, AG126 effects on the TLR signaling of microglia and the hierarchical involvement of AG-sensitive target(s) are presented. The identification of BTK as a putative AG126-sensitive target led to a detailed analysis of AG126 actions on this PTK, shown subsequently. An insufficient explanation for AG126 effects by PTK inhibition on the different readouts in TLR-activated microglia cells led to the analysis of PTK-independent modes, summarized in the next section. Additionally, data of NMR-analysis are shown which revealed chemical properties of AG126. The recognition of AG126 degradation in aqueous solutions was the reason to analyze the effects of AG126 degradation products on TLR-activated microglia. Finally, the effects of AG126-degradation products were tested in EAE again as shown in the last section.

4.1. AG126 reveals beneficial effects in EAE

In many animal models of inflammatory diseases, tyrphostin AG126 administration improves the severity of the disease outcome by attenuating the inflammation-associated dysfunction as well as damage and by promoting a more anti-inflammatory cellular phenotype. This could be shown, among others, in mouse models of septic shock and bacterial meningitis (Novogrodsky et al., 1994; Hanisch et al., 2001). The following study addressed the question whether AG126 also affects the disease outcome in mice with an induced experimental autoimmune encephalomyelitis (EAE), an animal model of MS. EAE is characterized by inflammatory reactions in the CNS combined with demyelination and subsequent axon injury. Apparent symptoms are ascending paralysis of distal to proximal extremities (reviewed by Gold et al., 2006).

4.1.1. AG126 treatment improved the clinical score

EAE was induced by immunization of C57/BL6J mice with MOG_{35-55} emulsified in CFA (details see Material and Methods). Animals were weighted daily and disease symptoms were scored according to the degree of severity (IMSF score) until day 22. On day 12, first disease symptoms could be detected. Henceforward, animals were treated with 500 µg AG126/animal/day or PBS (as controls, CTL) on three consecutive days. The disease progression of AG126- *vs.* PBS-treated animals is summarized in Fig. 4.1 *A*.

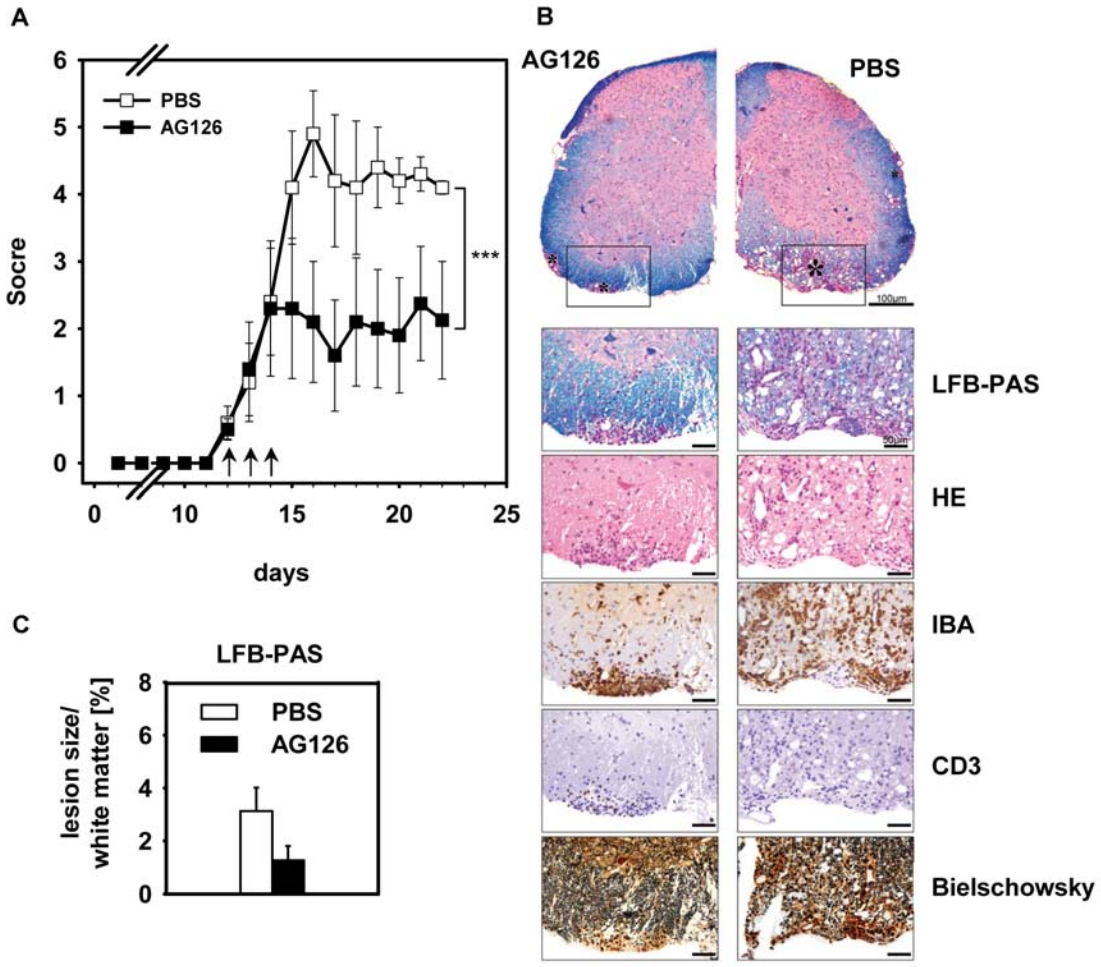

Figure 4.1.: AG126 improves the disease course in experimental autoimmune encephalomyelitis (EAE). *Wt* C57/BL6J mice actively immunized with MOG_{35-55} emulsified in CFA were treated at day 12 for three consecutive days (arrows) with 500µg AG126/animal/day (*i.p.*, closed square) or PBS (controls, open square). ***A*** Animals were weighted and scored daily for clinical signs of disease on a scale from 0 to 10 depending on the severity (details see Material and Methods section 3.2). $p<0.0001$ significant difference in interaction but not in total. ***B*** Animals were sacrificed on day 23. Histological analysis of spinal cord sections was performed to detect demyelinized white matter (LFB-PAS), infiltrated cells (HE), infiltrated macrophages and microglial cells (IBA1), infiltrated T cells (CD 3) or neuronal impairment (Bielschowsky). Representative stainings from the same tissue areas are shown. Asterisks indicate lesion sites (pink areas within the blue stained white matter). ***C*** Quantitative analysis of demyelinized spinal cord tissue in LFB-PAS-stained sections revealed a reduced lesion size in AG126 treated animals (Data are mean ± SEM, n = 5 animals/group).

While the maximal mean disease score for AG126-treated mice was reached on day 14 (2.4 ± 0.8), the PBS-CTL group reached its maximal score on day 16 (4.9 ± 0.6). From these maxima, an improvement of the disease symptoms could be reached in both groups on day 17 for AG (1.6 ± 0.8) and day 18 for the PBS-CTL (4.1 ± 1.0). The animals were sacrificed on day 22 with a mean score of 2.1 ± 0.9 and 4.1 ± 0.1 for the AG126 or PBS treatments, respectively. In conclusion, AG126 treatment improved the clinical score of EAE-induced mice. The CNS tissue of these animals was histologically analyzed as described in the following section.

4.1.2. AG126 treatment reduces the myelin lesion size

Representative (immuno-)histological stainings of spinal cord sections are shown in Fig. 4.1 *B*. Demyelinized white matter lesions were visualized by LFB-PAS-staining. Overall, T cell and microglia/macrophage infiltration of the tissue was visualized by HE, CD 3, or IBA1 staining, respectively. Bielschowsky staining revealed axonal injury. PBS-CTL animals presented with marked lesions of myelinated structures. A pronounced infiltration of immune cells was detected within the lesions as well as a diminished axonal density and looser tissue connections in the affected tissue regions. Tissue of AG126-treated animals showed a reduced damage of the white matter and attenuated lesion characteristics in general. The white matter lesions were quantitatively analyzed for consecutive sections, revealing a reduced size in AG126-treated compared to CTL animals (Fig. 4.1 *C*).

Taken together, AG126 reduces the white matter lesions in EAE-induced mice. These data are consistent with the improved disease severity score.

4.1.3. Therapeutic AG126 treatment is more effective than preventive treatment

To determine the 'kinetics' of the AG126 effect on the EAE outcome, *i.e.*, the most sensitive period, another EAE study was conducted. Compared to the first one, animals were now treated in two time windows. The first group received the tyrphostin in a preventive manner before the disease onset, starting with day 6 after immunization. The second group was treated in a therapeutic manner. AG126 was applied after disease onset. In contrast to the first EAE experiment, the animals were treated with 500 µg AG126/animal/day for five days, *i.e.*, on three consecutive days and thereafter every other day (Fig. 4.2). Moreover, the control group received DMSO as vehicle. Animals were weighted daily and scored according to their disease symptoms (ZTE score). The day after the three consecutive treatments, a blood sample was taken for analysis of immune cells, as described later.

In the preventive AG126 treatment first signs of disease could be detected on day 13 (Fig. 4.2 *A*). The preventive treatment caused a delay in the course of the disease but could not diminish the extent of extremity paralysis. While in the CTL group, the score maximum was reached on

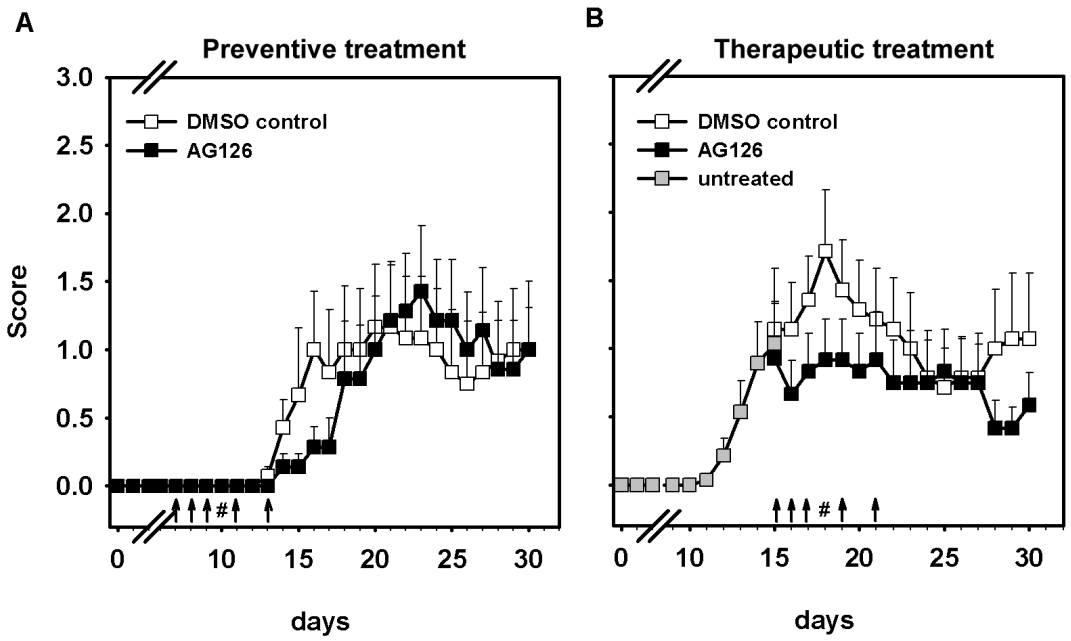

Figure 4.2.: AG126 improves the disease course by therapeutic but not preventive treatment in EAE. *Wt* C57/BL6J mice actively immunized with MOG_{35-55} were treated on five days (indicated by arrows) with 500 µg AG126/animal/day (closed square) or DMSO (control open square). ***A*** Treatment started before obvious disease symptoms on day 7 (preventive treatment). ***B*** Treatment started after disease onset on day 15 (therapeutic treatment). Animals were weighted and scored daily for clinical signs of the disease on a scale from 0 to 5 (details see Material and Methods section 3.2). Data are mean ± SEM, n = 7 animals/group. # Blood samples were taken and analyzed by FACS.

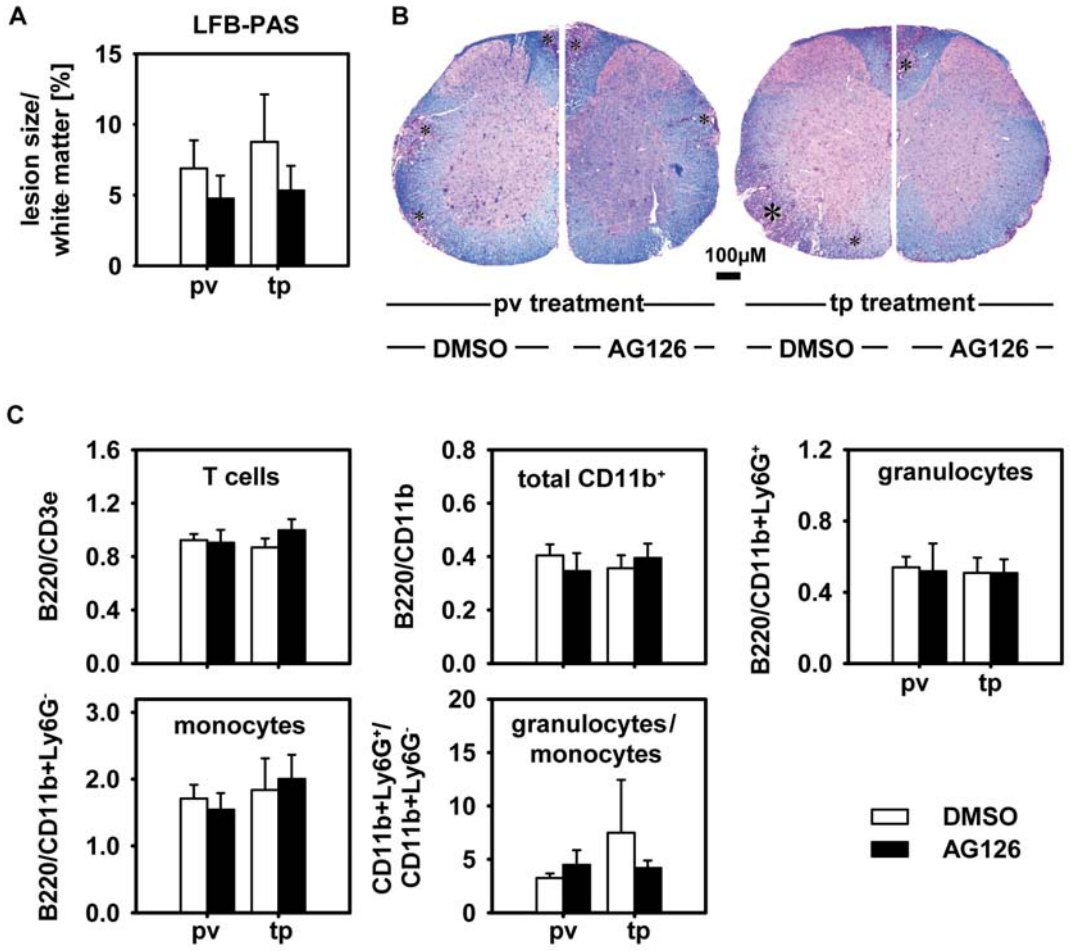

Figure 4.3.: AG126 shows effects on the CNS but does not affect immune cells in the periphery. Animals were sacrificed on day 30 (compare Fig. 4.2). Histological analysis of spinal cord sections was performed to detect demyelinized white matter (LFB-PAS). ***A*** Quantitative analysis of demyelinized spinal cord sections by LFB-PAS staining revealed a tendency for reduced lesion size in AG126-treated animals. Data are mean ± SEM (n = 7 per group). ***B*** Representative sections with LFB-PAS staining. Asterisks indicate the lesion sites (pink areas within blue stained white matter). ***C*** On day 10 (preventive treatment, pv) and day 18 (therapeutic treatment, tp) after MOG immunization, blood samples were taken for the analysis of peripheral blood leukocytes. No effects of AG126 on leukocyte counts in the blood was detectable. FACS analysis was performed for various cell populations (see text). Data are mean ± SEM (n = 7 per group).

day 20 (1.2 ± 0.5), the maximum was reached on day 23 (1.4 ± 0.5) in the AG126 group. The maximal mean disease score was even higher than in the DMSO-CTL group.

In the therapeutic treatment, the disease course improved as soon as AG126 administration was started (Fig. 4.2 *B*). No further aggravation (in mean) of clinical symptoms could be observed (1.1 ± 0.4). In contrast, in the DMSO-CTL group, the peak of disease was reached on day 18 (1.7 ± 0.4). Afterwards the disease course constantly declined in the CTL group until day 25 (0.7 ± 0.3). In contrast, the AG126 treated animals showed a relative constant mean disease score until day 27 (0.8 ± 0.3) with little variations between day 16 to 21. In the late phase of the experiment, still some benefit of the AG126 treatment was observed (AG126 0.9 ± 0.4, DMSO-CTL 1.2 ± 0.4). AG126 thus affected the EAE by suppressing the mean disease maxima.

The two treatment regimes came with a slightly different time of onset for the disease symptoms, *i.e.*, day 11 and 13 for the therapeutic and preventive AG126 administrations. Indeed, animal handling may induce stress, leading to an attenuated disease onset in both treated and control animals (Gold and Heesen, 2006).

Overall, the therapeutic treatment with AG126 suppressed the disease symptoms in comparison to the DMSO-CTL, whereas preventive treatment just delayed the development of the outcome of the disease symptoms.

Histological analysis of the lesions by LFB-PAS staining revealed reduced white matter damage even in animals with both, preventive or therapeutic treatment (Fig. 4.3 *A*). Representative tissue sections are shown in Fig. 4.3 *B*.

On the other hand, blood analysis for peripheral immune cells, like T cells, total $CD11b^+$ cells (covering monocytes, granulocytes, natural killer cells and macrophages), monocyte or granulocyte population revealed no differences between the AG126-treated *vs.* CTL groups (Fig. 4.3 *C*).

In conclusion, AG126 was able to influence the disease course of animals with an induced EAE. Depending on the time point of AG126 treatment, the tyrphostin attenuated the disease outcome. AG126 thereby represses effectively the disease symptoms, when being applied at onset of clinical signs (compare Fig. 4.1 *A* and 4.2).

Therefrom, we analyzed the mode of action of AG126 on microglial cells. Here we focused on cellular responses, when cells get activated by TLR ligands, pathogen-associated structures originating from bacteria or viruses.

4.2. Microglia as a target of AG126

Microglia are the innate immune cells of the CNS and their TLR's mediate responses to both exogenous as well as endogenous factors in infectious as well as non-infectious challenges. Our previous work had revealed that microglial activities, namely reactions to TLR stimulations are modulated by AG126 (Hanisch et al., 2001; Kann et al., 2004). We therefore focused on microglia for an investigation of cellular consequences and potential mechanisms of AG126 actions.

Primary mouse microglia cell cultures were activated by TLR stimulation and a cyto- and chemokine release pattern, based on nine factors was analyzed. The cyto- and chemokine induction pattern was than also measured for TLR stimulations in the presence of AG126 to elucidate a putative involvement of an AG126-sensitive target(s) in the TLR signaling of microglia. Cells deficient for either central signaling elements of the TLR signaling cascade (MyD88, TRIF) or the whole receptor (TLR4). Activation of the downstream-located MAPK's and NFκB in TLR-stimulated microglia was examined to obtain first information about the hierarchical position of the AG126-sensitive target(s) especially within the MyD88 route.

4.2.1. Multiple Toll-like receptor agonists activate a pro-inflammatory cyto- and chemokine release response in microglia

The first set of analysis examined the impact of the PAMP confrontation *via* diverse TLR's on the cyto- and chemokine release in microglial cells. Therefore, primary *wt* microglia cultures were exposed to the specific TLR agonists Pam_3CSK_4 (TLR1-2), Poly(I:C) or Poly(A:U) (TLR3), LPS *E.coli R515* (TLR4), Flagellin (TLR5), MALP2 (TLR6-2), Poly(U) (TLR7/8) and CpG ODN (TLR9) in pathophysiological relevant concentration range (Fig. 4.4). For a TLR3 stimulation, two different ligands were used, Poly(I:C) and Poly(A:U). While Poly(I:C) was used as a standard tool in TLR studies, it became more recently clear, that it is recognized by both the endosomal receptor TLR3 and cytosolic receptors, like the RNA helicases retinoic-acid-inducible protein I (RIG-I) and melanoma differentiation-associated gene 5 (MDA5; Kato et al., 2006). Thus, responses would be built on more than one signaling pathway. In contrast, Poly(A:U) signaling is considered to be more confined to the TLR3 pathway (Conforti et al., 2010). The spectrum of cyto- and chemokines determined upon TLR stimulation comprised:

- TNFα a pluripotent cytokine with general pro-inflammatory actions,
- IL6 as a pro- as well as anti-inflammatory cytokine, with multiple cellular targets and induction also upon injuries and a cytokine associated with recruiting T- and B cells,
- IL12 (covering all molecular versions containing the IL12p40 subunit in monomeric hetero- and homodimeric form, *i.e.* IL12p70, IL12p40 or $IL12p(40)_2$ as a cytokine associated with CD 4 T cell differentiation into the Th1 subtype.
- IL10 as a potent suppressor of macrophage functions and
- IFNβ as an interferon known to be involved in antiviral defense
- CCL2 (MCP1), as a chemokine to attract T cells, monocytes, basophile cells and activates macrophages,
- CCL3 (MIP1α) as a chemokine attracting monocytes/macrophages, T cells (Th1 > Th2), NK cells, basophil cells, and immature dendritic cells.
- CCL5 (RANTES) as a known attractor of monocytes/macrophages, T cells (T memory cells > T cells, Th1 > Th2), also involved in chronic inflammation.

- CCL22 (MDC) causing chemotactic migration of dendritic cells and Th2 cells.
- CXCL1 (KC) known to be involved in the attraction of neutrophil cells.

A pronounced cytokine and chemokine release was obtained in microglia exposed to Pam_3CSK_4, Poly(I:C), Poly(A:U), LPS and MALP2 (Fig. 4.4 *A*). Some release was also induced by Poly(U) and CpG ODN, whereas Flagellin failed to stimulate cells. Pam_3CSK_4, Poly(A:U), LPS and MALP2 triggered a release over a broader concentration range. Concentrations of 0.5 ng/ml for MALP2, 1 ng/ml for LPS, 50 ng/ml for Pam_3CSK_4 and 10 µg/ml for Poly(A:U) were sufficient to reach a release plateau. The amount of 5 µg/ml CpG ODN was sufficient for a plateauing release of MIP1α but not yet for other factors. Similarly, the release induction for TLR3 by Poly(I:C) and TLR7/8 did not reach maximal values over the agonist concentrations which could be afforded.

In general, the TLR agonists triggered a wide spectrum of cyto- and chemokines with primarily pro-inflammatory actions. TNFα, IL6, MCP1, MIP1α, RANTES and KC could be detected, to varying extent, upon induction by ligands for TLR1-2, TLR3, TLR4 and TLR6-2 as components of their respective spectra. Thereby, TLR1-2 and 6-2 exhibited similar release patterns, due to the sharing of TLR2 in their heteromeric configuration. Agonists of TLR7/8 and 9 induced only a weak release of MIP1α, RANTES as well as KC. Contrariwise, the anti-inflammatory and immunosuppressive IL10 or MDC were not found at all in the supernatants of microglia following TLR stimulations.

PCR analyses were performed to examine microglial TLR expression. PCR products could be detected for TLR1 to 4 and TLR6 to 9 (Fig. 4.4 *B*). Consistent with the absence of cyto- and chemokine release in TLR5-stimulated cells, TLR5 mRNA was virtually undetectable.

In further experiments, microglial cells were stimulated with 10 ng/ml of the TLR1-2, TLR4 and TLR6-2 agonists, 50 µg/ml of the TLR3 agonists and 5 µg/ml of the TLR9 agonist. These concentrations caused well detectable release responses and were in the relevant cases of TLR1-2, TLR3, TLR4 and TLR6-2 already in the range of maximal cellular effects.

4.2.2. AG126 affects the cyto- and chemokine release pattern

In order to determine dose-dependent effects of AG126 on the cyto- and chemokine profiles on TLR-stimulated microglia, the cells were preincubated with the tyrphostin for one hour, followed by combined incubation with the TLR ligands for 18 h and determination of the cyto- and chemokine content in the supernatants. The applied AG126 concentrations did not have an effect on the cell viability. TLR agonists were applied at concentrations selected from the previous experiments.

Pronounced effects of AG126 on the release pattern could be observed for all of the TLR ligands (Fig. 4.5 *A*). Interestingly, AG126 did not exert a simple inhibitory effect throughout. It caused a biphasic release modulation for some of the cyto- and chemokines depending on its concentration. AG126 administration up to 10 µM led in some cases to an increased release, such

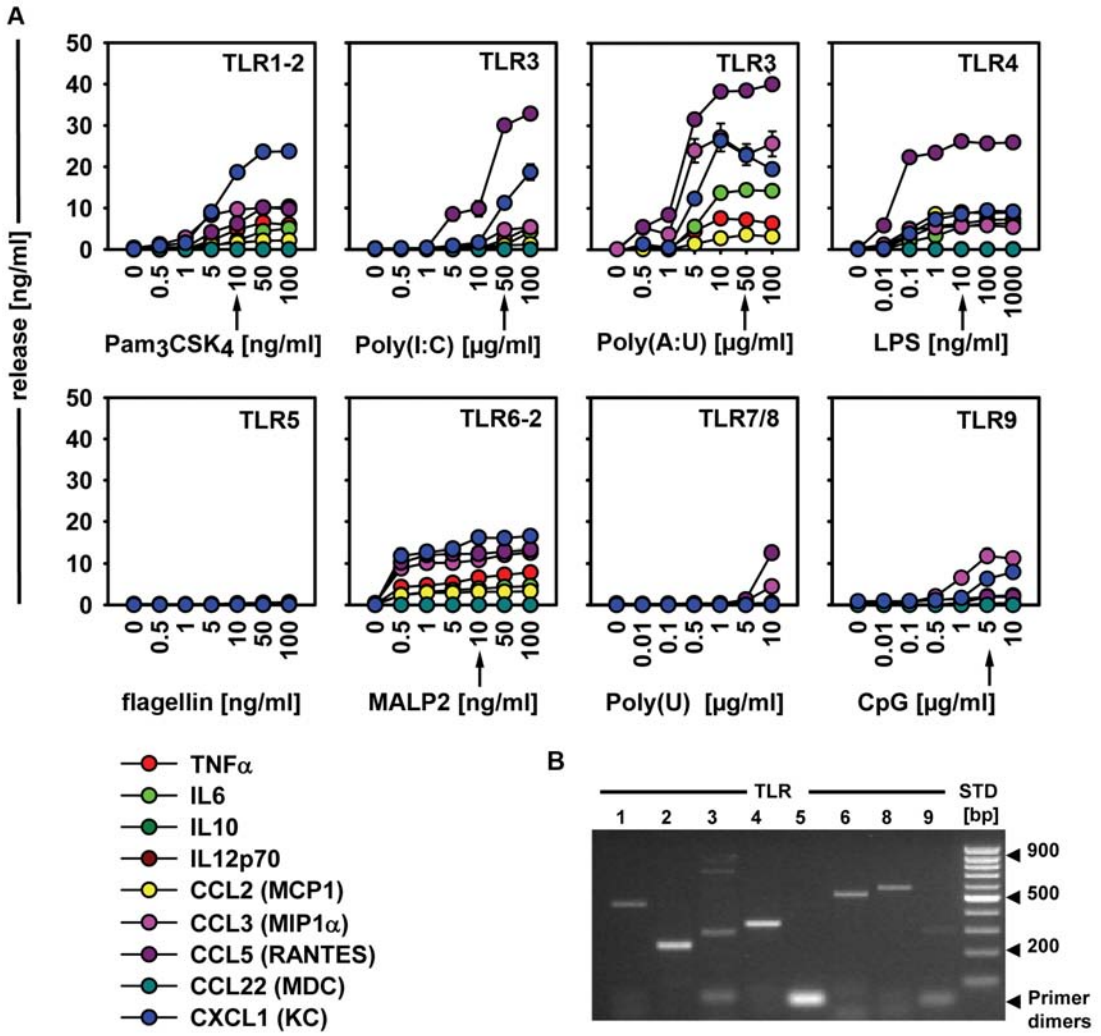

Figure 4.4.: Stimulation of TLR's in microglia leads to a pro-inflammatory cyto- and chemokine response. ***A*** Microglia were stimulated with the respective TLR agonists Pam_3CSK_4 (TLR1-2), Poly(I:C) and Poly(A:U) (TLR3), LPS *E.coli R515* (TLR4), Flagellin (TLR5), MALP2 (TLR6-2), Poly(U) TLR7/8 and CpG ODN (TLR9) for 18 h at various concentrations. Supernatants were taken and analyzed for cyto- and chemokine release by ELISA. Data are mean ± SEM, $n > 20$ per concentration as summarized from two experiments each. Arrows indicate standard concentrations used for subsequent experiments. TLR5 and TLR7/8 were not considered in further experiments. ***B*** mRNA of unstimulated microglia was analyzed by PCR for the expression of TLR1 to 9. 30 amplification cycles were performed. A PCR product could be detected for TLR1 to 4 and TLR6 to 9, but not for TLR5. A PCR product was also detected for TLR7 after 28 amplification cycles (not shown).

as for MIP1α, RANTES and KC, whereas this phenomenon was not seen for other factors. The biphasic profile for Pam_3CSK_4, Poly(I:C), MALP2 and CpG ODN-treated cells then covered a suppression of release with higher AG126 concentrations. Again, similarities were seen in the responses of TLR1-2- and TLR6-2- stimulated cells. With 100 µM of AG126, release activity nearly disappeared for several factors, such as TNFα, IL6, MCP1 and RANTES. Others were markedly down-regulated, like KC and MIP1α.

The AG126 effects on Poly(A:U)- and LPS-stimulated microglia differed from that seen for the other TLR agonists. Interestingly, both release patterns were very similar. Release of MCP1 was just partially diminished, and the production of KC even increased with increasing AG126 concentrations. Most surprisingly, in LPS-treated cells, the release of MIP1α revealed also a biphasic effect, however, in a reversed fashion compared to the stimulation of the other TLR's. There was a decrease at lower and an increase at higher AG126 concentrations. The release of RANTES was nearly unaffected by AG126. Apparently, the AG126-inducible modulations of cyto- and chemokine release would fall into two types. First, TLR's signaling through MyD88 exclusively (TLR1-2, TLR6-2, TLR9) reveal a biphasic profile. Second, TLR's signaling through TRIF only (TLR3) or in addition to MyD88 (TLR4) would present with a selective enhancement of certain release functions, while others are partially inhibited and again others are more or less separated. Poly(I:C) thereby joins more the first pattern, likely due to its RIG-I/MDA5-stimulating effects, and thus less appearing as a TLR3 agonist.

Overall, AG126 revealed a pronounced influence on the release induction by various TLR's. The effects on the release phenotypes were, however, far from a simple inhibition but exhibited a complex dose dependency with, in some cases, opposite outcomes. Consequently, the release-modulating influence of AG126 is not *per se* of suppressive or 'anti-inflammatory' nature.

4.2.3. AG126 does not alter the TRIF-dependent IFNβ induction

In order to further narrow down on the target of AG126, the release of IFNβ was analyzed. This response product depends on the adapter molecule TRIF (Fig. 1.1; Doyle et al., 2002; Yamamoto et al., 2003.

As before, cells were preincubated with AG126 (10, 50 or 100 µM) for one hour, followed by a combined stimulation with the TLR ligands Pam_3CSK_4, LPS and MALP in the presence of AG126 for 18 h. Cell culture supernatant was taken and the IFNβ release analyzed by ELISA. Induction of IFNβ release was seen only after TLR4 activation (Fig. 4.6 *A*). Regarding AG126, no regulatory effect on the IFNβ release was detectable. Together with the data from the Poly(A:U) stimulation in section 4.2.2, these data support the concept that the AG126-sensitive target does not affect the MyD88-independent signaling cascade.

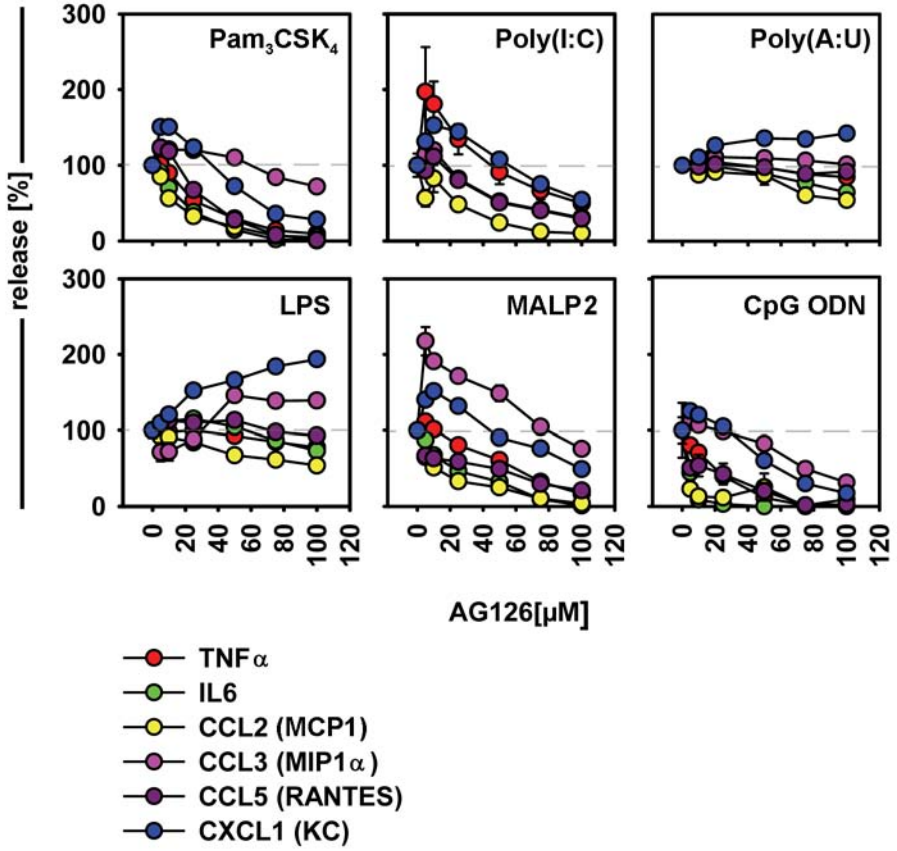

Figure 4.5.: AG126 treatment has complex effects on the cyto- and chemokine production in microglial cells stimulated with different TLR agonists. *Wt* microglial cells were stimulated with agonists of TLR1-2 (10 ng/ml Pam_3CSK_4), TLR3 (50 µg/ml Poly(I:C) or Poly(A:U)), TLR4 (10 ng/ml LPS), TLR6-2 (10 ng/ml MALP2) and TLR9 (5 µg/ml CpG ODN) without or with 5 to 100 µM AG126 as indicated for 18 h. Cells with AG126 treatment received a preincubation with the tyrphostin for one hour at the respective concentration. Cyto- and chemokine release was measured in the supernatants and expressed as percentages of the control amounts (AG126 absence). Data are mean ± SEM, n = 24 per treatment as summarized from two independent experiments.

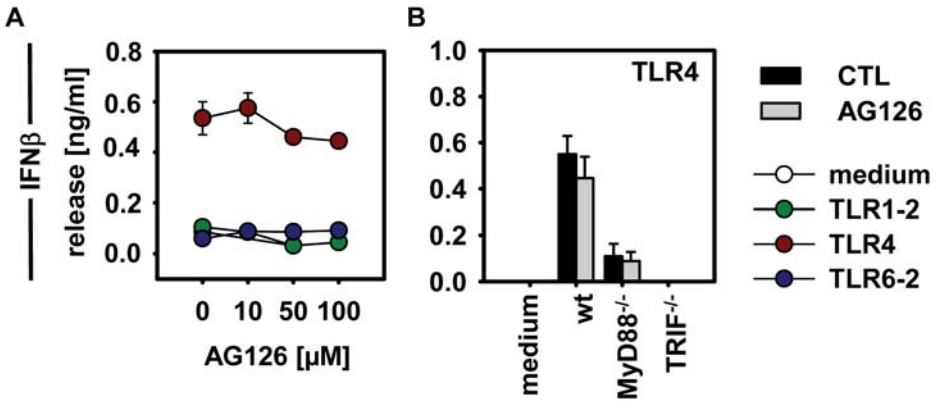

Figure 4.6.: AG126 does not affect the TRIF-dependent pathway.(***A***) NMRI or (***B***) C57/BL6 *wt* microglia and cells deficient in TRIF or MyD88 were preincubated with ***A*** 10, 50, 100 µM or ***B*** just 100 µM AG126 for one hour. Subsequently, TLR1-2- (10 ng/ml Pam_3CSK_4), TLR4- (10 ng/ml LPS) and TLR6-2- (10 ng/ml MALP) stimulated or unstimulated microglia were incubated without or with ***A*** 10, 50, 100 µM or ***B*** just 100 µM AG126 for 18 h. IFNβ release was measured by ELISA. Data are mean ± SEM, ***A*** n = 6 ***B*** n = 4.

4.2.4. AG126 effects on microglia with TLR signaling deficiencies

To get more information about the operating range of AG126 within the TLR signaling, the cyto- and chemokine release was analyzed for TLR-stimulated microglia from various *ko* animals with deficiency in the TLR pathways. Therefore, $TLR4^{-/-}$, $TRIF^{-/-}$ and $MyD88^{-/-}$ microglia were preincubated with 100 µM AG126 for one hour and following applied in combination with the TLR ligand Pam_3CSK_4, LPS or MALP. Microglia were stimulated for 18 h. Cell culture supernatant was taken and IFNβ, TNFα and KC release analyzed by ELISA.

Underlining the data from IFNβ *wt* microglia descibed in the previous section, AG126 did not significantly influenced the IFNβ release in $MyD88^{-/-}$ microglia (Fig. 4.6 $A + B$). Interestingly, the total release of IFNβ in the $MyD88^{-/-}$ microglia was much lower compared to the *wt* cells. This leads to the conclusion that both TLR4-associated signaling cascades (MyD88-dependent and -independent) crosstalk for a proper IFNβ release.

To examine, if AG126 may affect the MyD88-dependent signaling, the release of KC and TNFα was examined. As shown in Fig. 4.7, the release of both cytokines was abolished in all, Pam_3CSK_4-, LPS- and MALP-exposed, $MyD88^{-/-}$ microglia.

By contrast, the release of KC and TNFα stayed nearly unaffected in $TRIF^{-/-}$ cells *vs. wt* microglia, besides the KC release of TLR6-2-stimulated cells. Here, an overall release reduction by approximately 60 % was detectable in $TRIF^{-/-}$, suggesting that deficiency in this pathway may still affect some MyD88-controlled consequences. Nevertheless, the AG126 sensitivity remained in all $TRIF^{-/-}$ microglia. AG126 had a more or less pronounced inhibitory effect on the release of TLR-activated cells. Surprisingly, AG126 had even no enhancing effect on TLR4-activated KC release any more as seen in the *wt* situation.

As expected, no KC or TNFα release could be detected in TLR $4^{-/-}$ microglia when exposed

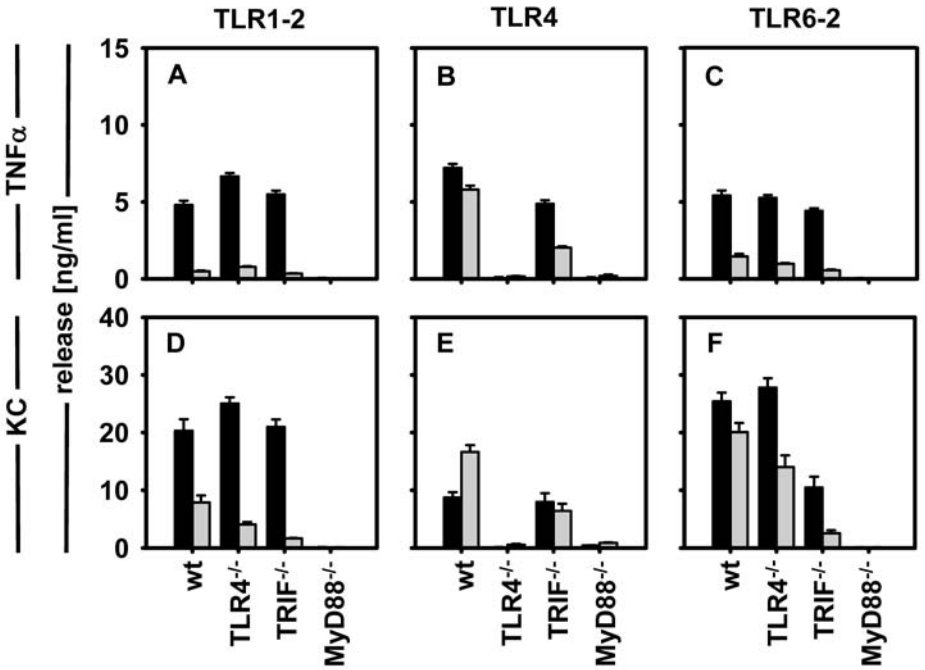

Figure 4.7.: Anti-inflammatory effects of AG126 are not restricted to TLR4 and are unaffected in a TRIF*ko* situation. C57/BL6 microglial cells deficient in TLR4, TRIF, MyD88 and *wt* cells were preincubated with 100 µM AG126 or received a media change for one hour. Subsequently, TLR1-2 (10 ng/ml Pam_3CSK_4, ***A, D***), TLR4 (10 ng/ml LPS, ***B, E, G***), TLR6-2 (10 ng/ml MALP, ***C, F***) stimulated or unstimulated microglia were incubated without or with 100 µM AG126 for 18 h. Supernatant was taken. KC, TNFα and IFNβ release was measured by ELISA. Data are mean ± SEM, ***A - F*** *wt* microglia ($n > 16$ per treatment summarized from two independent experiments). $TLR4^{-/-}$ microglia ($n = 24$, data were summarized from 4 *ko* animals), $TRIF^{-/-}$ microglia ($n = 18$, data summarized from 3 animals) $MyD88^{-/-}$ microglia ($n = 18$ summarized from 3 animals).

to LPS (Fig. 4.4 $B + E$). Moreover, the activation of TLR 1-2 or 6-2 was similar to the *wt* situation. In short, when microglia were stimulated with a TLR agonist, the cyto- and chemokine release was not much influenced by the deficiency in another TLR.

Summing up, AG126 does not affect the LPS-induced IFNβ release. Here, IFNβ is known to get activated by the TRIF-dependent pathway. However, the takeout of this signaling element leads to a strongly AG126-independent reduction of the total IFNβ release, assuming a crosstalk of both pathways. On the other hand, AG126 has a strong inhibitory affect on the KC and TNFα release. It could be shown, that these cytokines are under MyD88 control, and remained nearly unaffected if the TRIF-componend of the signaling cascade is abolished. This leads to the conclusion, that the AG126 sensitive target is localized with closer association to the MyD88 pathway.

Because microglial TLR stimulation leads to further responses others than the induction of soluble immunoregulary factors, we checked in the following experiments, whether AG126 may

also affect some of these. Therefore, the next section describes the effect of AG126 on TLR-induced expression of the MHC class I and II as well as effects on the myelin phagocytosis.

4.2.5. AG126 does not alter the MHC expression

The expression of MHC class I and II was analyzed to evaluate putative AG126 effects besides its influence on soluble factors. Both MHC class I and II are expressed on microglia and are essential for the antigen presentation to T cells. MHC class I is expressed on every nucleated cell. MHC class II is constitutively expressed on few cell types but can be induced on some cells, including the microglia, by various stimuli like IFNγ (Amaldi et al., 1989; Pazmany et al., 2000). The level of MHC expression itself is highly regulated. Including infectious agents, various factors have the potency to up-regulate MHC surface expression levels, also in microglia.

For this analysis microglia were preincubated with 100 µM AG126 for one hour and following treated with AG126 in combination with the TLR ligand Pam_3CSK_4, Poly(I:C), LPS or MALP. The microglia were stimulated for 48 h. Afterwards FcγR III/II were blocked and cells were labeled with the microglial marker isolectin(IL)B-4 and the respective α-MHC class I or II antibody. Histograms for the expression level of MHC structures are shown in Fig. 4.8. Here, an TLR-induced up-regulation of the MHC structures was very selective. Compared to the medium control, only TLR 3 and 4 stimulation resulted in an up-regulation of MHC class I. Yet, no pronounced AG126-effect was obvious. Only LPS-treated microglia in the presence of 100 µM AG126 showed a slight reduction of the MHC class I expression. There was no obvious effect on the low expression of MHC class I in unstimulated cells.

Consistent with the literature, there was no expression of MHC class II on the microglia. However, non of the TLR ligands had the potency to up-regulate MHC class II expression. We could confirm that IFNγ is able to induce MHC class II expression on microglia. As seen for MHC class I, AG126 had also no effect on the MHC class II expression/ induction. From these data we can conclude that AG126 does not affect the expression of MHC class I or II.

4.2.6. AG126 affects the myelin phagocytosis in TLR-stimulated microglia

To reveal AG126 effects on the myelin phagocytosis in TLR-stimulated microglia, cells were pretreated with 10 or 100 µM AG126 or received a medium change for one hour. Subsequently, cells were stimulated with agonists for TLR1-2 (Pam_3CSK_4, 10 ng/ml), TLR4 (LPS, 10 ng/ml) or TLR6-2 (MALP, 10 ng/ml) in the further presence or absence of 10 or 100 µM AG126 for 24 h. Afterwards, microglia were finally quantified by flow cytometry (FACS analysis).

Fig. 4.9 presents the intercorrelation among TLR stimulation of microglial cells in the presence or absence of AG126 and myelin phagocytosis. Broadly, TLR stimulation of microglia reduced the myelin phagocytosis, as compared to unstimulated cells, and the presence of AG126 rescued the myelin phagocytotic capacity (Fig. 4.9 *A*). Representative contour diagrams of the myelin load revealed two subpopulations in the unstimulated cells, a larger one loaded with a high

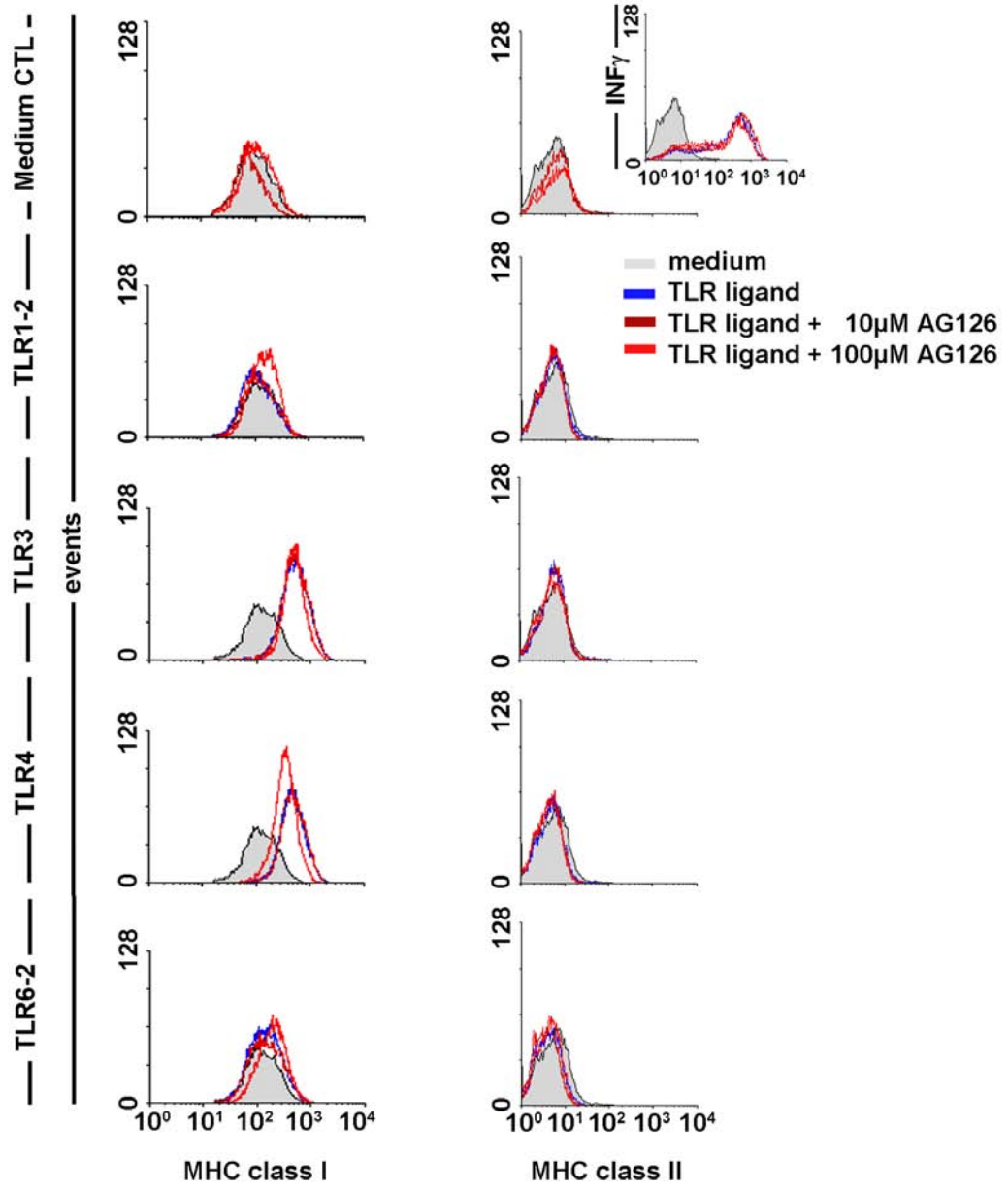

Figure 4.8.: AG126 does not affects the expression of MHC class I or MHC class II on microglial cells. Microglial cells were preincubated with 10 or 100 µM AG126 or received a media change for one hour. Subsequently, cells were stimulated with agonists for TLR1-2 (10 ng/ml Pam_3CSK_4,), TLR (50 µg/ml Poly(I:C)), TLR4 (10 ng/ml LPS), TLR6-2 (10 ng/ml MALP), IFNγ (10 ng/ml, positive CTL) with and without 10 or 100 µM of AG126 for 48 h. FcγR III/II blocked cells were labeled with FITC-ILB4 as a microglial marker and with APC-α-MHC antibodies. Samples were analyzed by FACS. Histograms for the expression level of MHC structures are shown. For each sample, 1×10^5 cells were taken into account. Representative of two independent experiments is shown.

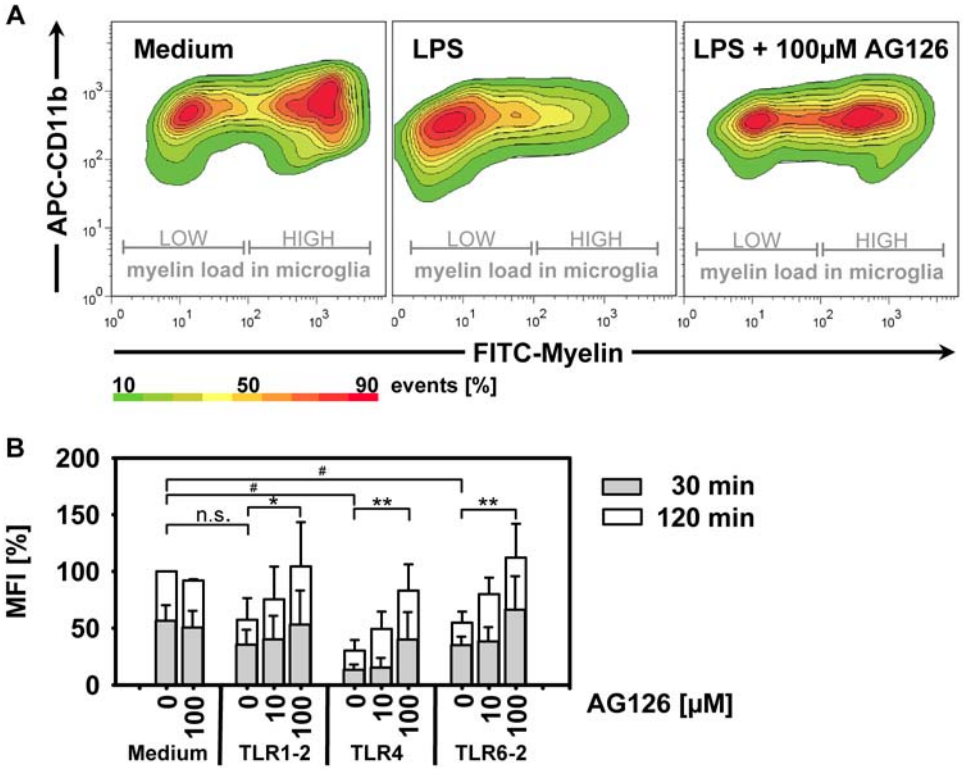

Figure 4.9.: AG126 affects the myelin phagocytosis in TLR-stimulated microglia. Microglial cells were preincubated with 10 or 100 µM AG126 or received a media change for one hour. Subsequently, cells were stimulated with agonists for TLR1-2 (10 ng/ml Pam_3CSK_4,), TLR4 (10 ng/ml LPS), TLR6-2 (10 ng/ml MALP) with and without 10 or 100 µM of AG126 for 24 h. Microglia were fed with FITC-mylin for 30 min or 120 min and labeled with APC-CD11b as microglial marker. Myelin load was determined by FACS analysis. ***A*** Contour blots are exemplarily shown for unstimulated, LPS and LPS + 100 µM exposed microglia after 120 min myelin phagocytosis. 15×10^3 cells were taken into account. Color code represent intensity of events. ***B*** Mean fluorescents intensity (MFI) was normalized to unstimulated medium control (120 min myelin exposure). Data are mean ± SEM, ***A*** n = 2 summarized from two independent experiments. Paired t-test was performed between medium to TLR stimulation (#) and AG126 effects normalized to respective TLR-stimulated control (*); #,* $p < 0.05$; ** $p < 0.01$; n.s. not significant.

amount of myelin and a second with considerably less myelin, with both being clearly separated. In the LPS-stimulated microglia, just one large population free — or nearly free — of myelin was detectable, and only a few cells revealed a higher myelin load. In contrast, the LPS-stimulated cells also treated with AG126 (100 µM) appeared as two subpopulations as well, as similarly seen with untreated cells. In comparison to these controls, more cells occurred in the 'transition state' between the segregated populations.

A quantitative analysis of the myelin load depending on the cell treatment is shown in Fig. 4.9 *B*. The mean fluorescence intensities (MFI)'s were normalized to unstimulated cells as analyzed at 120 min and then compared among the various treatments and time periods. Within 30 min of myelin exposure, the resulting myelin loads already revealed the impact of TLR stimulation, especially for TLR4. At the 120 min time point, TLR4- and TLR6-2-treated cells presented with significantly lower myelin uptake, while cells under the TLR1-2 agonist revealed at least a similar tendency.

TLR-stimulated cells exposed to myelin for 30 min in the presence of 10 µM of AG126 showed no differences in the myelin load as compared to the cells treated with TLR agonists only. However, at 120 min, they revealed increased intracellular myelin levels. This rescuing effect was most obvious for the TLR6-2-stimulated cells, whereas the higher AG126 dose then also resulted in a clear increase in the TLR1-2- and TLR4-stimulated cells. Throughout the TLR's, 100 µM of AG126 re-established myelin loads comparable to unstimulated cells.

Of course, the incorporated amounts of myelin at a given time point represent a snap-shot of a steady-state based on uptake and degradation, rather than a simple accumulation (van Rossum et al., 2008). The measurement also relies on the fluorescent signal which is affected by the pH of the phago/lysosomal compartments and a potential physico/chemical breakdown. The subcellular conditions may apply similarly to myelin in the differently treated cells, while the TLR activation may not only affect the incorporation but also the degradation rates. Yet from previous experiments we rather suggest an impact on the uptake. Overall, AG126 had a regulatory effect on myelin phagocytosis in TLR-stimulated microglia. Here, it can reverse the repressed myelin load or loading capacity back to the level of unstimulated cells. From these data, it can also deduce that AG126 effects are not restricted to the modulation of soluble immunoregulatory factors as described in section 4.2.2.

4.2.7. AG126 has only minor effects on NFκB and MAPK activation

In the following experiments, we wanted to obtain more information about the hierarchical localization of the AG126-sensitive target(s) as they would be affected in the TLR-stimulated microglia. Therefore, the activation of downstream located MAPK's and NFκB was analyzed following challenges with the TLR agonists, assuming a consequence (*e.g.* drop) for the activity for the respective pathways under AG126 (Fig. 1.1).

First, we addressed the activation of the NFκB transcription factor system based on the detection of a translocation of the NFκB subunit p65 to the nucleus (Fig. 4.10 *A*). For the

JNK activation, the protein phosphorylation state was determined by immunoblot (Western blot) analysis (Fig. 4.10 *B*). Total JNK protein amounts were detected as well to ensure equal sample loading. The state of the p38α^{MAPK} (Thr180/Tyr182) and ERK1/2 (p44/42$^{\mathrm{MAPK}}$, Thr202/Tyr204) phosphorylation — indicating activation — was determined quantitatively by ELISA, and such an analysis was also carried for the NFκB subunit p65 (Ser536), in addition to the translocation assay (Fig. 4.10 *C* to *E*), since this system conveys a large part of the MyD88- and TRIF-organized consequences upon TLR activation. Here, equal protein load in the assays was revealed by parallel immunoblot analysis (Western blot) for GAPDH.

As to the NFκB system, treatment of cells with LPS (for TLR4 stimulation) and MALP (for TLR6-2) clearly caused a translocation of the p65 subunit to the nucleus within 30 min. However, the presence of AG126 during the stimulation did not have an obvious effect (Fig. 4.10 *A*). For a quantification of the p65 phosphorylation, we performed a more detailed time course study (Fig. 4.10 *C*). Microglia were pretreated with 50 µM of AG126 or received just a medium change for one hour (for TLR activation in the absence of AG126). Subsequently, cells were stimulated with Pam_3CSK_4 (TLR1-2), Poly(I:C) (mainly TLR3), LPS or MALP for 5, 15, 30, 60 and 240 min. Afterwards, cellular lysates were prepared, cleared and analyzed. The Pam_3CSK_4 and Poly(I:C) treatments revealed only a slight increase in p65 phosphorylation, as being most obvious after 30 min incubation. In contrast, LPS and MALP2 stimulations led to a pronounce activation already after 5 min, with a further increase at 15 min in the case of a TLR4 activation. As of 30 min (TLR4) or already 15 min (TLR6-2), phosphorylation levels decreased — yet not reaching baseline levels within 240 min. Some AG126 effect was only detectable in the TLR4-stimulated cells. Here, the early phosphorylation at 5 min was lower, but for all other time points and throughout the TLR's, no impact of AG126 was noticed.

Focusing on a phosphorylation of p38$^{\mathrm{MAPK}}$ and ERK1/2, the time courses of responses revealed a similar pattern (Fig. 4.10 *D* and *E*). There was a slight to moderate increase in the phosphorylation states for TLR1-2 at 30 min, which rapidly run down thereafter. TLR3 stimulation gave only (very) weak activation signals, in the case of ERK1/2 even with some delay. Again in contrast, TLR4 and TLR6-2 challenges resulted in massive phosphorylation enhancements as of 5 to 15 min, with a lasting elevation especially under TLR4 control up to 30 min. Subsequently, phosphorylation intensities declined again, reaching for both MAPK types and both TLR's almost baseline level. Importantly, no pronounced AG126 affect was found for any of the TLR's at any time point of stimulation.

The analysis of TLR-induced JNK phosphorylation was based on Western blots (Fig. 4.10 *B*, in collaboration with Prof. Thomas Herdegen, Kiel, see also Materials and Methods). It considered the splicing variants of 46 kDa and 54 kDa in a comparison to the total amount of JNK protein. Under control conditions (unstimulated cells), phosphorylated JNK forms were nearly undetectable. Only some, yet very weak, signals could be seen in some control preparations under AG126, suggesting a certain impact on the basal activation status. A TLR1-2 stimulation provoked JNK phosphorylation between 5 and 30 min, which thereafter declined again. Interestingly, cells stimulated under AG126 revealed some delay in the JNK phosphorylation wave. The

54 kDa form was thereby well detectable, whereas the 46 kDa variant bands were rather weak. Total JNK protein amounts were approximately the same in all samples. TLR6-2-stimulated microglia showed sharp phosphorylation increases at 15 and 30 min. Here again, as for TLR1-2, AG126 shifted the JNK activation in time. AG126 thus delayed the TLRX-2-induced JNK activations — yet without reducing their intensity.

Poly(I:C) induced a strong phosphorylation at 15 min, which was already visible at 5 min and still obvious at 30 min. Here, both JNK versions, and especially the 46 kDa splicing variant, gave a signal. In the AG126 treated cells, the 15 min phosphorylation of the 46 kDa form was apparently weaker, but a global impact could not be determined. Interestingly, some late signal seen for both JNK forms under Poly(I:C) alone did not appear in the AG126 presence (compare the 240 min time points).

The blots from the LPS-stimulated cells showed strong phosphorylation intensities at 15 and 30 min, with a sharp increase and decline. AG126 did not show any obvious effect on this pattern. As in the case of Poly(I:C), the LPS treatment led to pronounced activation not only of the 54 kDa form, but also to the 46 kDa variant. Even though Poly(I:C) effects are not exclusively restricted to TLR3, it would activate the TRIF pathway, as LPS would do *via* TLR4. Comparing the phosphorylation patterns of TLR1-2 and TLR6-2 to those of TLR3 and TLR4, one may suggest that a stronger involvement of the 46 kDa JNK depends on TRIF.

It should be stressed that immunoblot analysis have less quantitative information than the ELISA studies. Moreover, even though equal amounts of total cell protein were loaded on the SDS-PAGE lanes, based on a reliable protein assay, immunostaining of the total JNK protein resulted occasionally in unequal band intensities. Such a phenomenon may relate to the complex activation patterns of individual JNK isoforms, including not only their selective phosphorylation, but also individual translocation events and scaffold incorporation, as we had previously shown (Waetzig et al., 2005). Yet the most relevant samples, *e.g.* those with effects on the phosphorylation, were not affected and thus allowed for an evaluation of the AG126 influence.

Overall, the analyses of the MAPK's and the NFκB system rendered unlikely that the AG126-sensitive target massively controls these signaling elements. On the other hand, the set of cy-

Figure 4.10. *(following page)*: AG126 does not affect the activation of NFκB, p38α^{MAPK}, ERK1/2 or JNK. Microglia cells were preincubated with 100 μM AG126 or received just a medium change for one hour. Cells were stimulated for various time periods with the respective TLR ligands, TLR1-2 (10 ng/ml Pam_3CSK_4), TLR3 (50 μg/ml Poly(I:C)), TLR4 (10 ng/ml LPS) or TLR6-2 (10 ng/ml MALP) alone or in combination with 50 μM AG126. ***A*** The activation of p65 NFκB was detected after 30 min of TLR stimulation by immunostaining. Translocation of p65 NFκB to the nucleus is shown by a red signal, with nuclei stained in blue (DAPI) and microglia in green (ILB_4-FITC). For ***B*** to ***E***, clear cellular lysates were prepared. ***B*** Phosphorylated and total JNK proteins were detected by Western blot analysis. The JNK analysis was performed twice. A representative set of blots is shown. In ***C*** to ***E***, phosporylated p65 NFκB (Ser536, ***C***), p38$^{\mathrm{MAPK}}$ (Thr180/Tyr182, ***D***) and ERK1/2 (Thr202/Tyr204, ***E***) were detected by specific ELISA. Total protein amounts were analyzed by the BCA method and equal loading of the samples was confirmed by Western blot analysis of GAPDH. Data are given as mean ± SEM, n = 3 as summarized from two independent experiments.

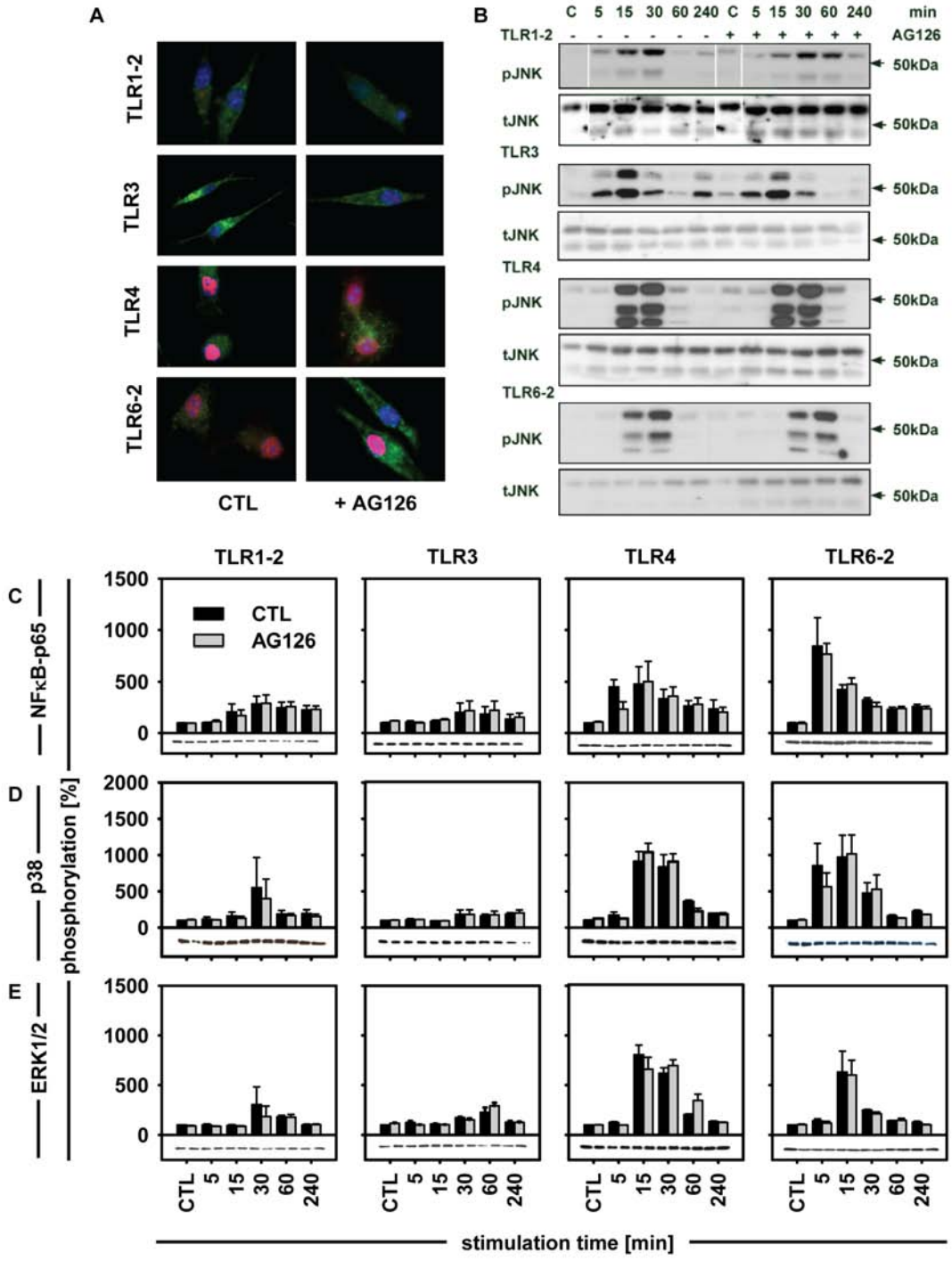
A
TLR1-2
TLR3
TLR4
TLR6-2
CTL
+ AG126
B
C 5 15 30 60 240 C 5 15 30 60 240 min
TLR1-2 - - - - - - + + + + + + AG126
pJNK
tJNK
TLR3
TLR4
TLR6-2
50kDa
C
D
E
NFκB-p65
p38
ERK1/2
phosphorylation [%]
TLR1-2
TLR3
TLR4
TLR6-2
CTL
AG126
1500
1000
500
0
2000
CTL 5 15 30 60 240
stimulation time [min]

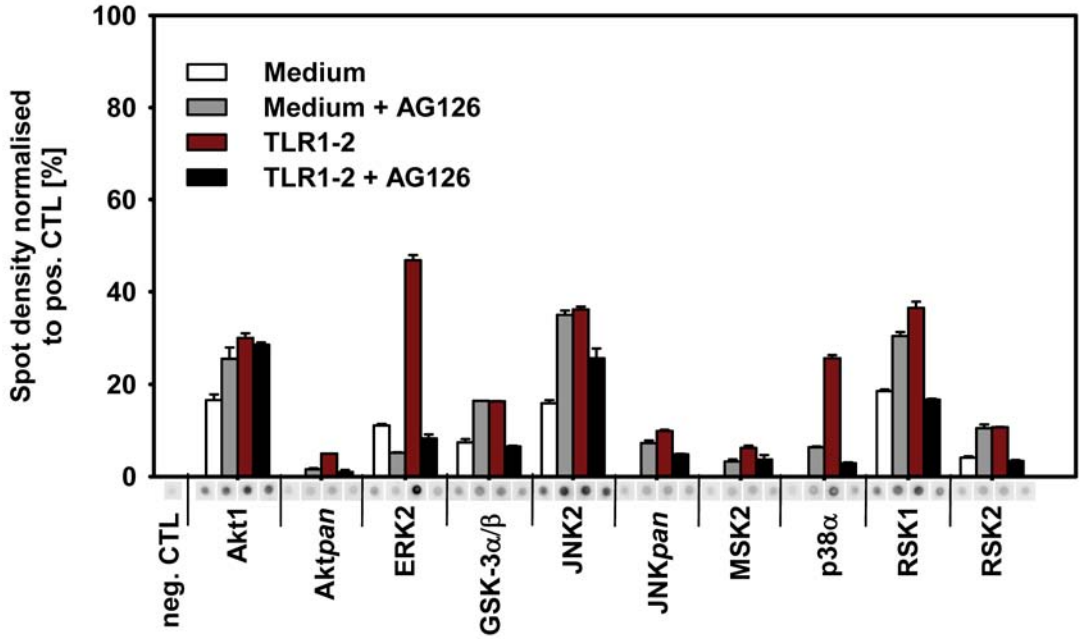

Figure 4.11.: AG126 treatment affects the phosphorylation of MAPK activated by TLR1-2 stimulation in microglia. Microglia cells $3x10^6$ were preincubated with 100 μM of AG126 or received a medium change for one hour. Subsequently, cells were either TLR1-2-stimulated (Pam_3CSK_4, 10 ng/ml) for 15 min with or without AG126 (100 μM) or just incubated with medium in the presence or absence of AG126. Cell lysates were prepared and subjected to a phospho-MAPK array according to the instructions of the manufacturer (for details see section 3.12 in the Material and Methods). The graph represents data for proteins which gave a (phosphorylation) signal higher than the negative control. Each spot intensity was determined and normalized to controls placed on each array to guarantee comparisons (100 %). Representative spots for each kinase are shown under the respective bars. No induction by TLR1-2 stimulation was obtained for Akt2, Akt3, Erk1, GSK-3β, JNK1, p38δ and p38γ. Importantly, this human protein array has been confirmed by the manufacturer to be applicable to mouse material as far as regarding the selected kinases as shown here. No or insufficient antibody cross-reactivity between the species resulted in the exclusion of JNK3, GSK-3α/β, p38β and HSP27. Data are mean ± SEM, n = 2.

tokines and chemokines affected by AG126 pointed to an interference with the MyD88-organized consequences. Thus, AG126 may either target the signaling flow just downstream of the MAPK's and NFκB p65 or alter the activity of molecular MAPK species as not properly covered by the above phosphorylation assays — or AG126 effects localize to a signaling element which is itself not inserted into the TLR ⟶ MyD88 ⟶ NFκB/MAPK chains of command and influences the TLR-controlled gene pattern independently of their successful signaling throughput. To further narrow down on these alternatives, a small phospho-protein array was performed.

Indeed, the phospho-MAPK array performed on microglia upon a 15 min stimulation with Pam_3CSK_4 indicated AG126 effects on MAPK subtypes and on certain kinases located downstream (Fig. 4.11). The TLR1-2 stimulation was chosen in order to focus on MyD88-dependent outcomes, while the stimulation period was selected as a compromise, based on the patterns obtained in Fig. 4.10. Interestingly, AG126 affected some kinase activities in the otherwise unstimulated microglia. For example, JNK2 showed some phosphorylation signal under basal conditions, which got apparently enhanced by the presence of AG126, the effect resembling the findings of Fig. 4.10 *B*. Also some additional proteins, which came already with a basal phosphorylation signal, revealed an increase upon AG126 exposure, such as Akt1, GSK-1α/β, RSK1 and RSK2. On the other hand, several kinases covered by the array did not reveal an activation upon TLR stimulation and were thus eliminated from a further consideration, such as Akt2, Akt3, Erk1, GSK-3β, JNK1, p38δ or p38γ.

Upon TLR1-2 agonist application, a pronounced phosphorylation was detectable for Akt1, Akt*pan* (covering all versions), ERK2, GSK-3α/β, JNK2, MSK2, $p38\alpha^{MAPK}$, RSK1 and RSK2 (Fig. 4.11). In most cases, AG126 had a slight or even pronounced repressive effect on the TLR1-2-activated phosphorylation, which reached for ERK2 a reduction by 80 %. It is important to state that stronger or weaker signals from the array spot as regarding individual kinases do not indicate the quantitative importance as the antibody-based detection cascade cannot allow for comparisons between kinase antigens. Indeed, this would require some reference to a standard curve each. Comparisons are only possible between treatments as they affect the phosphorylation state of a given kinase. Moreover, the effect obtained for a MAPK subtype in the array may not be reflected by the ELISA when the latter cannot truly differentiate between isoforms. The individual contributions of isoforms to the total signal in an assay may additionally be nonproportional. In other words, effects on a subtype could be easily overlooked in a more *pan*-specific detection system. This is important when taking the data for JNK(2), ERK2 and p38α into consideration. Actually, each MAPK family came with tendencies for AG126 effects in the studies of Fig. 4.10 (see the TLR1-2 groups with and without AG126).

It is thus the more interesting that RSK1 and MSK were apparently regulated in AG126 presence, even though in a complex fashion. ERK1/2 as well as $p38^{MAPK}$ can activate RSKs and MSKs (Anjum and Blenis, 2008; Zaru et al., 2007) RSK, in turn can activate GSK. From all of these data, we can see, that all the mentioned participants are AG126 may affect the TLR-stimulated signaling — yet not with global impacts on a major MAPK family. The AG126-sensitive target could be located upstream of the MAPK level as individual subtypes appeared

to be affected. Moreover, the respective PTK — or 'target' — seems to be also constitutively active, based on the AG126 effects on otherwise non-stimulated cells. Indeed, we had shown such a phenomenon already in our work on the calcium regulation in microglia (Kann et al., 2004). After all, AG126 influences the TLR signaling in the MyD88 environment by some more subtle mechanism.

4.3. BTK as a putative target for AG126

In the former sections, we had analyzed the AG126 effect on the cellular responses of TLR-stimulated microglia. AG126 affected the cytokine and chemokine release predominantly by repression, when applied at higher concentrations. Furthermore, the knockout experiments indicated that AG126 would not affect the TRIF-dependent pathway, but rather influence the consequences of MyD88 signaling. Assuming that AG126 is PTK inhibitor, its target would need to meet some key features as deduced from our previous and present data as well as the literature. The PTK should

- be involved in TLR signaling,
- be associated with MyD88-dependent signaling (in some way at some level),
- be localized in a chain of command above MAPK activation,
- be constitutively expressed as well as active and
- be involved in a regulation of calcium upon challenges and under basal conditions.

Based on the reported features, we considered the Bruton's tyrosine kinase (BTK) as one of the likely candidates (Kann et al., 2004) as it would fulfil the required criteria. In particular, the BTK (i) is involved in TLR signaling (Jefferies et al., 2003) in (ii) a MyD88-associated fashion as shown for TLR4 and TLR2 signaling (Gray et al., 2006) and plays a role in calcium signaling, as documented for the B cell receptor (BCR) and its signaling cascade (Takata and Kurosaki, 1996; Genevier and Callard, 1997; Fluckiger et al., 1998). From this work, it could be assumed that the BTK is also constitutively expressed .

4.3.1. Classical BTK-Inhibitor *vs.* AG126 - microglial responses differ

If AG126 affects the activity of BTK with the consequence of modulating the TLR-stimulated cyto- and chemokine production in microglia, one would expect a similar effect for the known BTK inhibitor, LFM-A13. The compound was specifically designed as an anti-leukemic agent with apoptosis-promoting and chemosensitizing properties mediated through BTK inhibition (Mahajan et al., 1999). Therefore, TLR1-2-, 4- and 6-2-stimulated microglia were treated for 18 h with LFM-A13 and AG126 at various concentrations. Supernatants were analyzed for TNFα and KC (Fig. 4.12).

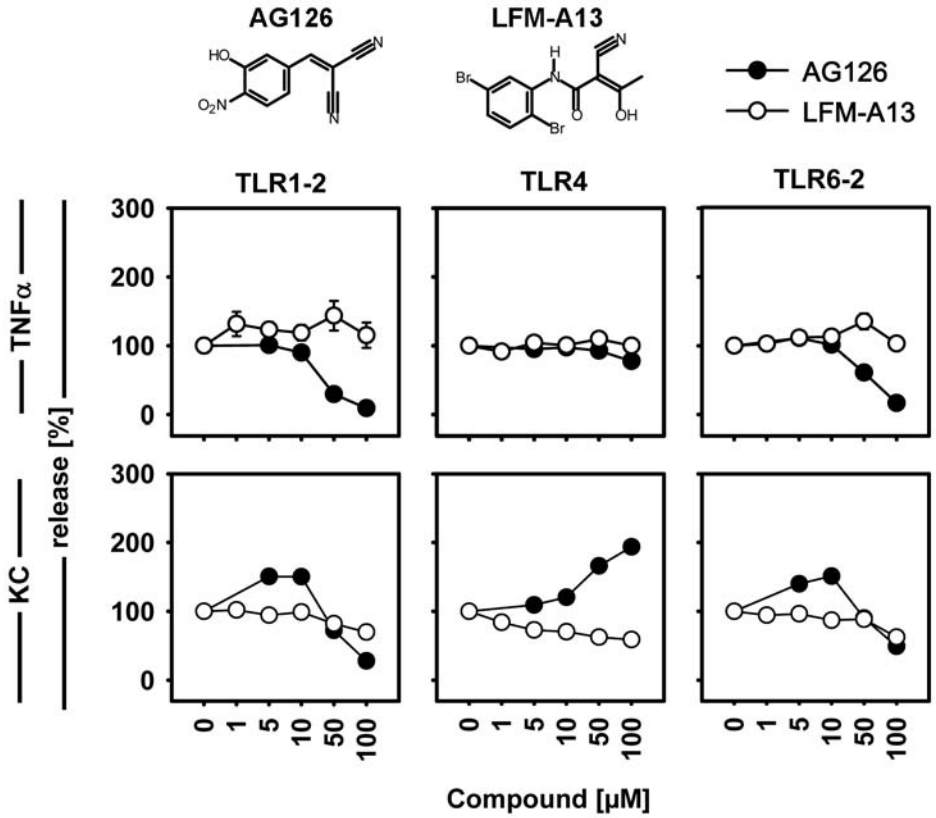

Figure 4.12.: AG126 and LFM-A13 have divergent effects on TLR-stimulated microglia cells. Microglia were preincubated with 1 to 100 µM of AG126 or LFM-A13 as indicated or received a medium change only for one hour. Subsequently, TLR1-2- (Pam_3CSK_4, 10 ng/ml), TLR4- (LPS, 10 ng/ml) or TLR6-2-treated (MALP, 10 ng/ml) or unstimulated microglia were incubated for another 18 h with or without 1 to 100 µM of AG126 or LFM-A13. TNFα and KC release were measured in the supernatants. Data are mean ± SEM with n = 12 as summarized from two independent experiments.

A comparison of the dose-response relations revealed, however, marked differences. While AG126 can repress the TLRX-2-stimulated TNFα release almost completely at highest concentration, LFM-A13 had no obvious effect. For the TLR4-activated cells, both response curves were similar (compare also to Fig. 4.5). Focusing on KC release, LFM-A13 had a mild but dose-dependent inhibitory effect, with up to about 30 % of inhibition at the highest dose. AG126 showed instead biphasic curves in TLR1-2- and TLR6-2-activated cells, and even an up-regulated KC release in TLR4-stimulated cells (as already described in section 4.2.2, see Fig. 4.5). Overall, presence of LFM-A13 and AG126 during TLR stimulations came with different consequences for TNFα and KC. Thus, if LFM-A13 is taken as a specific inhibitor of BTK, the AG126-caused influence on this microglia response cannot be simply explained by an interference with BTK. AG126 may either not affect this PTK or have additional targets.

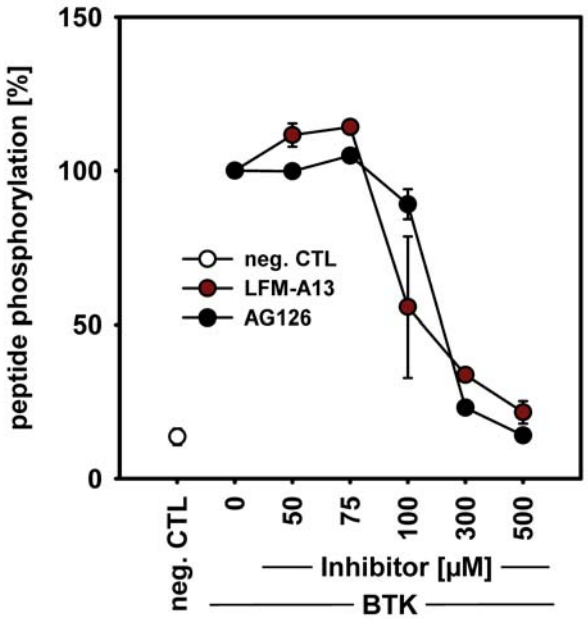

Figure 4.13.: LFM-A13 and AG126 directly inhibit recombinant human BTK activity. Random peptides containing tyrosine motives were coated on a 96-well plate. The addition of 50 ng/ml recombinant human BTK in the presence of ATP allowed for the phosphorlyation of the tyrosine residues. Inhibitory effects on the BTK were analyzed by the addition of LFM-A13 and AG126 at concentrations from 50 to 500 µM as indicated. The amount of phosphorylation was analyzed by a phospho-tyrosine-specific antibody labeled with HRP for catalyzing the conversion of a chromogenic substrate (see Materials and Methods, section 3.14, for details). Data are mean ± SEM with n = 4 as summarized from two independent experiments.

4.3.2. AG126 inhibits the phosphorylation activity of recombinant BTK

To either confirm or exclude a potential effect of AG126 on BTK, a PTK activity assay was performed. Peptides of random sequence containing tyrosine motives were phosphorylated *in vitro* by a recombinant, constitutively active human BTK (in the presence of ATP, over 30 min). The reaction was performed in the absence or the presence of 50 to 500 µM of LFM-A13 or AG126.

From the graph in Fig. 4.13, and as expected, it is obvious that LFM-A13 can inhibit the phosphorylation capacity of BTK at concentrations of 100 µM. The highest concentration tested here reduced the phospho-Tyr signal by more than 75 %. Most importantly, we could show for the first time directly that AG126 was also able to inhibit the kinase activity of BTK, even though less potent than LFM-A13 when applied at 100 µM. However, at concentrations as of 300 µM, AG126 was a effective as the established inhibitor. Thus, AG126 proved to be a BTK inhibitor. The different cellular actions of AG126 and LFM-A13 may thus result from BTK-independent effects.

4.3.3. Detection of BTK in microglia is challenging

We were then interested in analyzing the activation of BTK upon TLR signaling in microglia. According to Gray et al. (2006), BTK phosphorylates the MyD88 adapter-like protein (MAL), localized very proximal to TLR's. MAL actually mediates the contact of, for example, TLR4 to MyD88. We tested the activation of MAL by Western blot analysis. However, no clear data were obtained, most likely due to a failure of the respective antibody in revealing the low abundant protein in our cells (data not shown). Therefore, we decided to analyze some BTK-relevant and — indicating effects of AG126 in another cellular system, *i.e.* a human B cell line, which has been studied already and which would thus serve as a suitable model.

4.3.4. BTK in B cells: AG126 represses its target phosphorylation, the PLCγ

To confirm the repressive effect of AG126 on BTK we analyzed the activation of its known target in B cell receptor (BCR) signaling, PLCγ2. Ligand binding to the BCR leads to the activation of non-receptor kinases (such as PTKs) and the phosphorylation of residues within the intracellular BCR sequence, namely the immunoreceptor tyrosine-based activation motifs (ITAMs). This allows for the cytoplasmic Src family kinase Syk to bind to the ITAMs and its activation. Subsequently, the BTK is phosphorylated by the Src kinases Lyn or/and Syk. Afterwards, BTK is recruited to the plasma membrane. Binding of the scaffold protein SLP-65 to the BTK provides a docking site for downstream BTK targets, including PLCγ2. Activated PLCγ2 is known to be involved in the mobilization of calcium *via* IP_3 and diacylglycerol (DAG), and thus leading to an increase in $[Ca^{2+}]_i$ (as reviewed in more detail by Brunner et al., 2005).

For the experimental analysis, the starved cells of the mouse B cell line K46 positive for IgG were preincubated in with 50 µM of AG126 or LFM-A13 for one hour. Cells were stimulated with a Fab fragment specific for the BCR for 1 or 3 min in the presence or absence of AG126 or LFM-A13. Cleared lysates were prepared and Western blot analysis was performed. The phosphorylated form of PLCγ2 (Y759), PLCγ2 as load control and total tyrosine phosphorylation were detected (Fig. 4.14 *A*). It can be seen that the stimulation of the BCR leads to a fast upregulation of PLCγ2 phosphorylation within 1 min, yet there is also a basal activation detectable in the BCR-unstimulated cells. Differences in the phosphorylation of PLCγ2 after 1 or 3 min were only minor. Focusing on the effects of AG126 and LFM-A13, none of these compounds could repress the activation of PLCγ2. In the blot showing the total tyrosine phosphorylation pattern, LFM-A13 just caused a reduced phosphorylation of an unknown protein after 1 min of BCR stimulation. Overall, in this mouse cell line, AG126 failed to inhibit the PLCγ2 activation, and so did the known BTK inhibitor LFM-A13. This indicated that BTK is probably not accessible for these compounds in the mouse BCR complex or that species differences in the BTK binding region itself would exist. Therefore, a human B cell line was employed, because the inhibitory AG126 effect was actually demonstrated for the human recombinant BTK (see

previous section 4.3.2).

Ramos cells, a human B cell line positive for IgM, were stimulated with AG126 and LFM-A13 as done for the mouse counterparts. Additionally, a higher dose of 300 µM AG126 and LFM- A13 was applied, as revealing the repression of the BTK activity in this dose range in the phosphorylation array (compare Fig. 4.13). Again, a stimulation of the BCR led to a pronounced phosphoryation of PLCγ2 (Fig. 4.14 *B*). In comparison to the activation of the mouse cells, the basal phosphorlyation of PLCγ2 seemed to be much lower. The application of AG126 and LFM-A13 revealed a dose-dependent suppression of PLCγ2 phosphorylation. While LFM-A13 was more potent than AG126 at 50 µM, at the concentration of 300 µM the differences in the inhibitory potential between both compounds disappeared. Furthermore, both substances did not influence the basal PLCγ2 phosphorylation, as seen in the unstimulated cells.

We could thus show that AG126 can repress PLCγ2 phosphorylation, as a surrogate for the inhibition of BTK. In this cellular system, AG126 proved nearly as potent as LFM-A13. Therefore, BTK remained a relevant candidate for AG126-based actions. Yet some species differences may occur by variations in the arrangement of the signaling complex, knowing that the BTK is involved in a complex protein ensemble in the case of the BCR — and probably also in the still less understood arrangements of plasma membrane TLR's. Sterical hindrance may there also result in a species-dependent accessibility for inhibitors.

However, these data could, on the other hand, not explain all the effects on the cyto- and chemokine release. Low doses of AG126 were already able to modulate the release activity, which could neither be confirmed by the direct inhibition of BTK activity (Fig. 4.13) not by the functional experiments on cells (Fig. 4.14). Therefrom the question arose whether AG126 may affect the microglial release activity by additional modes of action, independent of BTK.

4.4. Alternative mechanisms of AG126 action

Even though the tyrphostins were originally designed as tyrosine kinase inhibitors Levitzki (1992), henceforward, several PTK-independent tyrphostin effects could be revealed. The AG18, for example, was described to be a mitochondrial uncoupler, in addition to inhibitory functions on epidermal growth factor receptor autophosphorylation (Soltoff, 2004). An antioxidative effect could be shown for AG490, while it also caused Janus kinase 2 inhibition (Gorina et al., 2007). According to the chemical structure, AG126 may not act as antioxidant as AG18 does, since it lacks a quinone-like body. On the other hand, an antioxidant feature cannot be completely ruled out yet when considering a chemical or enzymatically catalyzed conversion in a cell. Several alternative mechanisms could play a role when considering data from other tyrphostins or when keeping in mind the indispensible relatedness to tyrosine (see Fig. 2.1). To systematically test such alternatives, it was tested if AG126 was considered to act as a mitochondrial decoupler. Furthermore, potential agonistic functions of AG126 were studied, especially for receptors and pathways which were already shown to cause a repression of TLR-activated pro-inflammatory

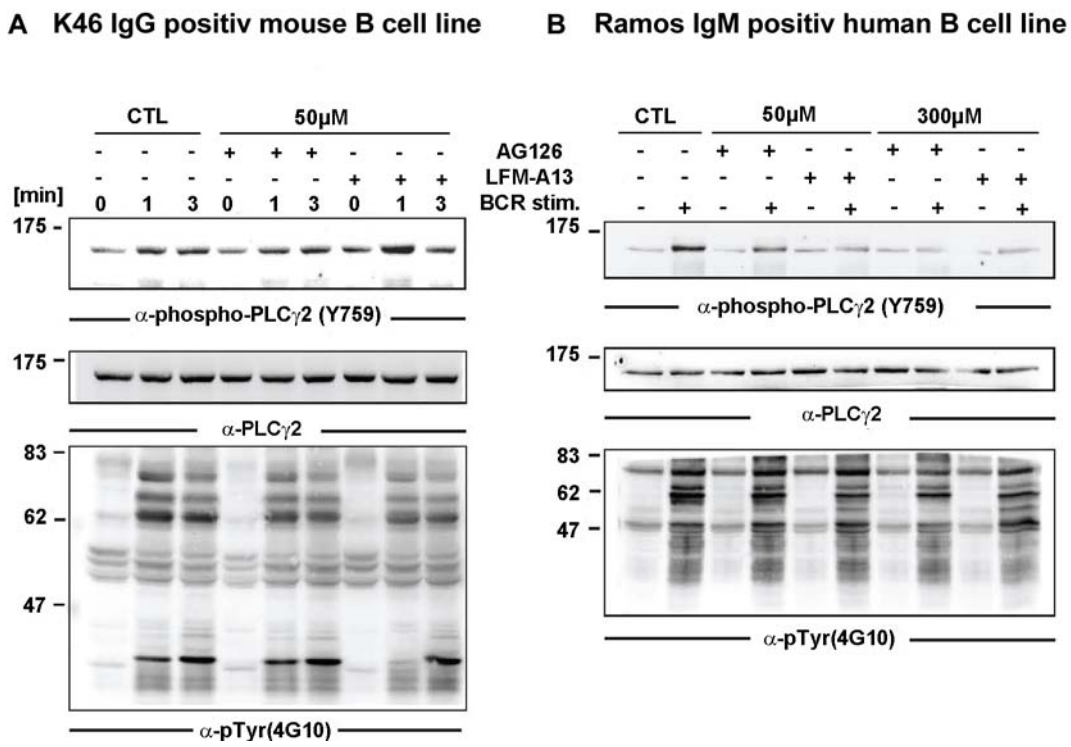

Figure 4.14.: AG126 and LFM-A13 can inhibit the PLCγ2 activation in human but not mouse B cells. ***A*** K46 cells and ***B*** Ramos cells were incubated in RPMI 1640 without FCS for one hour at 37°C with or without AG126 or the BTK inhibitor, LFM-A13. Afterwards, K46 cells were stimulated with α-mouse-IgG for 1 or 3 min. ***B*** Ramos cells were stimulated with α-human IgM for 1 min. Cells were lysed in lysis buffer. Cleared cellular lysates were processed by SDS-PAGE, blotted on membrane and probed with an α-phospho-PLCγ2 (Y759). Subsequently, blots were stripped, cut and probed for with an α-PLCγ2 and an α-phospho-tyrosine (G410). Representative blots of two independent experiments are shown.

response in microglia.

4.4.1. AG126 does not reveal decoupling activities in microglia

Besides AG10 and AG18, tyrphostin A9, also known as SF6847, acts as an uncoupler of the oxidative phosphorylation and the respiratory chain in mitochondria (Soltoff, 2004; Terada, 1990). To test for AG126 having also uncoupling properties, microglia were preincubated with 10 or 100 µM of AG126. Subsequently, microglia were stimulated with ligands for TLR1-2-, 4- and 6-2 in the further presence of AG126 for 18 h. Cells were then stained with JC-1, a fluorescent probe, to assess the mitochondrial $\Delta\psi$ as previously described (Salvioli et al., 1997). The $\Delta\psi$ was analyzed by a ratiometric measurement of green and red fluorescence. In intact cells with a normal mitochondrial membrane potential, red JC-1 'aggregates' occur in the organelles, while some 'diffuse' green JC-1 monomers can be found in the cytosol. The ratio was normalized to the respective control cells which were TLR-activated without AG126 treatment. As a positive control, cells were treated with the antibiotic valinomycin, which induces disruption of the mitochondrial membrane potential within 20 min and thereby a reduction of the red signal. Fig. 4.15 *A* gives an overview of the ratiometric analysis of the JC-1-based measurement and the panel in *B* shows representative pictures of the cellular staining. Valinomycin exposure strongly reduced the membrane potential, as indicated by a down-regulation of the red/green ratio to 50 %. In contrast, AG126-treated cells did not show signs of a $\Delta\psi$ reduction, in comparison to the controls. Just a slight reduction in the ratio was obvious for unstimulated cells treated with 100 µM of AG126. The effect of valinomycin was also obvious when microscopically examining the staining by JC-1 (see Fig. 4.15 *B* for some examples). A loss of the red JC-1 aggregate signal was induced in the otherwise untreated controls as well as in cells stimulated with TLR agonists. On the contrary, AG126 treatment did not affect the fluorescent signal at any concentration or in any combination with the TLR agonists. We concluded that AG126 would not affect the mitochondrial membrane potential in microglial cells.

4.4.2. AG126 has no agonistic functions for adrenergic receptors

Like tyrphostins, adrenalin and noradrenalin (NA) are derivatives of tyrosine. Both are very well known for their physiological actions on the autonomous nervous system, while NA is also a neurotransmitter in one of the diffuse modulatory systems of the CNS. Both mediate their cellular effects through adrenergic receptors. It has been shown for peripheral innate immune cells, such as macrophages, that adrenergic stimulation causes some suppressive influence on their pro-inflammatory functions — a feature that can be similarly shown for the microglia. As shown in Fig. 4.16, NA attenuated the cyto/chemokine induction as triggered by several TLR agonists. Microglia were stimulated with Pam_3CSK_4, LPS or MALP2 in the presence of NA for 18 h. Cyto- and chemokines were measured in the culture supernatant and compared to the release of cells TLR-stimulated without NA presence. Basically, AG126 and NA had a similar

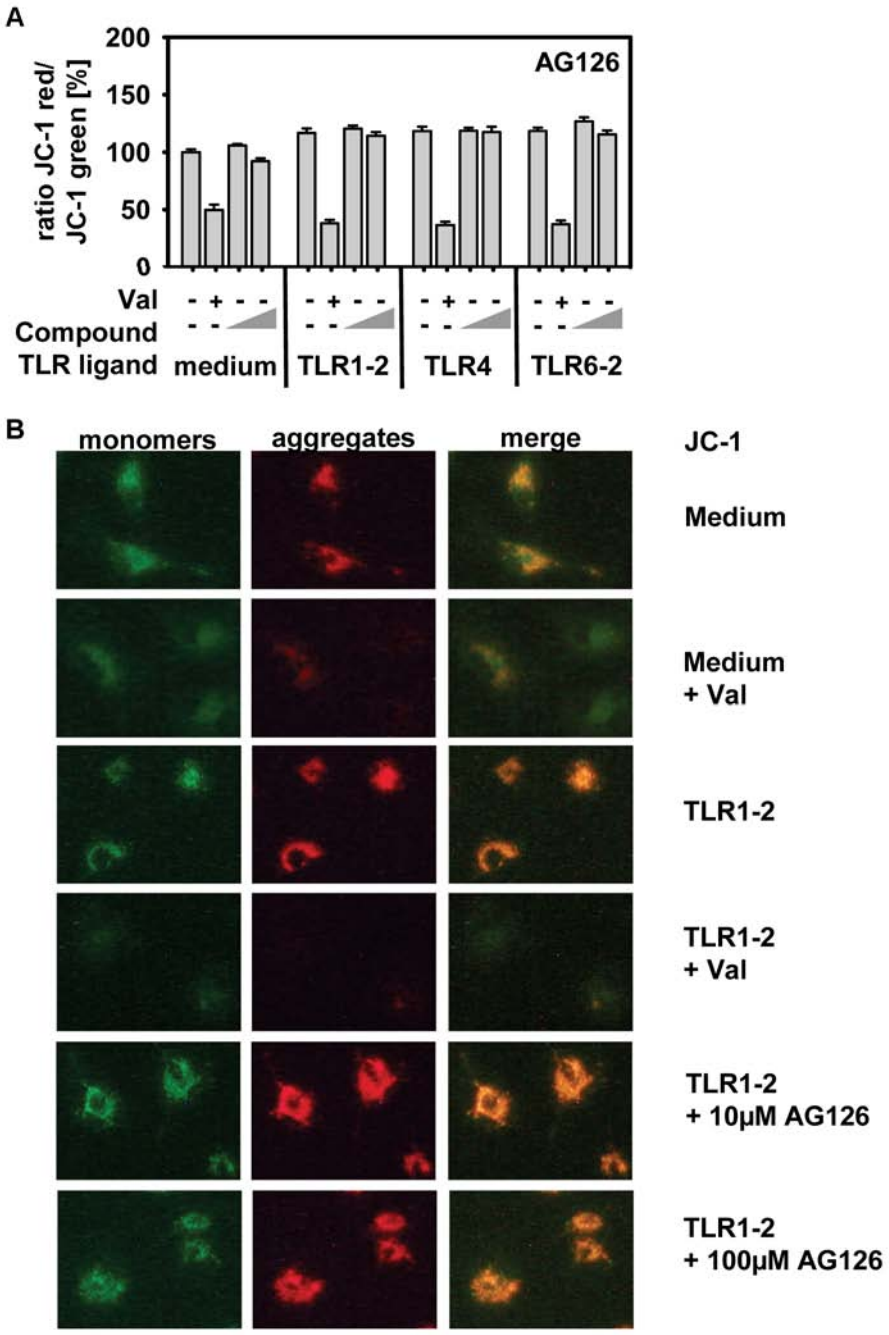

Figure 4.15.: AG126 does not affect the membrane potential of microglial mitochondia. Microglia cells were preincubated with 100 µM of AG126 or received just a medium change for one hour. Subsequently, microglia were incubated with TLR ligands as indicated for 18 h without or with 100 µM of AG126 (see Material and Methods). Cells were stained with JC-1 according to the manufactures instructions (see section 3.19). Some cell cultures were treated with valinomycin for 20 min as a positive control for an impairment of the membrane potential. ***A*** The fluorescence intensity of green stained JC-1 monomers and red stained JC-1 aggregates was measured and the ratio was calculated. Data are mean ± SEM, with $n > 12$ as summarized from two independent experiments. ***B*** Representative micrographs of JC-1-stained microglia (20x magnification). Also cells treated with valinomycin under a TLR stimulation are shown.

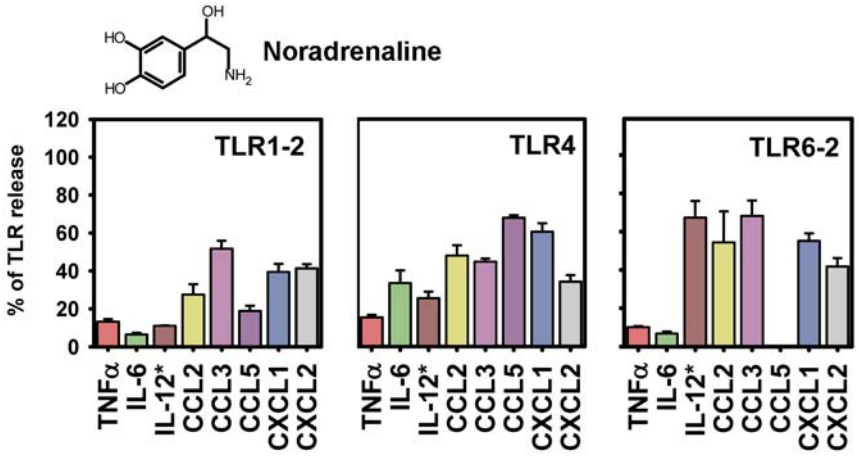

Figure 4.16.: Noradrenaline attenuates the TLR-induced cyto/chemokine production in microglia. Cells were stimulated with agonists for TLR1-2 (Pam_3CSK_4, 10 ng/ml), TLR4 (LPS, 10 ng/ml) or TLR6-2 (MALP, 10 ng/ml) in the presence of 8.2 µM of noradrenaline. Supernatant were taken after 18 h, the release of several cyto- and chemokines was determined and compared to controls, *i.e.* cells stimulated in the absence of noradrenaline. Data are mean ± SEM, with n = 8 as summarized from two independent experiments. Bars are presented in the same color code as in Fig. 4.4. *The IL12p40 assay determined the total amount of this IL12 subunit and thus covered the versions IL12p70, IL23, IL12p40 dimer and IL12p40 monomer, whereas IL12p70 and IL23 were selectively measured and combination of various assays in the past indicated that IL12 release in microglia thereby related to the p40 homodimer.

profile of suppressing the release of several of the cyto/chemokines, at least in the case of TLRX-2 stimulations. The profile differed for the TLR4 stimulated cells. Yet the similarities in the overall outcomes suggested to check whether AG126 might cause some of the cyto/chemokine modulation by agonistic functions *via* adrenoreceptors.

Therefore, microglia were preincubated with different concentrations of phentolamine methane sulfonate (PAMS), an antagonist for α_1/α_2 receptors, or propranolol, an antagonist for β_1/β_2 receptors, in the presence of 100 µM of AG126 for one hour. Afterwards, the cells were stimulated with Pam_3CSK_4 together with the respective antagonists and AG126 for another 18 h. The release of TNFα and KC was measured as described. Knowing that NA signals in microglia through β_2 receptors for the modulation of TLR-induced cyto/chemokines (data from our laboratory), its effects were completely abolished by propranolol (data not shown). The results of the experiments with AG126 are summarized in Fig. 4.17. It is obvious, that the stimulation of microglia with the TLR1-2 ligand led to an up-regulation of the TNFα and KC release, which could be attenuated by AG126. The addition of increasing PAMS or PR concentrations, however, did not interfere with the inhibitory effect of AG126, and both antagonists did also not affect the TNFα and KC release in unstimulated cells. It should be noted that, at high concentration, propranolol can develop some agonist behaviour, which is known, but which did not impair the present study and our conclusion from the data set. Despite the structural as

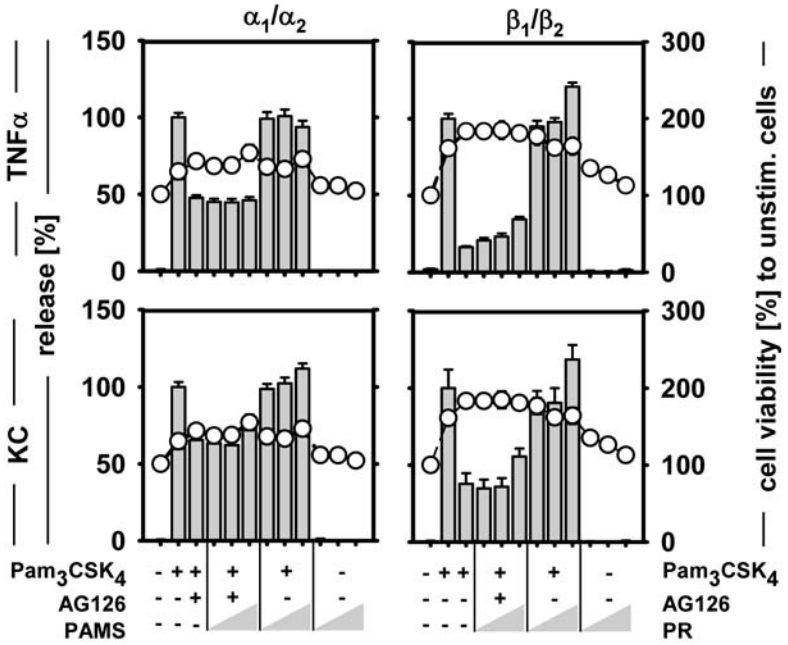

Figure 4.17.: AG126 does not act through α- or β-adrenergic receptors. Microglia were stimulated *via* TLR1-2 (Pam_3CSK_4, 10 ng/ml) for 18 h without or with 1.0, 10, 100 µM of PAMS or 0.1, 1.0, 10 µM of propranolol (PR) in the presence or absence of 100 µM of AG126. The TNFα and KC release was determined. Note that also TLR-unstimulated cells were included as controls. Data are mean ± SEM, with n = 16 as summarized from two independent experiments. Viability of the cells was determined in a WST-1 assay system (see Material and Methods for details).

well as functional similarities between AG126 and NA, there was no evidence that the tyrphostin would exert its microglial effects through adrenergic receptors.

4.4.3. Dexamethasone and Compound A affect the release responses in microglia

Alternatively, we hypothesized that AG126 could cause anti-inflammatory effects on our cells by serving as an agonist of the glucocorticoid (GC) receptor (GR). This assumption was based on three major indications. First, Sierra et al. (2008) reported evidence that *"...(adult) microglia are a direct target of steroid hormones and that glucocorticoids, through the predominant expression of GR and MR [mineralocorticoid receptor], are the primary steroid hormone regulators of microglial inflammatory activity."* Second, De et al. (2005) had stated *"...that Compound A (CpdA), a plant-derived phenyl aziridine precursor, although not belonging to the steroidal class of GR-binding ligands, does mediate gene-inhibitory effects by activating GR. We demonstrate that CpdA exerts an anti-inflammatory potential by down-modulating TNF-induced pro-inflammatory gene expression, such as IL6 and E-selectin."* Interestingly, this Cpd A has a

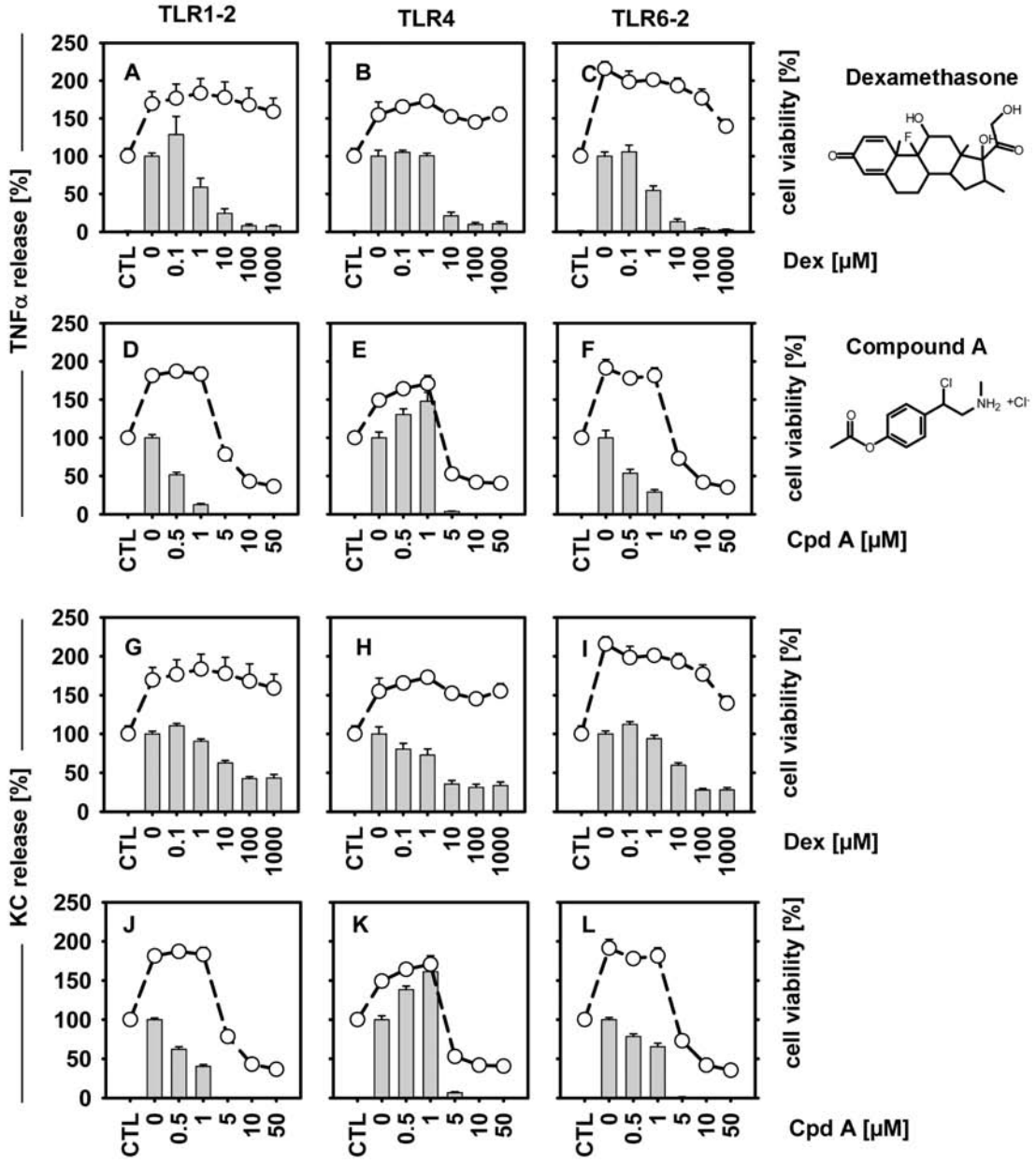

Figure 4.18.: Dexamethasone and Compound A affect the TLR-stimulated responses in microglia with similarities to AG126. Cells were pretreated with dexamethasone (Dex, 0.1 to 1000 µM) or Cpd A, 0.5 to 50 µM) for one hour and subsequently stimulated with the TLR1-2 (Pam_3CSK_4, 10ng/ml), TLR4 (LPS, 10 ng/ml) or TLR6-2 (MALP, 10 ng/ml) agonists in the absence or further presence of Dex or Cpd A for 18 h. TNFα and KC release was determined in the supernatants and compared to the amounts obtained with TLR stimulation in the absence of Dex or Cpd A. Data are mean ± SEM, with $n > 12$ as summarized from two independent experiments. Cell viability was analyzed in the WST-1 assay.

tyrosine-related structure. Third, the phytoestrogen genistein was originally found to interact with the estrogen receptor and only later, it became one of the first known substrate-specific PTK inhibitors (Martin et al., 1978; Akiyama et al., 1987). All together, structural and functional hints formed the hypothesis that AG126 might have a GR-dependent influence on the TLR signaling.

To test this concept, microglial cells were preincubated with different concentrations of dexamethasone (dex), the known ligand for the GR, or CpdA for one hour. Afterwards, cells were stimulated with Pam_3CSK_4, LPS or MALP in the presence or absence of dex or CpdA. The TNFα and KC release was determined and compared to the respective controls.

Both compounds down-regulated dose-dependently the TLR-induced release of TNFα and KC (Fig. 4.18). With regard to dex, under all TLR-stimulating conditions, it suppressed the release of TNFα (*A-C*) and, slightly less potent, that of KC (*G-I*). Considering the effect of Cpd A, concentrations as of 5 µM had to be excluded from consideration due to an indicated toxicity. We always examined the cell viability in an assay based on the cleavage of WST-1 (see Material and Methods). This assay determines oxidoreductase activity of the complex II and thereby allows to evaluate the vitality of the cells. While increases in the readout signal could be due to proliferation or increased enzymatic activity, a drop of activity can indicate impaired vital functions. Suppression of release by CpdA associating with a lowered WST-1 conversion was thus most likely not revealing an influence on the signaling flow, but simply a general impairment. Still, lower concentrations could repress the release of TNFα and KC in TLR1-2- (*D, F*) and TLR6-2-stimulated microglia (*J, L*), whereas the release of both of these factors was up-regulated in the TLR4-stimulated cells. Interestingly, unlike dex, CpdA thus presented with a comparable pattern of modulation with respect to the TLR-dependent profiles as known from AG126 (compare the profiles to those in Fig. 4.4). In contrast, dex affected the TNFα and KC release in LPS-treated microglia in a way not seen with AG126.

Due to the comparable effects of CpdA and AG126, we determined AG126 effects in microglial cells deficient for GR. Since a complete loss of GR is lethal for BL6 mice, only embryonic cells (from day 18.5) were used. Microglia with $GR^{-/-}$ and $GR^{-/+}$ genotype as well as from wildtype animals were preincubated with 0.1 µM of dex or 100 µM of AG126 and subsequently stimulated with Pam_3CSK_4 in their further presence for 18 h. The release of TNFα and KC was measured and compared. Cell viability was tested again by the WST-1 assay.

As shown in Fig. 4.19, the release of TNFα and KC in unstimulated cells treated with dex or AG126 was comparable to the medium control. For all cells, $GR^{-/-}$, $GR^{-/+}$ and *wt*, TLR1-2 stimulation provoked the release of TNFα and KC. The absolute values were slightly reduced in $GR^{-/-}$ (6.57 ± 0.32 ng/ml) and $GR^{-/+}$ cells (7.10 ± 0.31 ng/ml), when compared to the *wt* cells (7.92 ± 0.41 ng/ml). The addition of dex caused, as expected, a pronounced repressive release effect in the *wt*, but not $GR^{-/-}$ cells. In the $GR^{-/+}$ cells, the release was reduced, but not as strong as in the total *ko* situation. For AG126, the suppressive effect on the TNFα and KC release was apparent in all cell types, including the homozygous *ko* — indicating that AG126 would not act in a GC-like manner.

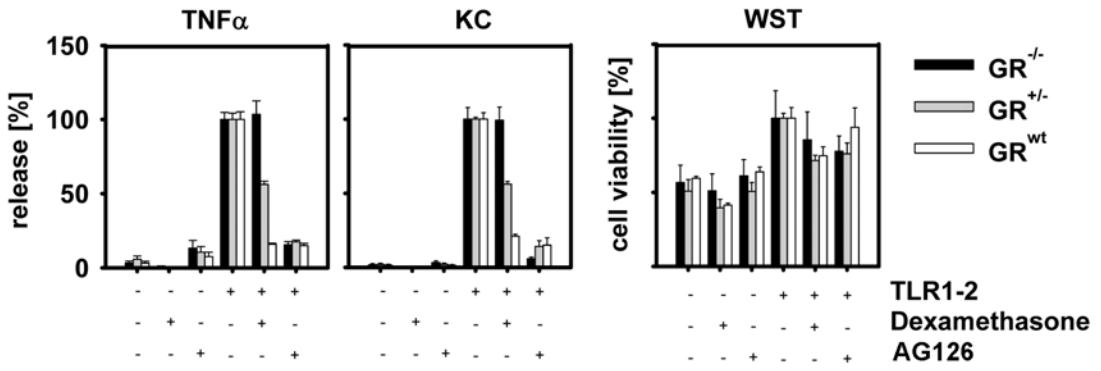

Figure 4.19.: AG126 does not act *via* GR. Microglia (of embryonic day e18.5) from $GR^{-/-}$, $GR^{-/+}$ or *wt* mice were preincubated with 0.1 µM of dex or 100 µM of AG126, or received a medium change for one hour. Subsequently, TLR1-2-stimulated or unstimulated cells were further incubated for 18 h without or with 0.1 µM of dex or 100 µM of AG126, as indicated. TNFα and KC release was determined. The cell viability was analyzed by the WST-1 assay. Data are mean ± SEM, with n = 16 as obtained from two microglia harvests.

Taken together, none of the alternative mechanisms held true in explaining the activity of AG126 beyond the effects as determined for BTK. Both the adrenergic as well as the GR pathway could be ruled out. Based on some earlier findings of an obscure disappearance of AG126 signals in a spectral HPLC analysis (data not shown), we then raised the hypothesis that AG126 may undergo some chemical degradation or metabolic conversion in aqueous solutions and/or the cellular environment. This would not only reduce the concentration of the AG126 itself but probably liberate biologically active offsprings.

4.5. Metabolization of AG126

4.5.1. Spectral analysis reveals instability of tyrphostins in aqueous solution

To get a first indication, tyrphostin stability was analyzed in aqueous environment, incubating several compounds for different time periods at 37°C. Therefore, 50 mM of AG18, AG82 and AG126, as dissolved in DMSO, were diluted to a concentration of 100 µM in medium and incubated with or without cells at 37°C, 5 % CO_2, *i.e.* conditions usually applied for cultures. The characteristic absorbance spectra were determined in 2 nm steps and normalized to the phenol red peak at 560 nm.

Fig. 4.20 *A* shows the summary of data for the measurement without cells. AG126 shows changes of its characteristic peak maximum at 435 nm. However, a time- dependent reduction of the signal cannot be clearly extracted from the array. In contrast, AG18 and AG82 showed time-dependent signal reductions at the characteristic absorbance maxima of 449 nm or 470 nm,

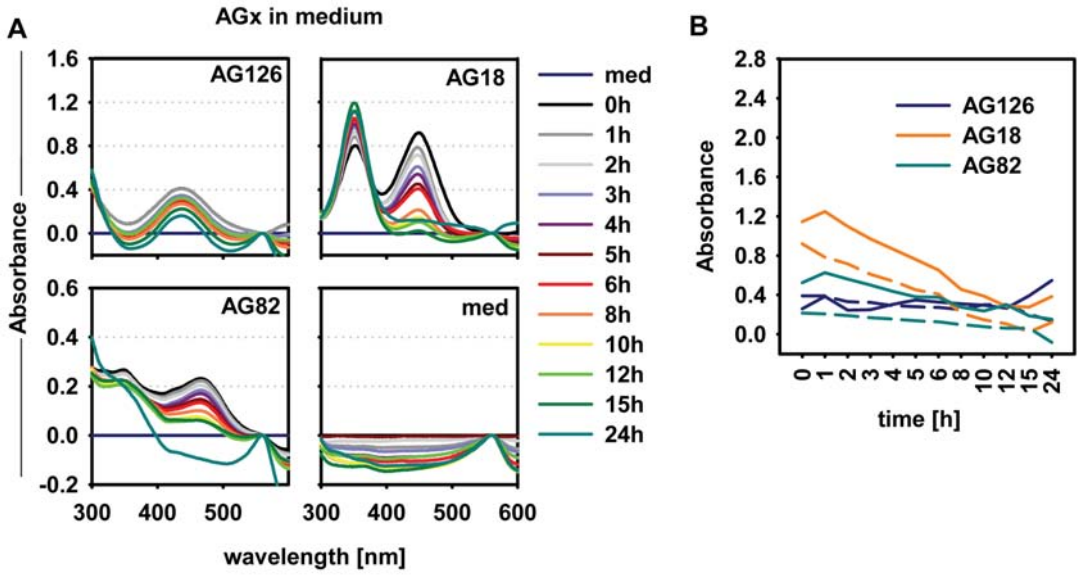

Figure 4.20.: Tyrphostin stability in medium as revealed by spectral analysis. AG126, AG18 and AG82 were diluted from a stock solution in DMSO to 100 µM with medium and incubated for different time periods without (solid lines) or with (dashed lines) microglia. ***A*** Absorbance spectra were analyzed (by 2 nm steps) and normalized to the phenol red signal at 560 nm. ***B*** The time-dependent degradation of AG18, AG82 and AG126 is shown based on their characteristic absorbance maxima at 449, 470 and 435 nm, respectively.

respectively. In Fig. 4.20 *B*, the specific maxima are plotted against time for both cell-free (medium only) conditions and recordings of tyrphostins upon an exposure to cells. It is obvious that the signal intensities of tyrphostins with a cell contact are lower than those taken without cell incubation. It can be suspected that microglia can even catalyze the degradation or incorporate the compounds, at least for A18 and A82.

In conclusion, the data provided a first direct indication for structural changes of certain tyrphostins within an aqueous environment, interpreted as an instability, and probably be cell-assisted. These data are thus in agreement with findings by Ramdas et al. (1994). They showed degradation of tyrphostin 23 (AG18) and 25 (AG82) and a therewith related potential for PTK inhibition. For AG126, the spectral analysis was not absolutely conclusive. Further proof was thus sought of by another analytical approach.

4.5.2. NMR spectroscopy reveals break down products of AG126

The more sophisticated method of nuclear magnetic resonance (NMR) spectroscopy was employed to elucidate the molecular fate of AG126 in aqueous solution. NMR spectroscopy reveals the electronic environment of individual atoms and their interactions with neighboring atoms. By this means, we were able to obtain more reliable information about the structure changes, *i.e.* the degradation, of AG126. To do so, the stability of AG126 as dissolved in absolute DMSO,

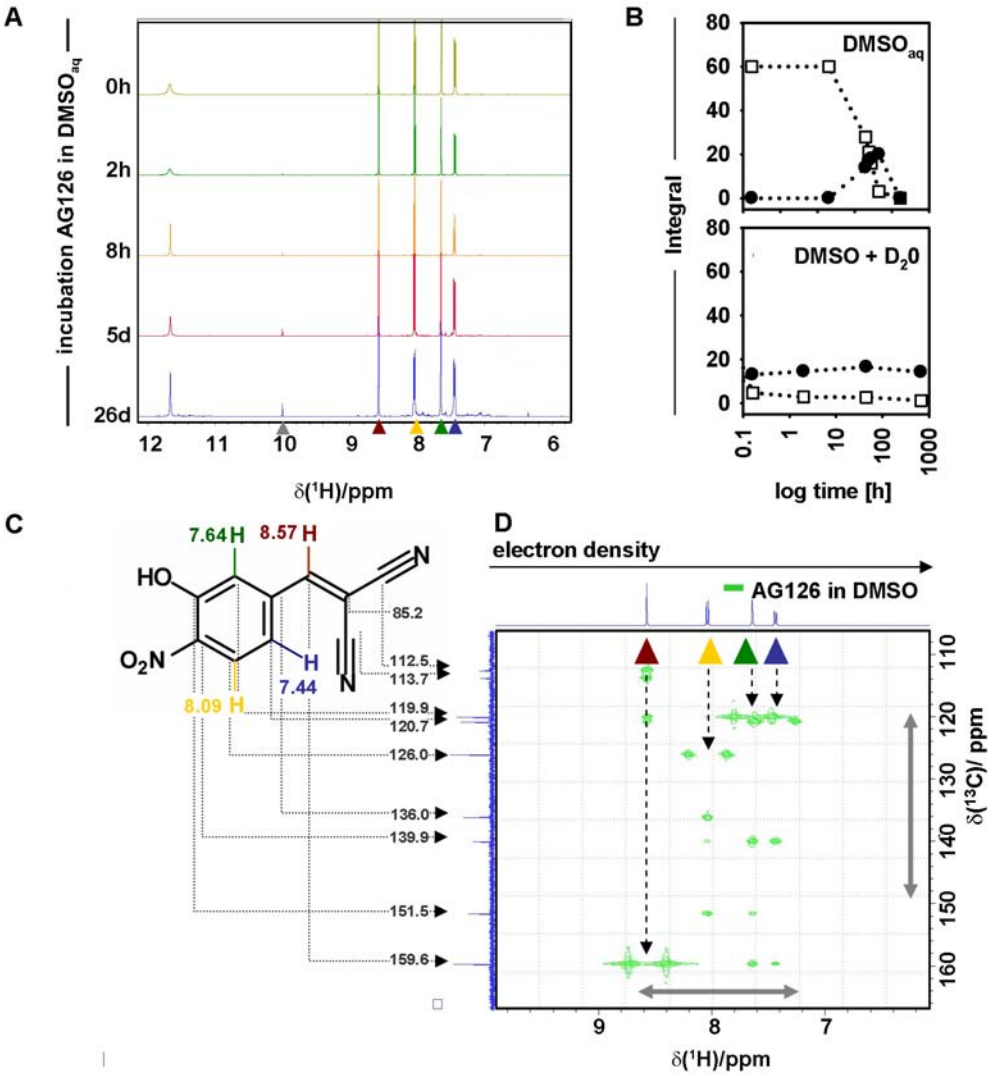

Figure 4.21.: NMR analysis of AG126 reveals its degradation in aqueous solution. ***A*** AG126 dissolved in DMSO$_{aq}$ was analyzed by ^{1}H NMR spectroscopy. Spectra were taken directly or after 2 h and 8 h as well as 5 and 26 days of incubation. Characteristic AG126 peaks are indicated by colored triangles and explained in ***C***. The gray triangle indicates a newly appeared peak (characteristic for aldehyde). ***B*** AG126 was diluted in DMSO$_{aq}$ or diluted in 1 volume of DMSO$_{aq}$ and 3 volumes of D_2O. ^{1}H NMR spectra were taken at the different time periods as indicated. The integral of the AG126 peak (white box, DMSO$_{aq}$, 8.57 ppm, DMSO + D_2O, 8.25 ppm, peak shift was caused by solvent) and an aldehyde peak (black box, 10.0 ppm) were plotted against time of AG126 dilution. ***C*** ^{1}H atoms with a corresponding ppm value are highlighted on the chemical structure of AG126. ***D*** The ^{13}C atoms are correlated to a 2D HMBC spectrum of AG126 dissolved in DMSO, with the ^{1}H NMR spectrum shown on top and the ^{13}C NMR spectrum shown on the left. Traces along the characteristic H atoms (again marked with colored triangles) are drawn as dashed lines. Observed ^{13}C resonances are connected to the corresponding C atoms in the AG126 structure by black arrows. The corresponding C atoms are highlighted in the structure as given in ***C***.

DMSO with a residual water amount ($DMSO_{aq}$) and in DMSO being added D_2O was monitored over time.

AG126 dissolved in absolute DMSO seemed to be stable over time although, after several weeks, traces of new compounds, presumably photo-dimerization products, were found (^{1}H NMR spectra not shown). Fig. 4.21 *A* shows ^{1}H NMR spectra of freshly dissolved AG126 (10.0 mg/ml in $DMSO_{aq}$) after different time periods. At any time, the characteristic NMR peaks of AG126 could be detected, described in detail *vide infra*. Furthermore, a new peak, which is characteristic of the -CHO group of an aldehyde, occurred and increased during the time of incubation. The ^{1}H NMR peak at 12.3 ppm belongs to the hydroxy group as located at the benzene ring.

To analyze the rate of degradation of AG126 as well as the formation of the aldehyde in regard to the water amount in the solvent, the tyrphostin was dissolved in $DMSO_{aq}$ or in $DMSO_{aq}$ + D_2O (1:4). ^{1}H NMR specta were taken during the proceeding degradation of AG126. The integral of the occurring aldehyde peak at 10.0 ppm and the AG126 peak at 8.57 ppm ($DMSO_{aq}$) or 8.25 ppm (DMSO+D_2O) was measured and plotted against time. The peak deviation resulted from the changes caused by the solvent environment. AG126 diluted in $DMSO_{aq}$ degraded quite slowly, while the signal for the aldehyde increased. After a very long time (26 days), the aldehyde peak also decreased as the aldehyde itself became further oxidized to the corresponding carbonylic acid by DMSO. AG126 in the DMSO mixture with D_2O revealed a faster degradation of AG126 and a constant presence of the aldehyde signal (Fig. 4.21 *B*). The AG126 degradation was nearly completed before the first recorded ^{1}H NMR spectrum. The lower amount of DMSO seemed to lower the rate of benzaldehyde degradation.

From these measurements, it can be safely concluded that AG126 does degradate in an aqueous environment. Higher amounts of water in the solvent clearly increase the rate of the reaction, suggesting that cellular and tissue environments create conditions in which the compound breaks down into products which could deliver own effects in addition to AG126 as the parent structure.

4.5.3. 3-hydroxy-4-nitrobenzaldehyde is an AG126 degradation product

To identify the substances that are newly formed during degradation of AG126 several 2D NMR techniques were applied. First, additionally to the ^{1}H NMR spectrum, the corresponding ^{13}C NMR spectrum was recorded. The obtained ^{13}C resonances were correlated to nearby H atoms with HSQC (heteronuclear single quantum coherence, one-bond correlation) and HMBC (two- and three-bond or heteronuclear multiple bond correlation) spectra.

This way, all C atoms of AG126 could be detected and assigned in the sample of AG126 in absolute DMSO (Fig. 4.21 *C* and *D*). In a second step, D_2O was added to the sample. HMBC and HSQC spectra were recorded once again. The corresponding AG126 signals were also found in the DMSO + D_2O samples, where a slight shift of the signals appeared resulting from the changed solvent environment. Again, the aldehyde-specific signal at about 10 ppm could be detected and correlated to its respective C atom (Fig. 4.22 *A*). This led to the assumption that 3-hydroxy-4-nitrobenzaldehyde could be a degradation product of AG126.

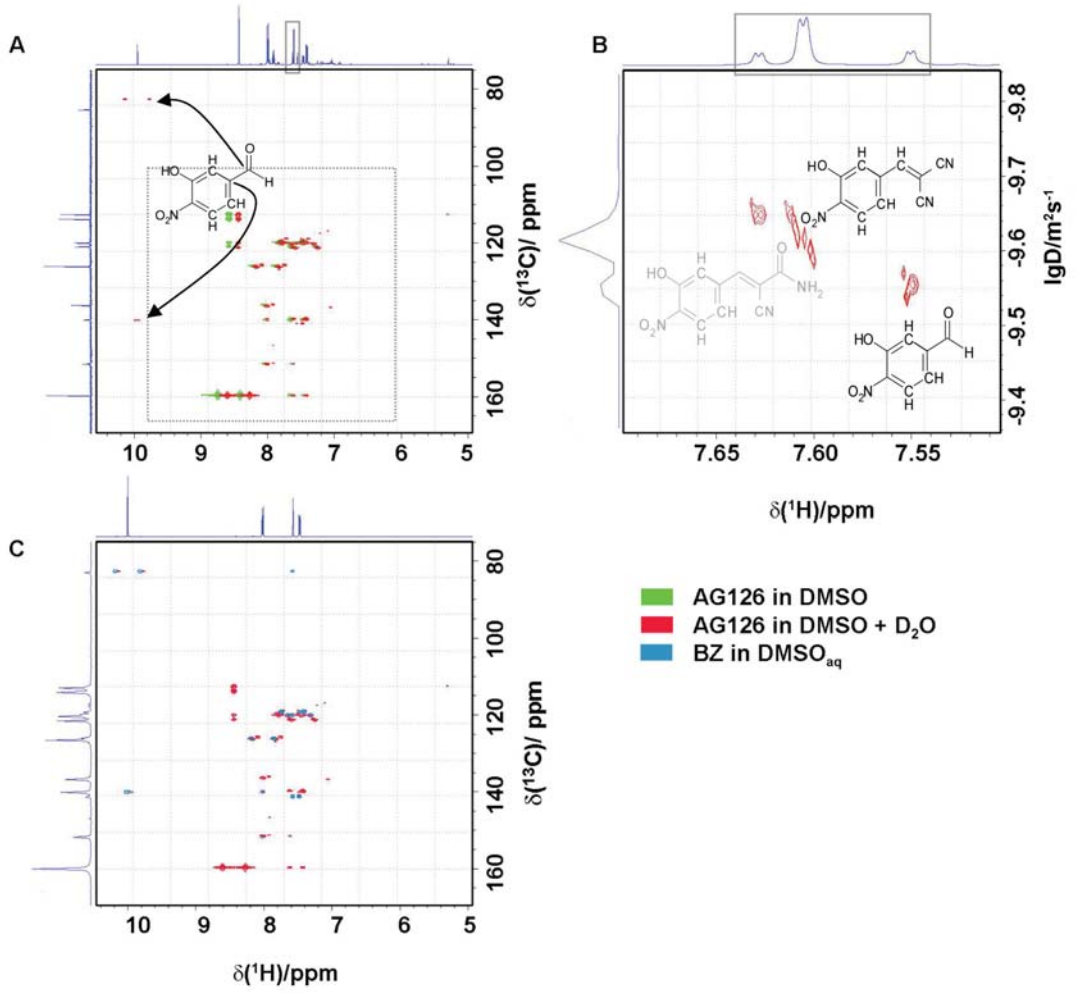

Figure 4.22.: 3-hydroxy-4-nitrobenzaldehyde is a degradation product of AG126. ***A*** Overlay of the 2D HMBC spectra of AG126 dissolved in DMSO (green) and DMSO + D_2O (red). The peaks in the two samples are slightly shifted due to the different solvent composition. The addition of D_2O to AG126 in DMSO led to the appearance of new signals corresponding to an aldehyde. The carbonyl ^{13}C resonance is at 192.7, but appears folded at 82.7. The gray dotted line illustrates the cutout shown in Fig. 4.21 *D*. The box in the ^{1}H spectrum indicates H_2 proton as analyzed by DOSY. ***B*** DOSY NMR spectrum of the AG126 sample in DMSO + D_2O, for the same sample as in ***A***. Next to AG126, two degradation products could be shown. The molecular size increases from bottom to top. Additionally, another tyrphostin derivate occurred, slightly larger as AG126, and putatively, but unproven, an amide compound. ***C*** Overlay of 2D HMBC spectra of AG126 dissolved in DMSO + D_2O and 3-hydroxy-4-nitrobenzaldehyde.

To confirm the presence of 3-hydroxy-4-nitrobenzaldehyde in the AG126 solution, a control sample was analyzed by HSQC and HMBC and was overlaid with the AG126 signals (DMSO + D_2O, Fig. 4.22 *C*). Note, that the aldehyde signal was present in both samples, whereas C atoms of the nitrile part of the AG126 could not be detected in the benzaldehyde sample.

In conclusion, we could demonstrate and confirm that 3-hydroxy-4-nitrobenzaldehyde (BZ) is at least one of the degradation products of AG126 in an aqueous environment.

4.5.4. AG126 is the precursor of more than one reaction product

For the determination whether BZ would be the only reaction product (which was unlikely), diffusion-ordered spectroscopy (DOSY) was performed. DOSY experiments allow for the separation of compounds in a mixture based on their translational diffusion coefficients and thus by substance size. The gray box in Fig. 4.22 *A* shows the region of isolated aromatic H atoms (H_2) used for the DOSY analysis. Compared to the signal originating from AG126 (7.60 ppm), the corresponding BZ signal (7.55 ppm) appeared at a substantially higher diffusion coefficient.

Additionally, a signal at 7.63 ppm with a diffusion coefficient similar or slightly smaller than that of AG126 belonged to a further degradation product — probaly a carboxyamide (resulting from hydrolysis of one of the nitrile groups of AG126). However, this putatively formed carboxyamide as detected by DOSY could not be confirmed yet.

On the other hand, the NMR analysis results allowed for the conclusion that AG126 is hydrolyzed in water to 3-hydroxy-4-nitrobenzaldehyde (BZ). Consequently, malononitrile (MN) should result as an expected byproduct (see the equation 4.1 below). This byproduct could, however, not be identified directly in ^{1}H NMR spectra, presumably because the CH_2 resonance was hidden under the residual water signal or because of a transformation into a CD_2 group by exchange with the solvent — or because MN itself got rapidly degraded to further products.

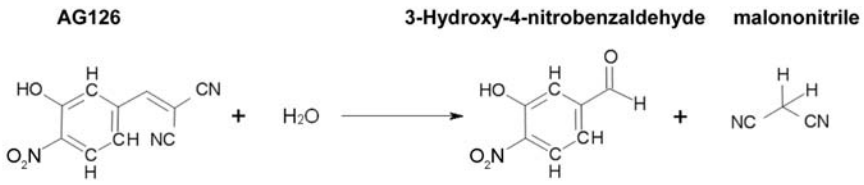

(4.1)

4.6. AG126 breakdown products have effects on microglia

Chemical analysis of AG126 revealed a fast degradation and conversion of the compound in aqueous solutions. Next to other putative products, a pronounced amount of BZ arose, with MN as the expected byproduct. Therefore, it was tested if one of the by/products would be sufficient to cause effects in microglia similar to those obtained with AG126.

4.6.1. MN but not BZ affects the cyto- and chemokine production similar to AG126

First, the modulatory capacity of MN and BZ on the pro-inflammatory cytokine pattern in TLR-stimulated microglia was analyzed. Microglia were pretreated with 1, 5, 10, 50 or 100 µM of MN or BZ *vs.* AG126 for one hour, followed by their stimulation with Pam_3CSK_4, LPS or MALP in the further presence or absence of MN, BZ and AG126 for 18 h. Cyto/chemokine release and cell viability were measured. MN and BZ had no effect on the cell viability, at any of the applied concentrations, as compared to controls.

The side-by-side comparison of AG126 and MN as to their effects on the TLR-induced release responses revealed a remarkably similar, partially even congruent pattern (Fig. 4.23 *A*). MN and AG126 did not affect the cyto- and chemokine release in unstimulated microglia, and the effects of AG126 on the TLR-stimulated cells were extensively described in section 4.2.2. MN largely followed these profiles, repressing the release of the various factors similar to AG126, such as for IL6 and MCP1 in TLR1-2- or TLR6-2-activated cells — or more or less sparing them when AG126 did so, like in some of the RANTES inductions. Interestingly, some of the more unusual regulations occurred with MN also in the AG126-like manner. This regared the biphasic influences on release patterns as described in section 4.2.2 or trends of increased release activity. Noticeably, MN exerted also little effects on the cyto/chemokines as released under LPS, as known for AG126.

In contrast, BZ did not show a comparable pattern of dose-dependent influences as it was seen with AG126- and MN-treated microglia (Fig. 4.23 *B*). Generally, BZ seemed to have little effect on the cyto- and chemokine release response of TLR-stimulated microglia. Divergence from the effects of AG126 is most obvious for the release of MCP1, RANTES or IL6 on TLR1-2- or TLR6-2-stimulated microglia. While AG126 clearly caused repression, BZ treatment did not change the release. In TLR4-stimulated cells, BZ as well as AG126 had little effect on the cyto- and chemokine release. Of course, two not existing effects are not a proof of similarity. Yet BZ did fail to exert any effect where AG126 was effective. Considering the reciprocal situation, AG126 being ineffective, but BZ presenting with an effect would be important as BZ would at least reveal microglia-active, and not just appear as dispensible. In certain cases, indeed, BZ even slightly increased the release in a dose-dependent manner, sometimes following the trend as set by AG126 (MIP1α, TLR1-2), sometimes with opposite direction (MCP1, TLR1-2). The overall correlations of AG126 and MN as well as AG126 and BZ demonstrate convincingly that the gross patterns of release modulation were most close for AG126 and MN (Fig. 4.6.1).

In general, AG126 and MN, but not BZ, can affect the cyto- and chemokine release in TLR-stimulated microglia in a similar fashion. This leads to the assumption that MN as a breakdown product of AG126 carries the essential pharmacological activities — at least as it regards this microglial function.

4.6.2. MN reveals the same MAPK and NFκB phosphorylation pattern as AG126

Focusing on the activation of MAPK's and NFκB in TLR-stimulated microglia we tested if MN would have a comparable outcome to AG126. Therefore, cells were treated and analyzed in the phosphorylation assays in the same manner as described for AG126 (see section 4.2.7).

Similar to AG126, MN did not significantly affect the phosphorylation profiles of the different MAPK's, *i.e.* ERK, JNK and p38, as well as those of NFκB (Fig. 4.24). As already seen for AG126, MN did not inhibit the activation of downstream these signaling molecules in the TLR pathway — with one exception. In Pam_3CSK_4-stimulated microglia, MN was able to suppress the activation of ERK1/2 after 30 min of stimulation, whereas AG126 showed a slight decrease. It is known that AG126 may inhibit the phosphorylation of ERK1/2 (Hanisch et al., 2004), and this could be confirmed by the phosphorylation array (Fig. 4.11). Yet both AG126 and MN did not cause a massive interference which could have served to explain their inhibitory or modulatory influence on microglia or which could have indicated distinct outcomes on the TLR signaling. Since we had obtained, however, indications for AG126 as inhibiting BTK, we addressed this potential mechanism for its breakdown products.

4.6.3. MN or BZ cannot inhibit BTK activity

The inhibitory potential of MN and BZ was tested on recombinant BTK in the enzyme activity assay as described above for LFM-A13 and AG126 (section 4.3.2). MN or BZ were tested at various concentrations and the data are summarized in Fig. 4.25. For a better comparison, the inhibition curves were overlaid with those from Fig. 4.13 (half transparent). It is obvious, that neither MN nor BZ inhibited the BTK activity. Only some slight reduction in the substrate phosphorylation by ~10 % was detected for BZ at 500 µM, probably caused by an unspecific interaction, but certainly not comparing to the effects noticed with AG126 or the established BTK inhibitor, LFM-A13. Overall, both AG126 degradation products on their own were not able to mimic the inhibitory potential of the parent compound.

Figure 4.23. *(following page)*: MN (*A*) but not BZ (*B*) shows a similar dose-dependent influence on the cyto- and chemokine release pattern in TLR-stimulated microglia as obtained with AG126. Cells were treated with MN, BZ or AG126 for one hour and subsequently stimulated with the respective agonists for TLR1-2 (Pam_3CSK_4, 10 ng/ml), TLR4 (LPS, 10 ng/ml) or TLR6-2 (MALP, 10 ng/ml) for 18 h in the further presence of MN, BZ or AG126. Cyto/chemokine release was determined in the supernatants. Data are mean ± SEM, with n = 6 as summarized from two independent experiments. ***C*** The overall correlations of the release modulation patterns as shown in *A* and *B* indicate striking similarity between AG126 and MN, but not between AG126 and BZ.

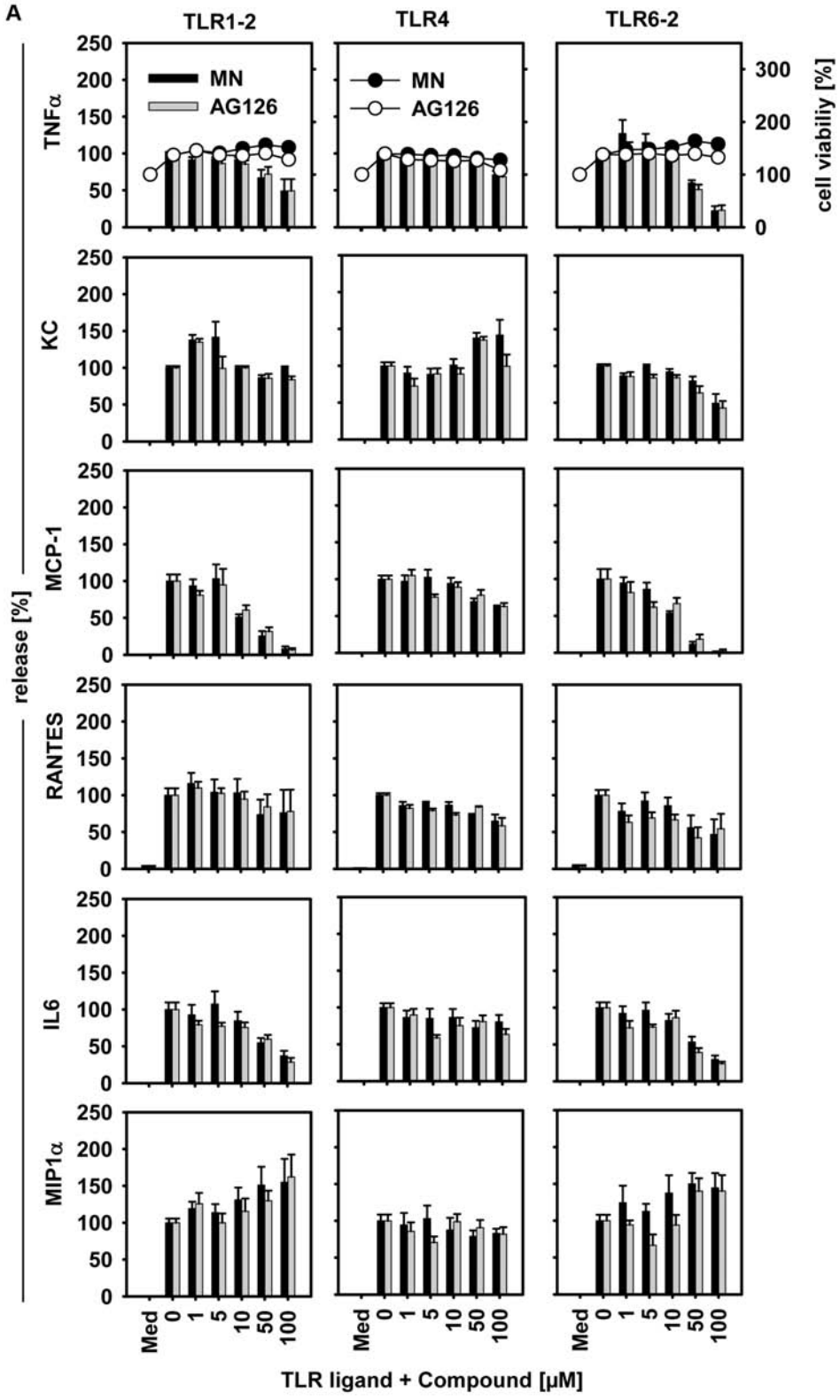
A
TLR1-2
TLR4
TLR6-2
MN
AG126
TNFα
KC
MCP-1
RANTES
IL6
MIP1α
release [%]
cell viabiliy [%]
Med
0
1
5
10
50
100
TLR ligand + Compound [µM]

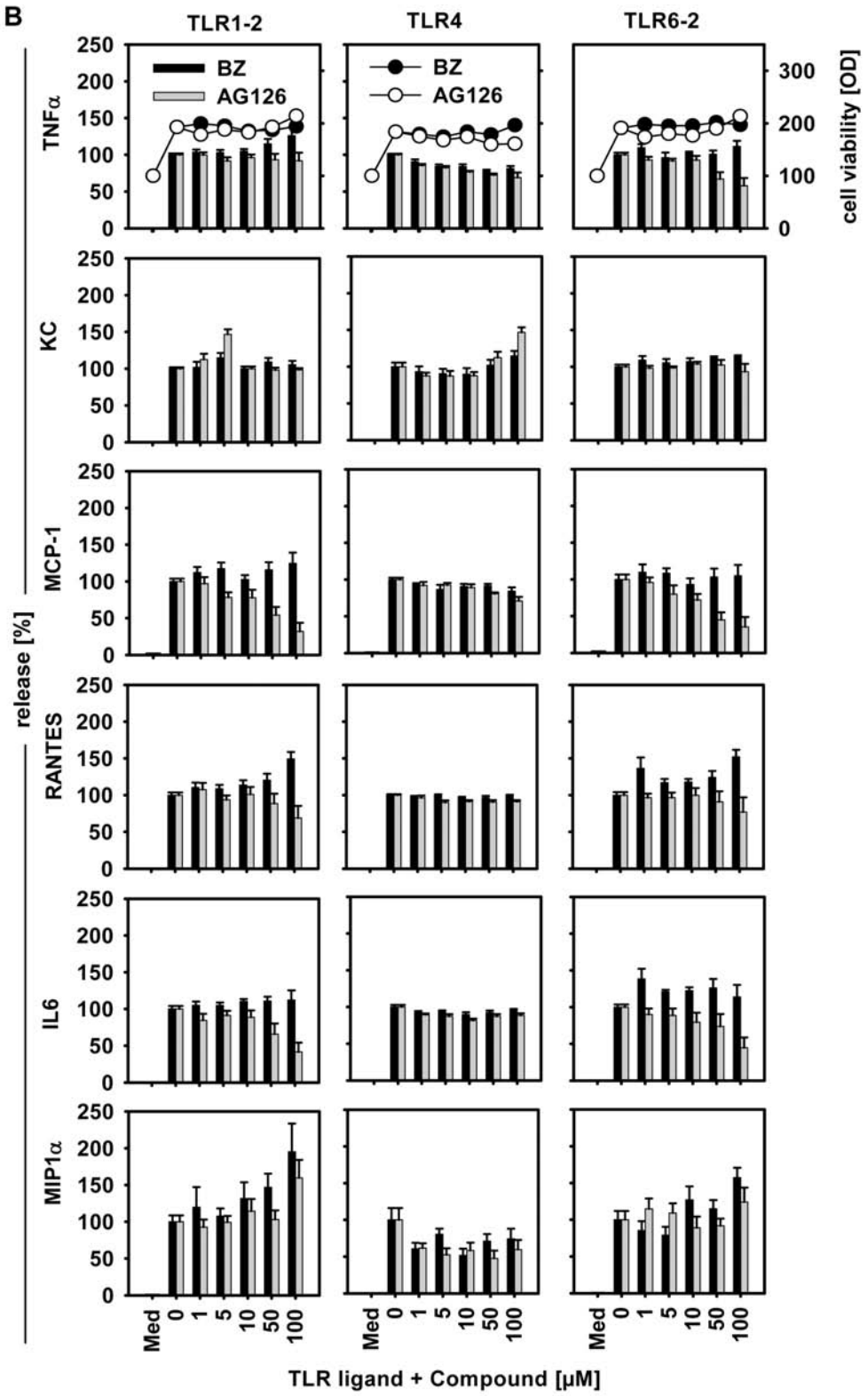
B
TLR1-2
TLR4
TLR6-2
BZ
AG126
TNFα
KC
MCP-1
RANTES
IL6
MIP1α
release [%]
cell viability [OD]
Med
0
1
5
10
50
100
TLR ligand + Compound [µM]

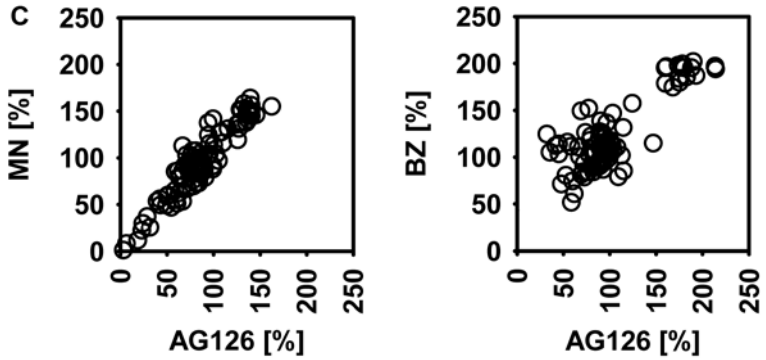

4.6.4. Other tyrphostins are able to inhibit the cyto- and chemokine release of TLR-stimulated cells in a similar fashion as AG126

While the previous data could show that AG126 as well as LFM-A13 were able to inhibit BTK activity, but not BZ or MN alone (section 4.6.3), MN seemed to suffice the modulation of the cyto- and chemokine release in TLR-activated microglia. In contrast to AG126, LFM-A13 — which was unable to affect the release (section 4.6.1) — lacks the molecular structure giving rise to MN. Currently, a large number of tyrphostins is on the market. While carrying diverse substituents on the benzene ring, many of them also have such a MN residue in common. It could be assumed that some of those tyrphostins could similarly degrade to a benzaldehyde structure (BZ) and MN. While the different structures may come with varying stability and thereby varying conversion to MN, they could probably exhibit some cyto- and chemokine modulation. If MN is the pharmacologically functional substance, then tyrphostins with and without this structural motif should fall into groups of proving or failing to be active on cells in TLR stimulation. A range of commercially available tyrphostins and of newly synthesized compounds with or without the MN structure were tested for their effect on cyto- and chemokine release of TLR-stimulated microglia. First, we tested the commercially available tyrphostins AG9, AG17, AG18, AG43, AG82 and AG1288. They have the MN 'residue' in common. Microglial cells were preincubated with 1, 5, 10, 50 or 100 µM of the respective compound for one hour, then incubated with the respective TLR ligand in their further presence for 18 h and the release of TNFα and KC was measured (Fig. 4.26). In comparison to AG126, the different tyrphostins affected the release in a similar, yet individual fashion. AG17 made an exception, since 50 and 100 µM were obviously toxic for microglia. Furthermore, it repressed the KC release in TLR4-stimulated cells, while all other tyrphostins did not affect KC release or even enhanced it, like AG126 did. In TLR6-2-activated cells, AG17 repressed the release of TNFα more potently than AG126. In comparison to the other tyrphostins, AG126 was consistently the most potent compound, with regard to a release suppression at its highest concentration. AG9, AG18, AG43 and AG83 effects did not reveal a clear order of responses when compared to AG126. All substances repressed more or

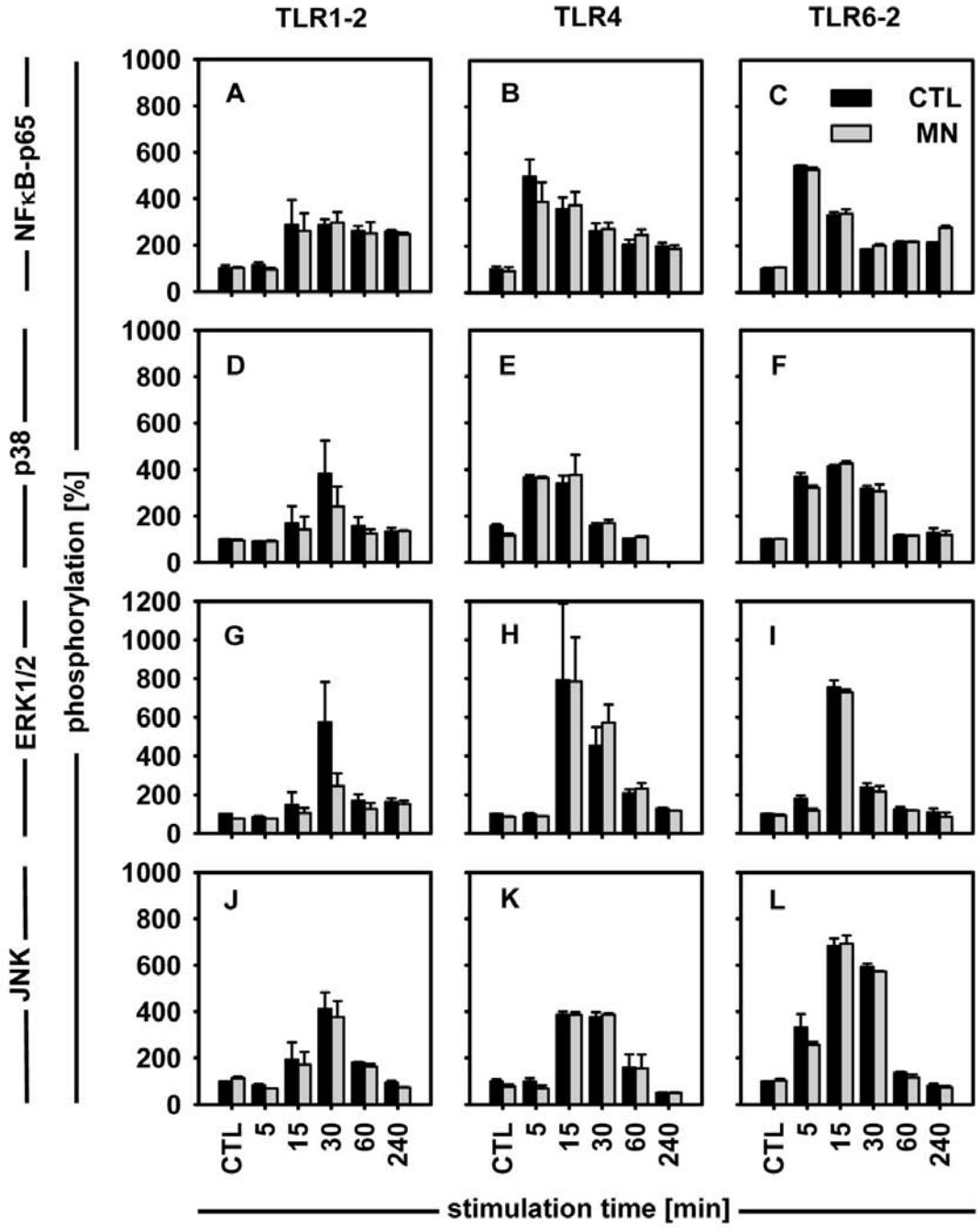

Figure 4.24.: MN does not affect the TLR-induced activation of NFκB or the MAPK, p38α, ERK1/2 and JNK. ***A***, ***D***, ***G*** and ***J*** show the phosphorylation pattern of TLR1-2-stimulated, ***B***, ***E***, ***H*** and ***K*** of TLR4- stimulated and ***C***, ***F***, ***I*** and ***L*** of TLR6-2-stimulated microglia. Cells were stimulated for various time periods with the respective TLR agonists alone or in combination with 100 µM of MN. Stimulations and (pre)incubations were performed as described in Fig. 4.10. Phosphorylated NFκB (Ser536, ***A-C***), $p38^{MAPK}$ (Thr180/Tyr182, ***D-F***), ERK1/2 (Thr202/Tyr204, ***G-I***) and JNK (Thr183/Tyr185, ***J-L***) proteins were detected by phosphorylation-specific ELISA. The total protein amount was determined by the BCA assay. Data are mean ± SEM, with n = 2 as summarized from two independent experiments.

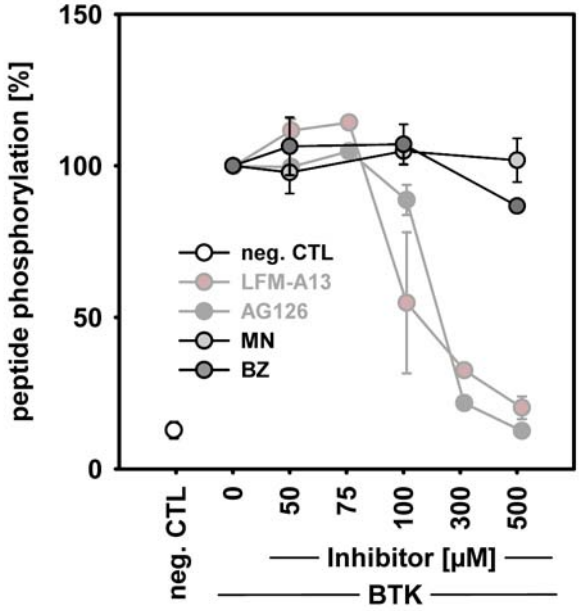

Figure 4.25.: MN and BZ do not inhibit the activity of recombinant BTK. Random peptides containing tyrosine motives were coated on a 96-well plate. Addition of 50 ng/ml of recombinant human BTK in the presence of ATP allowed for the phosphorylation of the tyrosine residues. Inhibitory effects on the BTK were analyzed by the addition of MN and BZ at concentrations ranging from 50 to 500 µM. The amount of phosphorylation was analyzed by a phospho-tyrosine-specific antibody labelled with HRP. The intensity of the colour reaction was determined and compared to the control, *i.e.* BTK-catalyzed substrate phosphorylation in the absence of MN. For details, refer to section 3.14 in the Material and Methods. Data are mean ± SEM, with n = 4 as summarized from two independent experiments. LFM-A13 and AG126 data (from Fig. 4.13) are shown as half-transparent curves for a comparison.

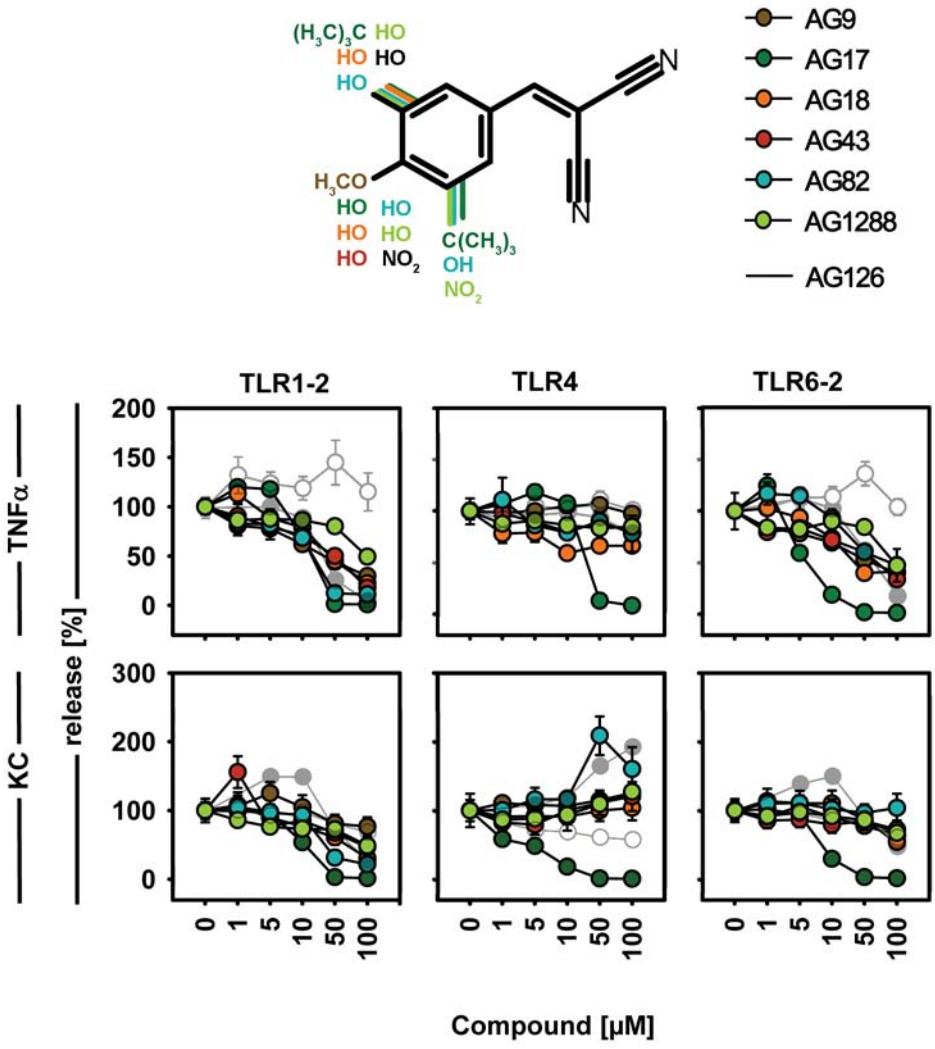

Figure 4.26.: Effects of tyrphostins on TLR-stimulated microglia. Microglia were preincubated with 1 to 100 µM of tyrphostin AG9, AG17, AG18, AG43, AG82 and AG1288 as indicated or received a change of medium only for one hour. Subsequently, TLR1-2- (Pam_3CSK_4, 10 ng/ml), TLR4- (LPS, 10 ng/ml) or TLR6-2-stimulated (MALP, 10 ng/ml) or unstimulated microglia were incubated without or with 1 to 100 µM of the respective tyrphostin for another 18 h. The TNFα and KC release was measured in the supernatants. Data are mean ± SEM, with $n > 8$ as summarized from two independent experiments. The WST-1 viability assay revealed that concentrations > 50 µM of AG17 had toxic effects on the microglia. Other tyrphostins showed no effect on cell viability. Structure formulas of the tyrphostins are shown in comparison to AG126 (black).

less effectively the KC or TNFα release in the TLR1-2- or TLR6-2-activated cells. Interestingly, the tyrphostins did not repress the release response in TLR4-stimulated cells. This phenomenon seemed to be a characteristic theme throughout the analyzed compounds. For example, AG82 seemed to be equally potent as AG126 in TLR1-2-activated cells. It also enhanced the KC release at 50 or 100 µM in LPS-stimulated cells. AG1288 showed the lowest inhibitory capacity release.

To correlate the cellular effect of tyrphostins to a presence of the MN 'residue' in their chemical structure more precisely, newly synthesized compounds were tested on microglia (see Material and Methods for details on their sources and the collaboration with scientists in Aberdeen, Scotland). Therefore, cells were preincubated with 10, 50 or 100 µM of ABD501, ABD517, ABD521, ABD571 (with a MN residue, Fig. 4.27) or ABD593, ABD604 or ABD642 (for a modified MN residue, Fig. 4.28) for one hour. Cells were then stimulated with Pam_3CSK_4 or LPS in the presence of the compounds for 18 h.

As seen for the commercially available compounds, TNFα and KC release responses to ABD509-571 and to AG126 were similar. Except for ABD571, the compounds (ABD509, AB5D17 and ABD521) revealed some differences to AG126 on the release of at least one chemokine, best seen for TLR1-2-treated cells. While AG126 repressed the release of MCP1, ABD509, ABD17 and ABD521 had no repressive properties, while ABD509 enhanced the RANTES release. On LPS-treated cells, ABDx with MN residues had minor repressive effects on the cyto/chemokine release. ABD509-571 enhanced the KC release. These results are rather comparable to those obtained with AG126. ABDx compounds with modified MN residues had mostly only slight repressive effects. ABD604 and ABD642 even enhanced the KC release in TLR4-stimulated cells.

Overall, structures with a MN residue seem to act similar to AG126, especially with regard to TNFα and KC release. In contrast, the compounds with a modified MN residue do not have effects comparable to AG126. From these data, it can be concluded that the MN structural component as being present in a wide range of tyrphostins seems to be important for the modulatory properties on cyto- and chemokine release inTLR-activated microglia.

4.6.5. Divergent effects of MN and BZ versus AG126 in EAE.

The previous experiments had shown that AG126 degradation products cannot inhibit the BTK function, as it applied to AG126 and LFM-A13. However, MN alone, but not BZ, could mimic the AG126 effect on the cyto- and chemokine response in TLR-stimulated microglia. From these data, the question arose whether the therapeutic effect in the animal disease models could be also caused by MN or whether it would still depend on the whole compound — considering relevant functions as only modified by the integral formula or as relating to the distribution and BBB penetration of the intact AG126. Consequently, the disease courses of mice with EAE mice were studied upon MN and BZ treatments.

C57/BL6J mice were actively immunized against the MOG peptide 35-55, as already described

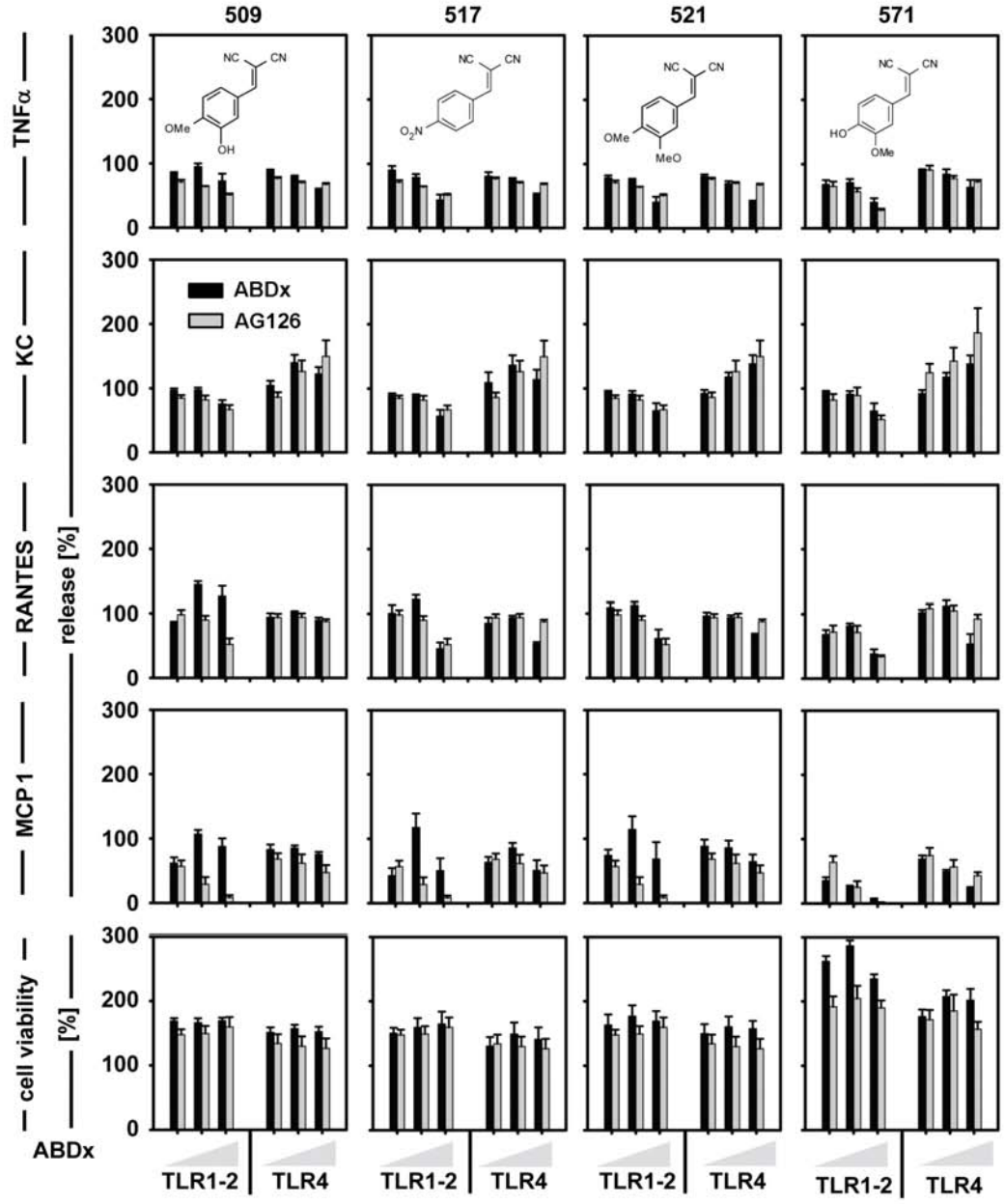

Figure 4.27.: Effect of ABDx compounds a MN residue on TLR-stimulated microglia. Cells were preincubated with 10, 50 or 100 μM of ABD501, ABD517, ABD521 or ABD571 or received a medium change for one hour. Subsequently, TLR1-2- (Pam_3CSK_4, 10 ng/ml) and TLR4-stimulated (LPS, 10 ng/ml) or unstimulated cells were incubated without or with 10, 50 or 100 μM of the respective compound for 18 h. Cyto- and chemokine release was measured in the supernatants. Cell viability was analyzed in a WST-1 assay. Data are mean ± SEM, with n = 8 as summarized from two independent experiments.

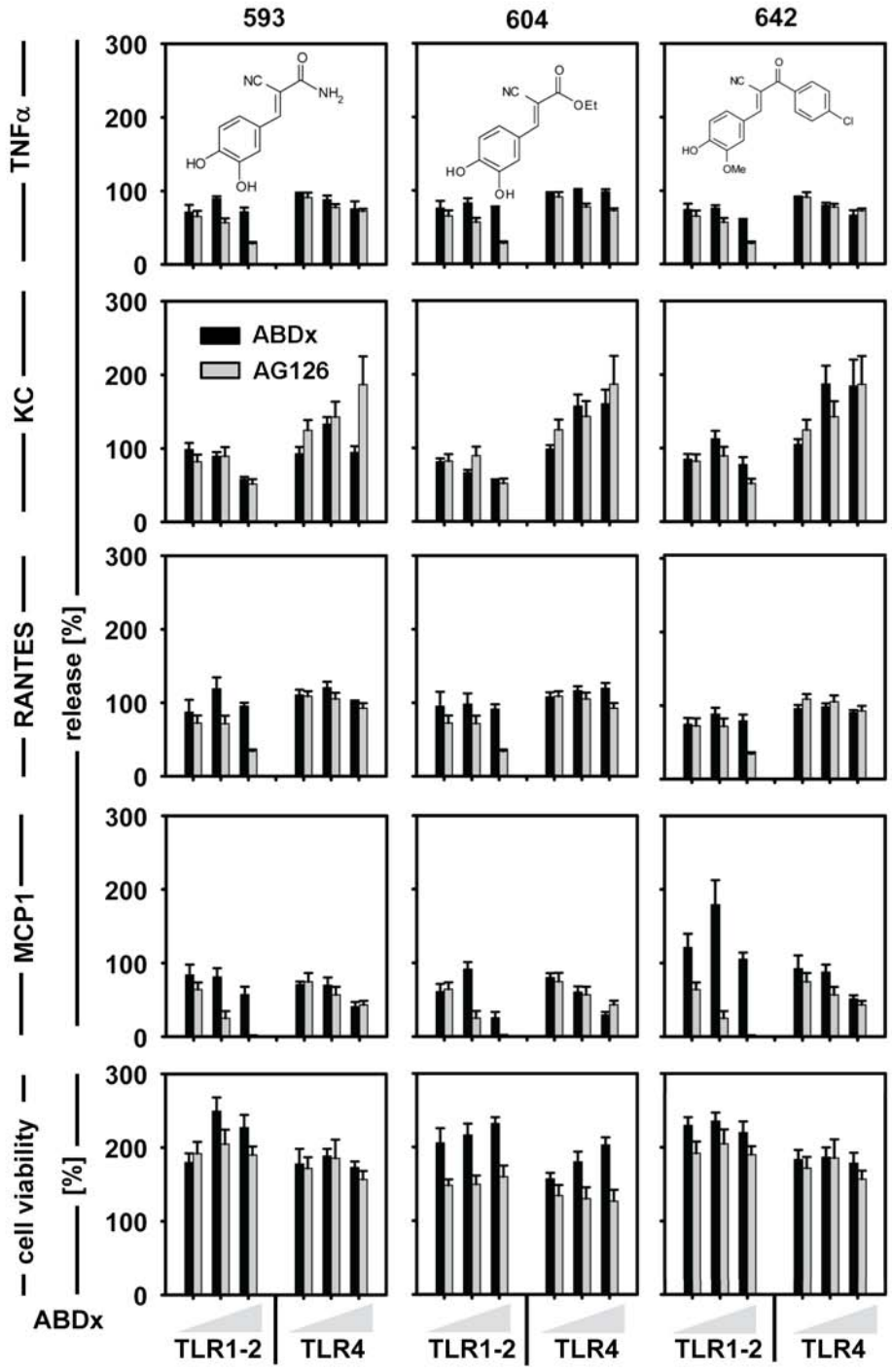

Figure 4.28.: Effect of ABDx with MN residue derivates on TLR-stimulated microglia. Microglia were preincubated with 10, 50 or 100 µM of ABD593, ABD604 or ABD642 or received a medium change for one hour. Subsequently, TLR1-2- and TLR4-stimulated or unstimulated cells (procedure as in Fig. 4.27) were incubated without or with 10, 50 or 100 µM of the respective compound for 18 h. The release activity and cell viability were analyzed as described above. Data are mean ± SEM, with n = 8 as summarized from two independent experiments.

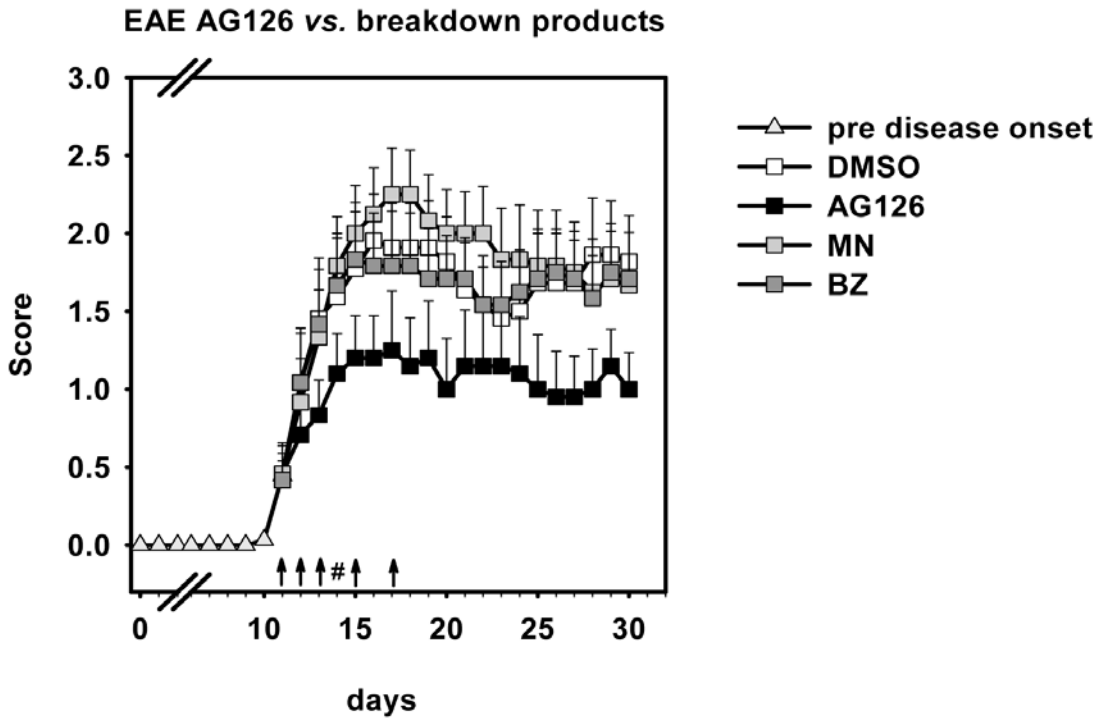

Figure 4.29.: Only AG126, but not MN or BZ, can improve the disease course in EAE. *Wt* C57/BL6J female mice actively immunized with MOG_{35-55} (emulsified in CFA) were treated after disease onset with 500 µg of AG126, MN or BZ (per animal and day, closed, bright and dark gray squares) or DMSO (as controls, open square), with n = 7 per group. Animals were weighted and scored daily for clinical signs of disease on a scale from 0 to 5 depending on the severity (for the details see Material and Methods section 3.2). Arrows indicate the days of treatment. # indicates the day when blood samples were taken for the analysis of cytokines (see the following figure).

(see also Material and Methods) After the disease onset, animals were treated at the indicated days (Fig. 4.29) with 500 µg/day of either AG126, MN, BZ or DMSO, the latter serving as the vehicle for these compounds and thus being taken as control treatment. The severity of disease symptoms was scored daily according to a scale from 0 to 5 (see for the details the Material and Methods section 3.2). On day 14 post immunization, blood samples were taken for cyto- and chemokine analyses. Animals were sacrificed on day 30 and tissue was prepared for histological analyses.

Fig. 4.29 provides an overview of the disease course. The first disease symptoms could be detected on day 11 after immunization. Depending on the treatment, a constant increase in the disease severity occurred up to day 15 (for BZ, 1.83 ± 0.37), day 16 (DMSO, 1.96 ± 0.3) or day 17 (MN, 2.25 ± 0.3, and AG126, 1.25 ± 0.38). Up to day 23, some general improvement of the disease symptoms could be detected (MN, 1.83 ± 0.35, BZ, 1.63 ± 0.27, DMSO, 1.50 ± 0.35 and AG126, 1.1 ± 0.36). Subsequently, a relative constant disease score could be detected until the animals got sacrificed on day 30 (with DMSO, 1.818 ± 0.30, MN,1.67 ± 0.34, BZ, 1.71 ± 0.30 and AG126, 1.00 ± 0.24).

While AG126-treated animals showed always the lowest mean score, BZ and DMSO treatment revealed a more severe and very similar disease progression. The disease course of MN-treated animals was even more severe than for BZ or DMSO (CTL), until day 23. From day 24 on, the disease progression and severity of MN-treated animals was similar to those under BZ and DSMO treatment. Overall, animals with AG126 treatment presented with an attenuated disease throughout the experiment.

As a conclusion, MN could not mimic the therapeutic AG126 effect. This result was also reflected by the histological analysis. Evaluation of the demyelinated areas by LFP-PAS staining revealed that AG126 treatment led to a decreased lesion size, as compared to the DSMO controls, whereas no rescuing effect was noticed for the treatments with BZ or MN (representative tissue section are shown in Fig. 4.30 *A* and *B*).

Selected cytokines were measured in blood samples as taken at day 14 to determine potential systemic influences of the compounds (Fig. 4.30 *C*). Interestingly, in MN-treated animals, IL12p40 levels were lower than in the other groups, including the controls and the animals treated with AG126 (with MN, 154.1 ± 25.8 pg/ml, AG126, 217.0 ± 51.5 pg/ml, BZ, 270.6 ± 51.9 pg/ml and DMSO, 262.6 ± 54.0 pg/ml). Focussing on TNFα, very low amounts were measured, yet the animals under MN showing again the lowest serum concentrations (with MN, 2.8 ± 2.9 pg/ml, DMSO, 9.2 ± 5.6 pg/ml, AG126, 6.7 ± 4.3 pg/ml and BZ 20.5 ± 18.8 pg/ml). The levels of IL6 were highest in the DMSO control animals (with 32.6 ± 6.2 pg/ml), with the AG126-, MN- and BZ-treated animals revealing lower serum contents throughout (AG126, 20.9 ± 3.3 pg/ml, MN 20.8 ± 2.1 pg/ml and BZ 17.9 ± 4.8 pg/ml). Interestingly, AG126 always caused a tendency for lower cytokine levels, even though the decrease did not reach significance. MN revealed even more of a reducing effect, such as in the values of IL12p40 and TNFα.

In Fig. 4.30 *D*, the data of the cytokine levels were plotted against the disease score. From this correlation it is obvious that animals with a lower disease score showed the higher amounts,

independent of their treatment. This phenomenon can be detected for all of three measured cytokines, but the trend is most obvious for IL12p40. From these data we can conclude, that AG126, but not its breakdown compounds MN or BZ, improves the disease course and outcome in EAE mice, represented by the clinical symptoms and the analysis of tissue lesions. While MN may develop some effects in the periphery, and while it was shown to mimic much of the immunomodulatory activity profile of AG126 when directly applied to cells, it fails to deliver the *in vivo* benefits of the complete tyrphostin structure — probably due to a lack of sufficient BBB penetration. The similar mode of action of MN and AG126 on microglia cannot be simply explained by a PTK inhibition. AG126 may hit BTK, but also other signaling elements. At least one of them, however, is then also addressed by MN — which seems to sufficient to interfere with the TLR-induced cyto/chemokine production. For any further development of compounds which such a profound activity in inflammatory diseases (or their models) as it has been demonstrated for AG126, the chemical design needs some elements only provided by the parent structure to reach the CNS and should consider the MN part for cellular efficacy.

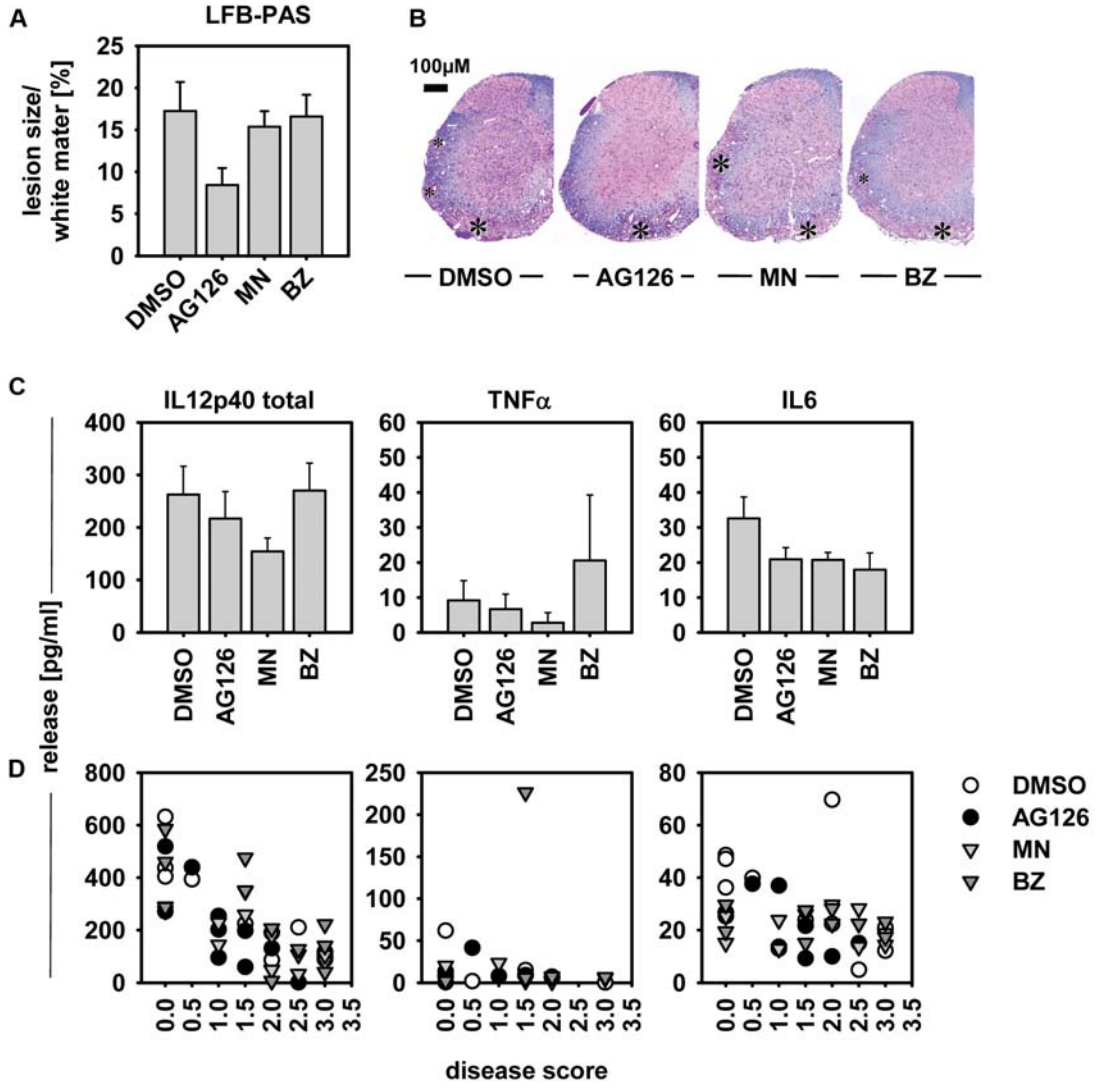

Figure 4.30.: Only AG126, but not MN or BZ, affects CNS lesions in EAE. ***A, B*** Animals were sacrificed on day 30 (see Fig. 4.29) Histological analysis of spinal cord sections was performed to detect demyelinated structures, *i.e.* white matter lesions (LFB-PAS). ***A*** The quantitative analysis of demyelinized spinal cord sections in LFB-PAS-stained slices revealed a tendency for reduced lesion size in AG126-, but not MN- or BZ-treated animals (n = 10 to 12 animals/group). ***B*** Representative stainings from the respective tissue areas. Asterisks indicate lesion sites (pink areas within the blue stained white matter). ***C + D*** Blood samples were taken on day 14. Inflammatory factors, like IL12p40 total, TNFα and IL6, were measured by ELISA in the serum. ***D*** The individual cytokine levels were plotted against the disease score of each animal.

5. Discussion

5.1. Inflammation — protective *versus* harmful consequences

Inflammation is an important response to various infectious and non-infectious challenges which primarily aims at protection. It is required for the host defense against microbes, but can also be mounted in the absence of infectious agents as a process of sterile inflammation. Inflammatory components are, in addition, also playing a role in wound repair. However, uncontrolled or chronic inflammatory processes can come with a substantial damage of the affected tissues. In many cases, the tissue may tolerate these consequences with only minor lasting functional impairment.

In the case of the CNS, however, the special vulnerability of the complex neur(on)al structures as well as the limited capacity for regeneration render (neuro)inflammatory events more likely to cause detrimental outcomes. Even though inflammation as initiated and driven by innate immune cell of the CNS, *i.e.* microglia, may have beneficial effects, inflammation appears to participate in neuropathologies of diverse etiology, including Alzheimer's (AD) or Parkinson's disease (PD), Amyotrophic lateral sclerosis (ALS), multiple sclerosis (MS) and even schizophrenia. Understanding of maladapted microglial response and pro-inflammatory mediators would thus have a substantial impact on potential CNS disease treatments (van Rossum and Hanisch, 2004b). In particular, microglial involvement is known, among others, for PD (Long-Smith et al., 2009), AD (Cameron and Landreth, 2010), ALS (Henkel et al., 2009) or bacterial meninigits (Angstwurm et al., 2004).

5.1.1. Microglia — master of innate immune and inflammatory responses in the CNS

Microglia, the tissue macrophage equivalent 'proper' within the CNS, play central roles in the immune response. Microglia reveal diverse inducible phenotypes as similarly known from the extraneural macrophages (Hanisch and Kettenmann, 2007; Mosser and Edwards, 2008). A specific phenotype 'to start with' depends on the environmental conditions, factors usually present in the extracellular space, *e.g.*, neurotransmitters or ATP. The gross anatomy with or without major myelin tracts or vicinity of the vasculature of varying BBB properties may also contribute

the the tissue adaption of local microglia. Reactive phenotypes, on the other hand, are also instructed differently depending on challenging signals and their context — factors usually absent from a 'homeostatic' tissue, such as DAMPS (fibronectin) or PAMPS (bacterial or viral structures). Their functional options and the gene inductions providing the basis can be diverse while revealing overlap at the same time (Hanisch and Kettenmann, 2007). For the activation and modulation of microglial function, the cell express a wide range of receptors, including PRR's , and among those the TLR's. The range of the microglia-expressed receptors is yet by far bigger and includes also those for glucocorticoids (GC)s or adrenergic signaling. Together they control the activity states of 'resting' and 'activated' microlgia, and they shape the actual reactive phenotype taken by a particular challenge.

Activation of microglia can trigger expression of surface molecules, including antigen-presenting structures for the initiation of adaptive immune responses upon T cell encounter, or the release of reactive oxygen as well as nitrogen species and immunoregulatory signals, such as cyto- and chemokines. The release products of activated microglia can widely and critically influence not only invading leukocytes, but also neuronal and other glial cells. Also by virtue of these pro-inflammatory messengers, microglial activation through their TLR's can bear a significant neurotoxic potential (Butovsky et al., 2005; Schwartz et al., 2006).

Previous work has shown that the tyrphostin AG126 affects the cyto- and chemokine release in microglia and that it exerts anti-inflammatory effects in numerous disease models, including CNS-associated complications. AG126 efficacy was previously demonstrated in the animal model of meningitis in our laboratory (Angstwurm et al., 2004; Hanisch et al., 2001).

In the present work, we showed its beneficial outcomes in EAE, a common model of MS. We addressed in detail how the tyrphostin AG126 — intentionally designed to serve as a PTK inhibitor — acts on microglia.

5.1.2. AG126 as a therapeutically relevant compound

Since the development of AG126 and other tyrphostins, the compounds were tested in both *in vivo* settings and cell culture models (Levitzki, 1992). Besides studies on AG126 in a CNS-associated disease (Hanisch et al., 2001), AG126 was also applied in mice under LPS-induced septic shock (Novogrodsky et al., 1994), in acute and chronic inflammation models employing carrageenan-induced pleurisy or collagen-induced arthritis in rats, in experimental colitis in rats (Cuzzocrea et al., 2000a,b), in multi-organ failure induced by zymosane in rats (Dugo et al., 2002), in renal ischemia/reperfusion injury in rats (Chatterjee et al., 2003), in pancreatitis in mice (Balachandra et al., 2005) and in intestinal ischemia in rats (Marzocco et al., 2006). In these studies AG126 reduced the disease symptoms of the respectively disease models generally associated with a reduced infiltration of immune cells and a reduced production of pro-inflammatory cyto- and chemokines. The present study could also show beneficial effects of AG126 in the animal disease model for MS, *i.e.* EAE, as discussed later (Fig. 4.1, 4.2).

For the validation of molecular effects, AG126 was also tested in various cell culture models,

such as bovine retinal microvasular endothelial cells (Bullard et al., 2003), leishmanial-infected or lipoteichoic acid (LTA)-activated murine macrophages (Chakraborty et al., 2000; Dasgupta et al., 2000; Kao et al., 2005), in platelet-activating factor (PAF)-stimulated human eosinophils (Dent et al., 2000), in oxidative stress of the retinal pigment epithelium (Garg and Chang, 2003), in benzopyrene-induced human embryo lung diploid fibroblasts (Du et al., 2006), in epithelial-like Caco-2 cells (Hosoi et al., 2003) and in the PCW as well as LPS-activated microglia (Kann et al., 2004).

During these studies AG126, was either used as 'general' PTK inhibitor to analyze the involvement of PTK's in diverse pathways (Hirasawa et al., 1999; Wang et al., 1999; Zakar et al., 1999; Dasgupta et al., 2000; Garg and Chang, 2003; Hosoi et al., 2003; Wewers and Sarkar, 2009) or as an assumed inhibitor of ERK1/2 (Bullard et al., 2003; Aramoto et al., 2004; Yu et al., 2005; Du et al., 2006) previously shown by (Hanisch et al., 2001). While many cellular effects were described, no molecular target could be assigned. The PTK was merely deduced from the tyrphostine nature of the compound, and the inhibition of ERK1/2 was not necessarily due to the direct action — leaving potential upstream kinases undefined. Whether a particular or more than one PTK — or any PTK at all — would be affected by AG126, the discrepancy between multiple proven *in vivo* benefits and an enigmatic mechanism of action has been remaining up to now.

5.2. AG126 actions in TLR-stimulated microglia

As the main focus, we aimed at the identification of the AG126-sensitive target(s), mainly in microglia, but assuming that such knowledge would also be generally useful also in other cell types. Previously it was shown in our laboratory that AG126 affected microglia as challenged by TLR agonists. The meningitis-relevant pathogenic structures of PCW contain ligands for TLR1-2 and TLR6-2 (Hanisch et al., 2001). Furthermore, AG126 suppressed the phosphorylation of ERK1/2 in TLRX/2- and TLR4-activated microglia (Hanisch et al., 2001; Kann et al., 2004). So far, there was no detailed analysis regarding the effect of AG126 as to the modulation of immune response profiles of microglia when stimulated *via* TLR's other than TLR4 and TLR2. Now, we could show, that AG126 affects the release of selected, typically pro-inflammatory cyto- and chemokines when cells were stimulated with agonists for TLR1 to TLR9 (Fig. 4.4). Effects on TLR5 could not be demonstrated since microglia did not respond to its agonist, as supported by the lack of TLR5 mRNA. Thus, from the original description of rescuing effects in LPS-challenged mice (*i.e.* septic shock as induced through TLR4) to our present data on several TLR family members, there is a line of evidence for AG126 modulating the signaling of these important innate immune receptors.

5.2.1. TLR-stimulated microglia

Microglia organize reactions to microbial invasion, viral infections and DAMPs by TLR's, as a major family of PRR's. They thus represent essential molecular sensors for the function of microglia to detect exogenous as well as endogenous factors indicating (or occasionally also causing) a homeostatic disturbance. The activation of the different TLR pathways by specific TLR ligands generates a pro-inflammatory release profile, similar to the one known from the M1-like (classical) phenotype of extraneural magcrophages, with little to no induction of anti-inflammatory factors (Fig. 4.4, Mantovani et al., 2002). For example, the expression of IL 10 or MDC (CCL22) known for their anti-inflammatory, immunosuppressive and neuroprotective feature typically products of M2-like (alterantive) macrophage phenotypes, could not be detected (Hanisch, 2002; Mantovani et al., 2002; van Rossum et al., 2008).

A potential attraction of neutrophils by KC (CXCL1) could be observed for most of the TLR- activated microglia, except for Flagellin- (no response at all) and Poly(U)-activated cells. Neutrophils are among the first cells occurring at a site of infection, and besides CXCL2, CXCL1 serves as a major chemoattractant. Furthermore, MIP1α (CCL3) and RANTES (CCL5) are involved in the attraction of T cells, monocytes/macrophages and microglia. Their release was induced upon stimulation of TLR1-2, 3, 4, 6-2, 7/8, 9. Thus, recruitment of further microglia and the attracted infiltration of peripheral monocytes and macrophages across the BBB might be supported (Hanisch, 2002; Guillemin and Brew, 2004). T cell recruitment enables microglia to present antigens by MHC structures. Knowing that all nucleated cells express MHC class I, this study could also show that activation of TLR3 and TLR4 even increased the expression of MHC class I — complementary to CD8 T cell-expressed structures and important for cytotoxic actions of these cells. The expression of MHC class II can also be induced on microglia/macrophages, namely by the Th1 T cell- and natural killer (NK) cell-derived factor, IFNγ (Amaldi et al., 1989; Pazmany et al., 2000; van Rossum et al., 2008). TLR-activation did, however, not induce microglial MHC II expression, as required for a CD4 T cell interaction and 'professional' antigen presentation and thus suggesting a selective enhancement of MHC I only (Fig. 4.8).

Activation of cytokines, like IL6 and TNFα support the initiation and coordination of pro-inflammatory responses and help limiting the spread of infectious agents. TNFα is thereby a pluripotent factor, and interruption with its signaling can be protective in CNS injuries, but can also cause more damage. IL6, on the other hand, has ambivalent inflammatory actions and is often induced upon tissue injury, much like acute phase response elements. However, activation of microglia within AD plaques in combination with factors like TNFα can drive neurotoxic cascades (Hanisch, 2002). We found both to be part of the TLR-inducible profiles. In general, the functional responses upon TLR stimulation agreed with the expression pattern of mRNAs for the respective TLR's. Again, microglia did not express mRNA for TLR5. This fact was consistent throughout with the lack of responses in the Flagellin-stimulated microglia (Fig. 4.4). Previously, Olson and Miller (2004) analyzed the mRNA expression of TLR's as well as selective inductions of cytokines and chemokines as a result of their stimulation. They could also show,

that IFNγ stimulation of microglia up-regulated the expression of TLR5. Cytokines, like IFNγ and TNFα affect the expression of receptors in microglia (van Rossum and Hanisch, 2004b). Thus, it can not be exclude that microglial cells may harbor the potential of expressing also TLR5, under certain conditions at least.

Depending on the TLR's, Olson et al. also described different cyto- and chemokine release patterns, but analyzed them on the mRNA level. The induction of mRNA does not have to correlate with actually released protein amounts. They detected, for example, an up-regulated IL6 mRNA upon Poly(I:C), LPS and CpG ODN stimulation, IL10 induction upon CpG ODN stimulation and TNFα in LPS-activated microglia. In agreement, the TLR-induced release of several of these and additional factors could be seen also in the our study. On the contrary, our study could not detect TLR-induced IL10 release.

5.2.2. AG126-sensitive target(s) reveal a complex involvement in the signaling of TLR-activated microglia

AG126 at higher concentrations was able to down-regulate the cyto- and chemokine release as triggered by TLR stimulation. Exceptions, however, were found with microglia in the LPS and Poly(A:U) experiments (Fig. 4.5). AG126 had also influences on other functions. TLR stimulation reduced the myelin phagocytosis by microglia, as seen with TLR1-2-, 4- and 6-2-activated cells. AG126 treatment could restore the phagocytotic capacity, much to the level of the unstimulated control cells (Fig. 4.9).

On the other AG126 did not affect the expression of MHC structures. The MHC class II expression were not altered by TLR stimulations (Fig. 4.8). Only MHC class I levels were found to be elevated under certain TLR activations. TLR3 and TLR4 agonists were effective — not those TLR1-2 and TLR6-2. This pattern indicates that TRIF is essential, as TLR3 and TLR4 employ this pathway. AG126, however, could not manipulate the MHC I enhancement, an additional hint to the sparing of TRIF signaling as we had deduced from the cytokine and chemokine profiles and the studies in TRIF *ko* animals. Thus, AG126 may counteract overshooting inflammatory responses by microglia without affecting the antigen presentation, and even restoring phagocytotic functions. These TLR effect-manipulating activity profile could be useful in infections, as it would — theoretically — allow for clearance of microbes, while ameliorating the concomitant inflammatory reaction upon microglial encounter of the germs. AG126 would then, however, also affect TLR activations due to DAMPs. These selective AG126-induced effects may serve as an explanation for the reduced development of acute and chronic inflammation in different animal disease models (Hanisch et al., 2001; Cuzzocrea et al., 2000b). Yet phagocytosis of myelin and bacteria can be rather differently regulated, and generalized interpretations of PAMP- and DAMP-triggered effects are not supported by data at the moment.

A detailed analysis of the release experiments revealed a more complex modulatory, rather than simply inhibitory effect of AG126. The biphasic release profiles of some cyto- and chemokines

suggested either a complex involvement of the putative AG126-sensitive target, *i.e.* specific PTK(s), or a multiple hit action. For the latter, also PTK-independent mechanisms had to be considered. Our data, indeed, provide now the support of this concept.

Biphasic release profiles were especially detected for KC upon Pam_3CSK_4-, Poly(I:C)-, MALP and CpG ODN-stimulation, but not in the LPS- or Poly(A:U)-activated microglia. In comparison to TLR-only activated cells, KC release was elevated, when low concentrations of AG126 were applied. AG126 treatment at higher concentrations revealed a strong inhibitory effect. Conceivably, AG126 could specifically affect a single kinase, as involved in more than one step of the pathway organizing the release. Increasing concentrations could then progressively block its activity, which would interfere with conceivably opposite effects on the net release. Such scenarios are imaginable when the PTK would first be needed for induction, then, however, also for negative feedbacks. AG126 could also act on two different kinases, depending on the concentration. In the latter model, the first kinase would have a lower affinity for AG126 and would be involved in the pathway towards release induction. The second kinase, with a higher affinity to AG126, could be involved more in a feedback control, leading to some reduced cyto- and chemokine release. Such a biphasic release profile was seen with AG126 already earlier for IL6 in LPS-stimulated microglia (Hanisch et al., 2001).

Interestingly, AG126 treatment affected the cyto- and chemokine release profiles of LPS- and Poly(A:U)-stimulated cell less than those of Pam_3CSK_4-, Poly(I:C)-, MALP- and CpG ODN-activated cells (Fig. 4.5). Here, highest AG126 concentrations led to an enhanced release of KC and MIP-1α in LPS-treated cells. Only enhanced KC release was observed in Poly(A:U)-activated cells. Furthermore, AG126 had no or just a slight inhibitory effect on the release of the other factors measured in this stimulations. In the case of LPS, this result could be explained by the fact, that the TLR4 signaling pathway is differently regulated when compared to other TLR pathways. Ongoing studies in our laboratory give indications that Poly(A:U) may also signal *via* TLR4 and is, in addition, not superior to Poly(I:C) in terms of a sole restriction to TLR3 (unpublished data). The cyto- and chemokine release was abolished in Poly(A:U)-treated microglia deficient for TLR4. The assumption, that Poly(A:U) signals *via* the TLR3 only derived from the work of Alexopoulou et al. (2001). Later it was shown, that Poly(A:U) also signals *via* the TLR7 (Sugiyama et al., 2008) In comparison to the other TLR's, TLR4 signals alternatively or in concert with two adapter proteins, MyD88 and TRIF. All other TLR's recruit only TRIF. First, there is more cooperatively among the two pathways than originally believed and, second, AG126 would affect the outcomes in TLR stimulations largely through MyD88, but this might come with influences also for TRIF-dependent factors and especially cause mixed consequences when certain factors are controlled by both adaptor protein pathways.

5.2.3. Hierarchical involvement of AG126-sensitive target(s) in TLR signaling

Obvious difference of AG126 effects depending on the specific TLR-activation led to a closer look of the different TLR signaling cascades. This study comes to the conclusion, that the AG126-sensitive target(s) is/are associated with the adapter molecule MyD88, but not with TRIF.

To obtain further information about AG126 effects on the MyD88-independent (TRIF-dependent) signaling pathway, IFNβ release was measured upon a TLR1-2, 4- and 6-2-stimulation. IFNβ production is induced by the activation of TLR3 and TLR4 through the MyD88-independent pathway, which involves the adapter molecule TRIF (Oshiumi et al., 2003b,a). This study also could show that an interruption of the MyD88-independent pathway in $TRIF^{-/-}$ cells led to the lack of the IFNβ release. In agreement with the literature, a reasonable IFNβ release in LPS-activated *wt* cells was detected. However, no significant modulatory effect of AG126 on the IFNβ release could be seen. IFNβ release was still present in $MyD88^{-/-}$ cells. Importantly, this induction was also not modulated by AG126 (Fig. 4.6). Together with the data from the MHC I regulation, AG126 presented with a more TRIF-sparing action.

Focusing on the MyD88-dependent signaling, TNFα and KC release was abolished in $MyD88^{-/-}$ cells (Fig. 4.7). Previously it was shown, that IL6 and TNFα mRNA expression was abolished in LPS-activated macrophages deficient for MyD88 (Kawai et al., 1999). This study could show, that the MyD88-dependent release of KC, TNFα and IL6 was suppressed in microglia, at least for TLR's signaling exclusively through MyD88 (Fig. 4.5). The data thus indicated the location of an AG126-sensitive target within or in association with the MyD88-dependent pathway.

It was next analyzed whether the AG126-sensitive target would be up- or downstream of NFκB and MAPKs, as they are elements in the chain of command of TLR signaling (see the schema in Fig. 1.1). Therefore, the activation (in terms of phosphorylation) of NFκB, JNKs, $p38^{MAPK}$ and ERK1/2 upon TLR1-2, 3, 4 and 6-2 stimulation was measured (Fig. 4.10). NFκB reveals a very complex involvement in the TLR signaling cascades (Akira and Takeda, 2004). Yet our data did not show any AG126 effect on TLR-induced NFκB activation (Fig. 4.10).

With regard to the MAPKs, AG126 was able to affect some of their activation in a, however, quite complex manner. We found that the phosphorylation of JNKs could not be inhibited by AG126 in microglia as activated through different TLR's. AG126 rather delayed the activation of JNKs. Delayed activation of JNK could, indeed, be seen in macrophages deficient for MyD88 (Kawai et al., 1999). Thus, an effect in a MyD88-dependent fashion was the cause of the time shift in our study. The assay used here covered the phosphorylation of various isoforms. Previous studies have shown that TLR4-activated microglia present with a distinct activation the respective isoforms, *i.e.* JNK1, 2 and 3 (Waetzig et al., 2005). In this publication, we found back then a revealed up-regulation of JNK2 upon a microglial TLR4 activation. The present study could show that TLR1-2 stimulation also activated JNK2 phosphorylation in microglia (Fig. 4.11). Interestingly, in unstimulated cells, AG126 caused a JNK2 activation as strong as

in TLR-activated microglia.

JNK(s) get(s) activated by MKK7 (Tournier et al., 1997). Although some AG126-sensitive target would not directly be localized upstream of MKK7, AG126 had an influence on the activation of JNKs. How could this still be conceived? AG126 effects on unstimulated cells were previously shown by Kann et al. (2004). In this additional study from our group, AG126 reduced the basal $[Ca^{2+}]_i$ in unstimulated microglia. A direct link to activation events on JNKs could be possible. A calcium-mediated activation of JNKs was shown in J774A.1 murine macrophage cells (Kim and Sharma, 2004). However, cadmium treatment of the cells led to a rise $[Ca^{2+}]_i$ and a subsequent activation of JNKs, whereas in our study AG126 treatment increased the JNK2 phosphorylation level in TLR-unstimulated microglia, where — according to Kann et al. — AG126 lower the $[Ca^{2+}]_i$. So, whether $[Ca^{2+}]_i$, is linked to JNK activation cannot be clarified at this stage.

A suppressive effect of AG126 on the phospho-p38α^{MAPK} (Thr180/Tyr182) could be detected by our protein array (human specificity with murine cross reactions), but not by the phospho-p38α^{MAPK} (Thr180/Tyr182) ELISA-based analysis (murine specificity).

Similarly divergent results were obtained for the ERK activation analysis. An ERK2 activation could be suppressed by AG126 in TLR1-2-activated microglia, analysed by the phosphorylation array. The phospho-specific ELISA did not show AG126 effects on ERK1/2 phosphorylation upon TLR-stimulation. Activation of ERK1/2 in the presence of AG126 upon microglial stimulation with PCW (TLR2) and LPS (TLR4) was investigated earlier (Hanisch et al., 2001), indicating some AG126 effect.

Interestingly, AG126 effects on unstimulated cells could also be seen for GSK-3α/β, RSK1 and RSK2. All these kinases revealed phosphorylation levels as high as in the TLR-activated microglia (Fig. 4.11). They are known to be localized downstream of ERK1/2 and p38^{MAPK}, respectively (Anjum and Blenis, 2008). Ananieva et al. (2008) showed that MSK1 and MSK2 are key components of negative feedback mechanisms needed to limit TLR-driven inflammation. MSKs are closely related to RSKs (in our study affected by AG126). Both belong to the class of cAMP-dependent protein kinase/protein kinase G/protein kinase C (AGC) family of kinases (Proud, 2007). They seemed to be involved in some negative feedback of TLR signaling — phosphorylation levels of all these kinases were down-regulated in TLR-activated cells treated with AG126, in comparison to the TLR-only activated microglia.

Thus, the results are not unequivocally pointing to or against an AG126 effect. The detection of or bias for an isotype or subversion of MAPK can play a rather relevant role, as shown in the case of JNKs (Waetzig et al., 2005). AG126 does affect MyD88-controlled genes, and some MAPK pathways could be targeted further downstream of their level. Thus, lack of effects for MAPK themselves does not exclude that genes controlled through them are not influenced. However, for the localization of a target for AG126, the questions remained not really answered as to whether some upstream impact would be involved. It was thus still hypothesized that an AG126-sensitive target might be localized upstream of MEK1/2, and even MKK3/6, both being the activators of ERK1/2 and p38^{MAPK}, respectively (Denhardt, 1996; Moriguchi et al., 1996).

The effects observed with otherwise unstimulated (not TLR agonist-treated) cells lead to the conclusion that AG126-sensitive target(s) would be constitutively expressed, and assuming that AG126 is an inhibitor for a PTK, we searched for one which could be involved in the TLR signaling — in association with MyD88, and probably rather proximal to the adapter protein.

5.3. Tyrosine kinases and TLR signaling

While many PTK's play a central role in the innate immunity, only few are known be involved in the TLR signaling. However, a range of PTK's like Tec family members (BTK, Bmx/Etk), Src family members (*Lyn, Hck, Fgr*) and tyrosine phosphatases (CD45) modulate the TLR signaling which results in an pro-inflammatory cytokine response (Johnson and Cross, 2009).

Activation of TLR's can induce the phosphorylation of tyrosine residues on TLR's and MAL in TLR2 and TLR4. MAL phosphorylation is caused by the BTK (Gray et al., 2006). Interaction of Bmx with the MAL and MyD88 was reported recently (Semaan et al., 2008). The responsible PTK for TLR phosphorylation still has to be elucidated, although the Src family kinases were implicated, identified by Src family kinase inhibitors and mutational analysis. These inhibitors affect the TNFα release, the activation of NFκB and (other) transcription factors (Orlicek et al., 1999; Ferlito et al., 2002; Napolitani et al., 2003; Sarkar et al., 2003).

5.3.1. A putative target for AG126

The expression of 21 PTK's, including receptor PTK's, non-receptor PTK and kinases of the Src family members (hck and fgr) have been for activated microglia (Krady et al., 2002). Kann et al. (2004) had postulated several potential candidates when studying the calcium regulation by AG126 in the context of TLR's. Among them, we also kept the BTK as a potential target, due to several criteria. Functional proximity to TLR's, constitutive presence in the cells, a role in calcium regulation and finally some preferential association with MyD88 — all these aspects should be found for the potential PTK, the fact to be a PTK coming from the assumed inhibitor action of a tyrphostin. In the present study, the expression of BTK in microglia could be shown at mRNA level by real time-PCR, whereas its detection as a protein was extremely challenging (data not shown). We thus also considered functional interference, based on the (only) known BTK inhibitor, LFM-A13, as previously also shown in microglia (Mahajan et al., 1999; Shideman et al., 2006).

5.3.2. BTK as a putative target

The BTK is a kinase well investigated in the BCR signaling, but also known to be involved in the TLR functions (Brunner et al., 2005). The BTK belongs to the Tec family kinases and is characterized by an N-terminal plecktrin homology (PH) domain as well as Src homology regions SH3 and SH2. The PH region allows its binding to the membrane, the SH3 and SH2

support interactions with proline-rich protein sequences and binding to sequences harboring phosphorylated tyrosine residues, respectively. These adapter sequences give then rise to complex interactions (Brunner et al., 2005).

In B cells of X-linked agammaglobulinaemia (XLA), a defect in BTK causes that the mobilization of Ca^{2+} is impaired in response to BCR activation (Genevier and Callard, 1997). Regulatory functions on $[Ca^{2+}]_i$ have been also shown for the AG126-sensitive target in our microglia cells (Kann et al., 2004). The elevation of the basal $[Ca^{2+}]_i$ in LPS- (TLR4) and PCW-treated (TLR2) cells can be prevented by AG126. BTK is involved in the TLR signaling of TLR2, TLR4, TLR8 and TLR 9 (Gray et al., 2006; Doyle et al., 2007). Furthermore, TLR2 activation also requires Ca^{2+} influxes to induce NFκB activation (Chun and Prince, 2006). In BCR signaling, NFκB is repressed in cells deficient for BTK (Bajpai et al., 2000). Our study could show, that TLR stimulation leads to the activation of NFκB, as expected (Fig. 4.10). However AG126 was not able to affect its activation (Fig. 4.10).

Horwood et al. (2006) demonstrated, by using XLA peripheral blood mononuclear cells, that BTK is needed for TNFα, but not IL6 expression in TLR2- and TLR4- stimulated cells. Consistently, this study was able to show that AG126 affects the TNFα release on TLR2- stimulated microglia. Inconsistently, AG126 could also affect the release of IL6 in TLR2-stimulated cells, but neither the release of TNFα nor that of IL6 in TLR4-activated microglia (Fig. 4.5). A possible reason for this difference could be the different cell types and lines. Indeed, there is growing evidence for differential organizations of TLR's varying by the cell type, such as endothelial, dendritic or mast cells, macrophages and — indeed — CNS microglia.

As a more straight forward approach, the comparison of the effects of AG126 and the specifically designed BTK inhibitor LFM-A13 (Mahajan et al., 1999) on TLR-activated cyto- and chemokine release suggested that BTK could not explain the AG126 activity spectrum, since both compounds behaved quite divergent (Fig. 4.12). However, analyzing AG126 effects on the BTK kinase activity directly, AG126 was confirmed to inhibit its enzymatic function. The peptide phophorylation assay revealed quite similar effects as obtained with LFM-A13. Interestingly, both developed inhibitor effects at considerably high concentrations (Fig. 4.13). It could well be that the specific assay conditions, namely the use of an already active BTK, deliver some artificial results and that both compounds would be more potent when studied within an intact natural environment. As another possible explanation, we considered degradation of the compounds in aqueous media, which could lower the effective concentrations and thereby affect the enzymatic inhibition.

To confirm this the inhibitory effect in more natural setting, AG126 was applied to the BTK manipulation in BCR-activated B cells. BTK is involved in the BCR signaling and mediates the activation of PLCγ2, which in turn plays a role in the calcium regulation (Takata and Kurosaki, 1996). Indeed, AG126 and LFM-A13 were able to prevent the phosphorylation of the PLCγ2, taken as the readout of BTK inhibition (Fig. 4.14).

Surprisingly, inhibitory effects were detectable in human but not in mouse B cells — for both compounds. Species barriers may lead to distinct access to the BTK in the complex BCR

arrangements, resulting in a different effectiveness of the inhibitory compounds. Importantly, proven efficacy as well as failure to demonstrate BTK effects were thus always applying to AG126 and the established BTK inhibitor.

Taken together, AG126 is able to inhibit the BTK activity within and outside of cellular systems. Yet the microglial effects of AG126 could not be reduced to BTK — and we thus had to evaluate alternative, PTK-independent mechanisms.

5.4. Alternative mechanisms of AG126

Tyrphostins as a novel class of PTK inhibitors were originally designed as chemotherapeutic agents to fight cancer. PTK's have a plethora of regulatory functions in signaling cascades of metabolism, cell proliferation, angiogenesis and immune system of multicellular organisms. PTK malfunction can lead to diseases with their abnormal activity affecting whole signaling pathways (Levitzki and Mishani, 2006). During the developmental process, tyrphostins were synthesized and tested for selective inhibitory capacity on epidermal growth factor receptor (EGFR) kinase, leading for example to AG18 and AG213, also known as RG50864 and RG50810 (Yaish et al., 1988; Gazit et al., 1989; Lyall et al., 1989). For other tyrphostins, additional specific PTK's targets could be assigned, such as for AG879 to nerve growth factor pp140^{c-trk} (Ohmichi et al., 1993), AG490 to Jak2 (Meydan et al., 1996) and AG1295 to the platelet derived growth factor receptor (Kovalenko et al., 1994). However, most if not all the specific inhibitory effects of these tyrphostins were determined in special assay systems.

Over the years, additional PTK-independent functions could be observed, especially in cellular systems. Antioxidative features, decoupling functions on oxidative phosphorylation and binding capacities to hormone receptors could be shown for certain tyrphostins.

We thus raised the question whether PTK-independent modes of action could also help explaining the biological profile of AG126. Antioxidative properties for AG126 as shown for the JAK2 inhibitor AG490/B42 (Gorina et al., 2007) or AG18 and AG82 (here named as A23 and A25, Sagara et al., 2002 were not tested because AG126 does not exhibit quinone-like structures. Of course, a chemical degradation or metabolic modification of AG126 in an aquous environment or by enzymatical conversion in a cell cannot be ruled out fully to also lead to a compound with antioxidative features. Yet reactions towards such a structure are not obvious and we, therefore, rendered antioxidant mechanisms unlikely.

5.4.1. AG126 does not act as a decoupler

Oxidative phosphorylation guarantees the synthesis of ATP by ATPase in mitochondria. The reactions of electron transport, providing energy for ATPase activity, and phosphorylation of ADP to ATP by ATPase are coupled. Decoupling substances have the ability to separate these two processes and to thereby suppress the ATP synthesis (Fig. 2.1). Tyrphostin AG17

(A9 or SF6847) can decouple the respiratory chain (Terada, 1990). Tyrphostin AG10 and AG18 are also able to act as mitochondrial uncouplers (besides inhibitory functions on EGFR autophosphorylation and antioxidative features, Sagara et al., 2002; Soltoff, 2004). Because of these published effects, we examined such potential functions for AG126.

Using JC-1 for a membrane potential-depending fluorescence staining of mitochondria in TLR-activated or control microglia with and without AG126 treatment, we could not detect a clear effect. For a potent uncoupler a dissociable group and a hydrophobic moiety (given by BZ residue) as well as a strong electron withdrawing group are required (given by the MN residue, Terada, 1990. Yet for AG126, no decoupling property seemed to play role (Fig. 4.15).

In contradiction to our results, Sagara et al. (2002) concluded from there experiments that AG126 acts as a mitochondrial decoupler. They induced cytotoxcicity in the hippocampal neuronal cell line HT-22 by glutamate treatment, causing cell death as well as membrane disruption, with a low JC-1 monomer/aggregate ratio. Tyrphostins A9 and AG126 were able to increase the JC-1 monomer/aggregate ratio as the known decoupler FCCP (cyanide p-trifluoromethoxyphenylhydrazone) did. Different to our experimental setup, they dissolved the tyrphostins in Me_2SO instead of DMSO. Furthermore, Sagara et al. tested cells in a state of oxidative stress, caused by glutamate and following excessive production of ROS in mitochondria (Davis and Maher, 1994). ROS accumulation is caused by insufficient ROS elimination. Our microglia, however, were in a 'endangered' and activated state, but not in a cytotoxic environment. Nevertheless, AG126 may affect mitochondrial functions, even though not like a classical decoupler. Regulation Ca^{2+} influx (Tan et al., 1998) and $[Ca^{2+}]_i$ could be an AG126-relevant feature. In this regard, our earlier observations on $[Ca^{2+}]_i$ may require some re-consideration (Hoffmann et al., 2003; Kann et al., 2004).

5.4.2. AG126 does not signal *via* the GR

For some 'master template' tyrphostins, such as the genistein (inhibits EGFR $pp60^{v-src}$ and $pp110^{gag-fes}$, Akiyama et al., 1987), PTK-independent functions are known. The compound was originally known as a phytoestrogen ligand to the estrogen receptor (Martin et al., 1978). Later on, Young et al. (1993) published genistein to have inhibitory effects on the fatty acid synthesis, lactate transport, mitochondrial oxidative phosphorylation as well as on aldehyde dehydrogenase.

We considered AG126 to probably use the steroid receptor, the GR in microglia, for intracellular signaling. Indeed, GR expression in microglia and GR interaction with TLR's in macrophages were previously shown (Sierra et al., 2008; Ogawa et al., 2005). Protective functions of GRs during innate immune responses, also in the brain, have been described (Glezer and Rivest, 2004)

GRs are ligand-induced transcription factors that are localized in a non-active state in the cytoplasm, in association with some heat shock proteins (hsp) 90, 70 and 56 (Pratt, 1993). Ligand binding leads to a conformational change, dissociation from the hsp complex and translocation

to the nucleus (Picard and Yamamoto, 1987). GR then influence gene transcription by binding to the GC response element or by the interaction with transcription factors (Nancy Ing and O'Malley, 1995).

In agreement with a AG126 effect, GR modulation is regulated by the TLR adapter protein MyD88. LPS activation of IRF3-dependent genes, that were dexametasone (dex)- sensitive in *wt* macrophages became dex-resistant in MyD88*ko* cells (Ogawa et al., 2005). This study revealed that dex was able to repress the release of TNFα and KC in TLR1-2- and TLR6-2-activated cells, quite similar as AG126 did. In some contrast to AG126, dex also repressed the release activities of TLR4-activated microglia (Fig. 4.18).

Moreover, the aziridine precursor from the African shrub *Salsola tuberculatiformis Botschantzev*, CpdA, is able to bind to the GR, although it has no steroid structure, but rather a tyrosine-related one. As a GR ligand, this compound is able to mediate gene-inhibitory effects on TC10 endothelial cells (De et al., 2005). In the TLR-activated microglia, CpdA revealed then a similar release profile as described for AG126. Interestingly, while CpdA repressed the release in Pam_3CSK_4- and MALP-activated microglia, it could not repress the release of KC and TNFα in LPS-activated cells — another striking parallel to AG126. High concentrations of CpdA were toxic to microglia, as it decomposes into aziridine intermediates known to act as alkylating pro-apoptotic agents (Fig. 4.18; Wüst et al., 2009).

Despite similar impacts on the release profiles obtained with CpdA and AG126 and the tyrosine relatedness of both compounds, GR*ko*-based studies excluded a potential action of AG126 *via* the GR signaling pathway (Fig. 4.19).

5.4.3. AG126 does not act *via* adrenergic receptors

Noradrenaline (NA) is a stress hormone as well as a neurotransmitter and is known — along with adrenaline — for its impact on the 'fight or flight' response of the autonomic nervous system. NA is primarily produced by the *Locus caeruleus* in the CNS, and by the adrenal gland in the periphery, and signals *via* the adrenergic receptors. The amino acid tyrosine is the starting product for its biosynthesis. Regarding its tyrosine-related structure, the question arose whether AG126 may signal — similar to NA — through the adrenergic receptors. Many aspects support the idea that AG126 may act in a comparable fashion.

In the periphery, NA is known to modulate innate immune function, *e.g.* phagocytosis and TNFα response of macrophages (Gosain et al., 2006; García et al., 2003; Hu et al., 1991; Spengler et al., 1994). As a neurotransmitter, NA has excitatory and modulating functions on neurons (Benarroch, 2009). NA has also modulating functions for inflammatory gene expression in the brain and, thereby, influences CNS diseases, including also MS, AD or PD. It reduces cytokine expression in microglial, astroglial and brain endothelial cells *in vitro* (Feinstein et al., 2002). Influences of NA on microglia have been documented several times (Colton and Chernyshev, 1996; Färber et al., 2005; Prinz et al., 2001). The expression of the respective adrenergic receptors (α1, α2, β1 and α2 receptors) for (nor)adrenalin on microglia was previously shown (Mori et al.,

2002; Tanaka et al., 2002). We confirmed such patterns for our own microglial preparations (van Rossum, unpublished).

In accordance with reports of Prinz et al. (2001); Feinstein et al. (2002); Heneka et al. (2010), to which our group contributed, the present study could show, that NA is able to reduce the release of diverse pro-inflammatory cytokines in a TLR-activated microglia (Fig. 4.16). We thus assumed that AG126, like NA, could act as a adrenergic agonist. However, experiments involving antagonists could not confirm such AG126 activity. The studies were based on Pam_3CSK_4-activated microglia, but ruled out the $\alpha 1/\alpha 2$ or $\beta 1/\beta 2$ adrenergic receptors to mediate the suppressive influence of the tyrphostin (Fig. 4.17).

5.5. AG126 as a precurser

The need for high concentrations of AG126 to be active in the inhibition of BTK may also be caused by the degradation of the compound (Fig. 4.13, 4.14). Photoinstability of tyrphostin RG13022 and RG12462 was demonstrated by Kumar et al. (1995). Similarly, Ramdas et al. (1994) published that the degree of inhibition of the respective PTK by tyrphostin 23 and 25 (AG18 and AG82) related to their instability. The degradation product inhibited the proto-oncogene proteins $pp60^{C-Src}$ then even more potent than its parent structure. Therefore, AG126 was always kept in the dark to minimize light-driven conversion of the compound. Cell culture experiments were generally performed under dimmed light. Importantly, when AG18, AG82 and AG126 were diluted in aqueous solutions, *i.e.* culture medium, chemical conversion could be confirmed by spectral analysis.

NMR analysis confirmed the AG126 instability and its degradation to more than one product. In particular, a formation of 3-hydroxy-4-nitrobenzaldehyde (BZ) could be confirmed (Fig. 4.21, 4.22). Previously, BZ was published as a chromophoric substrate for probing the catalytic mechanism of horse liver alcohol dehydrogenase (MacGibbon et al., 1987) and as a starting product for the synthesis of the anti-rheumatic agent epoxyquinomicin B (Matsumoto et al., 1998). Subsequent NMR analysis confirmed AG126 instability and its degradation to more than one product. The formation of 3-hydroxy-4-nitro-BZ could be confirmed.

Conversion of AG126 to BZ led to the assumption that the stoichiometric by-product malononitril (MN) should also is present. The use of MN as a pharmacological substance is not documented in the scientific literature. Nowadays, MN is described as a starting structure for the synthesis of many pharmacologically and agrochemically active compounds. In the 1950ies, however, MN and substituted MNs were tested for effects on tumors. This is quite an interesting parallel to the original intention of further developing tyrphostins as anti-cancer drugs. Indeed, some substituted MNs retarded the growth of certain transplanted tumors in mice (Gal and Greenberg, 1951).

Gal et al. (1952) analyzed the effect of MN on rhodanase in normal and tumor-bearing tissue and found that MN neither inhibited the rhodanase activity nor competitively displaced cyanide.

Also, the effect of MN administration was tested as to the excretion of thiocyanate in normal and Walker carcinoma 256-bearing rats (Greenberg, 1953). Here, a shift of maximum thiocyanate excretion was observed in tumor-loaded rats treated with nitro-substituted MN products (as AG126), but not MN or benzal-MN. Electron microscopic observations in spinal ganglion cells of the grass frog (*Rana pipiens*) showed several structural changes of the endoplasmatic reticulum, the Golgi complex and mitochondria following injection (*i.p.*) of MN (Anderson and van Breemen, 1958).

Comparing BZ and MN with AG126 as to their effects on the cyto- and chemokine release in TLR-stimulated microglia, MN clearly mimicked much of the AG126 profiles, while BZ did not affect the release. These data underline the present hypothesis that AG126 may reveal PTK-independent cellular functions. Interestingly, the MN motif, but no BZ structure, was needed to cause the modulation as seen with the parent formula (Fig. 4.23). This leads to the conclusion that AG126 is rather the precursor of the active compound and that the modulation of TLR signaling, *e.g.* towards the cyto- and chemokine inductions, is not caused by a PTK inhibition.

5.6. Tyrphostins as MN donors

Gazit et al. (1989, 1991) synthesized a broad range of tyrphostins. Subsets of them have the MN residue in common. Potential biological effects were examined as to their inhibitory activities for PTK's, especially EGF receptor kinase by *in vitro* approaches. The stability of these compounds in aqueous solution has not been reported yet. However, performance of assays with short durations may not reveal a stability-dependent potential of PTK inhibition. There, it was noted that Compound 15 showed quite a good inhibitory activity. However, less activity in intact cells was noted, which can be explained by a reduced permeability or rapid metabolization. In addition to their PTK-inhibitory capacity, these compounds may thus also have PTK-independent effects when entering water-based media or cellular system. It could well be that sharing the precursor potential for MN has an impact on their performance, still varying by the degree of MN donor activity, which in turn depends on the in/stability.

The findings of pharmacological actions of MN in this study led thus to the question whether — besides AG126 — other tyrphostins could modulate the release. Indeed, the tested tyrphostins revealed a similar modulatory cyto- and chemokine pattern as AG126 did (Fig. 4.26). It has, therefore, to be considered that the physiological outcomes of tyrphostin treatments are probably not exclusively caused by the (assumed or verified) PTK target inhibition, but also *via* PTK-independent mechanisms, such as by MN for potential MN donors. The individual substituents at the benzen structure may then influence the stability of the respective tyrphostin — in addition to the structural variations influencing the substrate competition.

This idea is supported by Turpaev and Drapier (2009). They tested AG126 upon expression of NO-dependent genes in U-937 monocytic cells. They came to the conclusion that the gene induction capacity of AG126-like tyrphostins is not related to the inhibition of PTK's. They

thereby showed AG126 activator properties regard to the expression of heme oxygenase 1 (HO-1), H-ferritin, activating transcription factor 3, IL8 and further NO- and redox-regulated genes. Structurally related tyrphostins, such as AG9, AG10, AG18 and AG1288, were also able to up-regulate the expression of HO-1 and of several other genes, but with less efficacy. In contrast, AG30 and AG490 were ineffective for regulating gene expression. The authors further argue, that for transcriptional activation of target genes, the presence of either the 4-nitro or 4-methoxy groups in the benzene ring and two CN-groups of the MN residue are most important. Indeed, all functional compounds revealed a MN residue.

As previously discussed, several PTK-independent effects as antioxidant, decoupler or hormone receptor ligand could be assigned to several tyrphostins already. We present MN as the offspring of AG126 and thus offer a common mechanism of action for potential donors — serving as the main or as an add-on feature. The identification of the ultimate target of MN represents thus a major goal of our future research.

5.7. AG126 as a potent modulator of the clinical course and tissue consequences in EAE — a function not matched by MN and BZ

The tyrphostin AG126 has beneficial properties in many animal disease models, including septic shock and bacterial meningitis (Novogrodsky et al., 1994; Angstwurm et al., 2004). With the present work, it could be shown that AG126 also improves the disease outcome in EAE, the established animal model for MS (Fig. 4.1 and 4.2). No toxicity was seen during the treatment of AG126. This is in agreement with the observation of Brenner et al. (1998), who tested the toxicity of AG126 by daily injections in mice. Furthermore, these authors also demonstrated some suppressive effects for tyrphostin AG556 in EAE.

For AG126, the time point of treatment is essential to produce an improvement of disease symptoms. While preventive treatment delayed the onset of the disease (symptoms), therapeutic treatment reduced the disease severity. In contrast to many experimental set-ups, AG126 thus effectively attenuated the disease outcome after the onset of symptoms (Fig. 4.1, 4.2, 4.29). Such an option, *i.e.* to treat an established disease, meets the desired time window for treating human diseases. In humans, a therapeutic interference usually starts when clinical signs already surfaced. Moreover, in contrast to many animal research-derived approaches based on gene knockouts, AG126 offers pharmacological treatment of a diseases.

The MS/EAE disease pathology is reflected by the formation of focal inflammatory demyelinating lesions in the white matter (Gold et al., 2006). AG126 was able to reduce the size of such demyelinated areas (Fig. 4.1, 4.3). Furthermore, it was then tested if one of the AG126 breakdown products, MN or BZ, would be sufficient to improve the disease outcome. Neither

MN nor BZ, however, influenced the disease score or lesion size (Fig. 4.29, 4.30). From all of these findings it can be concluded that MN on its own cannot deliver the beneficial effects and that the BZ part of the AG126 is required as the 'carrier' — or in better words, AG126 has to act as the precursor. Upon presence at and in the cells, MN is active and can unfold a repertoire of effects as observed with the AG126 as the parent compound. Thus, tyrphostin AG126 itself remains an interesting candidate for the development of anti-neuroinflammatory drugs.

5.7.1. Microglia in MS/EAE

Currently, the involvement of microglia cells in the pathology of MS is a point of discussion (Napoli and Neumann, 2009). On the one hand it is believed that microglia have neurotoxic properties in the disease, on the other hand it becomes clear that the microglia cell plays a central role in neuroprotection through the release of factors that stimulating the neural repair. As phagocytes, microglia are able to remove apoptotics cells and debris at the lesion site, the latter being a prerequisite for attempts of remyelination.

Reduced myelin phagocytosis, up-regulated MHC class I expression and up-regulated secretion of pro-inflammatory cyto- and chemokines could be shown for the TLR-stimulated microglia (Fig. 4.4, 4.8, 4.9). AG126 managed to reverse the capacity of myelin phagocytosis to the level of unstimulated microglia, whereas it had no effect on the MHC expression (Fig. 4.8). Furthermore, AG126 treatment repressed the pro-inflammatory cyto- and chemokines of TLR-stimulated microglia (Fig. 4.5). In conclusion, AG126 enables the microglia to suppress the pro-inflammatory phenotype and may, therefore, help to increase its capacity of debris removal, without concomitant inflammatory activation. So, AG126 seems to be a feasible drug to treat disease situations with chronic inflammation by suppressing the establishment of a pro-inflammatory environment.

5.7.2. TLR's in EAE

The expression of TLR's could be shown for all neural cells, microglia (Olson and Miller, 2004), oligodendrocytes (Bsibsi et al., 2002), astrocytes (Bowman et al., 2003), as well as neurons (Tang et al., 2007). The involvment of the TLR signaling in EAE could be shown by Prinz et al. (2006). Mice deficient for the adapter molecule MyD88 do not develop EAE. Furthermore, a decreased clinical score could be shown for TLR4 and TLR9 deficient mice (Prinz et al., 2006).

Using microglial cell culture experiments, it could be shown that AG126 dramatically reduces the release of pro-inflammatory cyto- and chemokines of activated TLR's as signaling *via* the MyD88 adapter protein. AG126 has a more modulatory than repressive effect on the release induction by certain TLR's, especially when their signaling operates through MyD88 and/or TRIF (Fig. 4.5, 4.6). Nevertheless, AG126 may diminish cellular responses and the disease outcome in our model by affecting largely MyD88-controlled cascades.

The exact mechanism of TLR signaling in MS is still largely enigmatic, because of the absence of infectious agents *in vivo* (Sospedra and Martin, 2005). Yet, in the animal model of EAE, the

disease is actually induced by the help of Freund's complete adjuvant, containing *Mycobacterium tuberculosis* as a gram-positive bacterium — which mainly serves to activate TLR's (Stenger and Modlin, 2002). In EAE and MS, the roles of TLR's are certainly complex, also due to the likely engagement of endogenous factors with TLR activity (Hanisch et al., 2008; Zhang and Schluesener, 2006). DAMP-like ligands may not only initiate and/or further enhance inflammation in such CNS autoimmune diseases by acting on innate immune cells — TLR's are more and more reported for actions on lymphocytes, the carriers of adaptive immunity (Carpentier et al., 2008; Hanisch et al., 2008). Compounds, like AG126, may thus even prove of additional value.

5.8. Promising clues could lead to further AG126-relevant targets

Despite the detailed analysis of mechanisms as presented in this work, the PTK-independent target of AG126 or AG126-derived products still needs to be found. A PTK-independent target is assumed, since MN affected the cyto- and chemokine release in TLR-activated microglia in the same fashion and as potent as AG126 — without bearing a tyrosine-related structure. Our previous and preliminary data, in combination with hints from the literature, indicate that AG126-sensitive signaling elements or those affected by AG126 degradation products could localize in Ca^{2+}-regulatory mechanisms as active in mitochondria or the ER. Structural changes of the ER, the Golgi complex and mitochondria were observed for MN (Anderson and van Breemen, 1958), and we had published on impacts of AG126 in microglial calcium mechanisms (Hoffmann et al., 2003; Kann et al., 2004).

5.8.1. Calcium regulation and AG126

Ca^{2+} is a highly versatile signal in cellular systems (Berridge et al., 2003). Microglial TLR4 activation leads to a chronic elevation of basal $[Ca^{2+}]_i$ as required for the release of IL12, IL6 or KC. It also suppresses the UTP- and C5a-induced Ca^{2+} signals, detectable in unstimulated cells (Hoffmann et al., 2003). AG126 prevents the TLR-induced elevation in basal $[Ca^{2+}]_i$ and the suppression of C5a- and UTP-evoked calcium signals. Furthermore, AG126 could lower the basal $[Ca^{2+}]_i$ even in unstimulated microglia. Effects of MN on $[Ca^{2+}]_i$ should thus be analyzed in the future.

Ca^{2+} signaling plays a central role in cell survival and death (Orrenius et al., 2003). Signaling Ca^{2+} is derived from either internal stores (ER) or from the external medium. The release of intracellular calcium is controlled by Ca^{2+} itself or a series of messengers, which stimulate or modulate the release channels of the internal stores (Berridge et al., 2003). According Koss et al. (2009), AG126 affects store-operated Ca^{2+} channels (SOCCs) in hippocampal neurons of neonatal rat.

5.8.2. AG126 and mitochondria

Mitochondria take up Ca^{2+} rapidly from the cytosol through a uniporter and can release it again by different routes. It was also found that Ca^{2+}-mediated mitochondrial permeability triggers apoptosis (Berridge et al., 2003; Orrenius et al., 2003). Indeed, AG126 prevented splenic cell apoptosis in murine sepsis (Wewers and Sarkar, 2009).

Recently, preventive effects of AG126 in 7-ketocholesterol (KCL) toxicity were investigated in relation to the mitochondria-mediated cell death process by Kim and Lee (2010). They could show that AG126 attenuated the 7-KCL-induced decrease in cytosolic Bid and Bcl-2 levels and that it increased cytosolic pro-apoptotic Bax levels. Furthermore, AG126 attenuated mitochondrial membrane potential loss, cytochrome c release and subsequent caspase-3 activation. The authors assumed that AG126 may prevent the 7-KCL toxicity by suppressing mitochondrial membrane permeability changes, which leads to the cytochrome c release and caspase-3 activation.

Additionally Wewers and Sarkar (2009) showed that ATP activates the caspase-1 inflammasome *via* $P2X_7$ receptors ($P2X_7R$). AG126 prevented the activation of $P2X_7$ and thereby the activation of the caspase-1 inflammasome. $P2X_7R$ contributes to the entry of calcium and the cellular responses evoked by higher levels of ATP (McLarnon, 2005). Recently, a direct link of caspase-1 to the MyD88-dependent cell signaling was reported. Caspase-1 targets the TLR adapter MAL at the TIR-domain interaction site (Ulrichts et al., 2010). MAL, in turn, is a substrate of BTK, shown in our work to be a potential PTK target of AG126.

5.9. Conclusion

In conclusion, the tyrphostin AG126 affects many cellular processes in microglia summarized in Fig. 5.1. This study could show that AG126 inhibits the BTK, however, just at very high concentrations. A further AG126-sensitive target still has to be identified. Alternative actions of AG126 as an agonist of the GR or adrenergic receptors can be ruled out. This study revealed that AG126 affects the TLR-activated, MyD88-dependent signaling, as it leads also to the induction of cyto- and chemokines. Yet AG126 affects the MyD88 signaling outflow apparently without a massive interference with typical downstream elements within its hierarchy. This study showed the degradation of AG126 in aqueous solution, with at least two degradation products, MN and BZ. MN was able to mimic many of the influences that the parent structure AG126 had in TLR-activated microglia. Therefore, degradation product(s) of AG126 might serve as the true carrier of effects on cellular processes. However, AG126, but not MN, had beneficial effects in EAE as an animal disease model for MS. Therefore, AG126 stays an interesting tool to suppress pro-inflammatory TLR-driven processes in the microglia and probably beyond. The ultimate identification of the AG126-sensitive target(s) would reveal a central 'control unit' for (neuro)inflammatory processes. This could facilitate a development of improved compounds for therapeutic interventions.

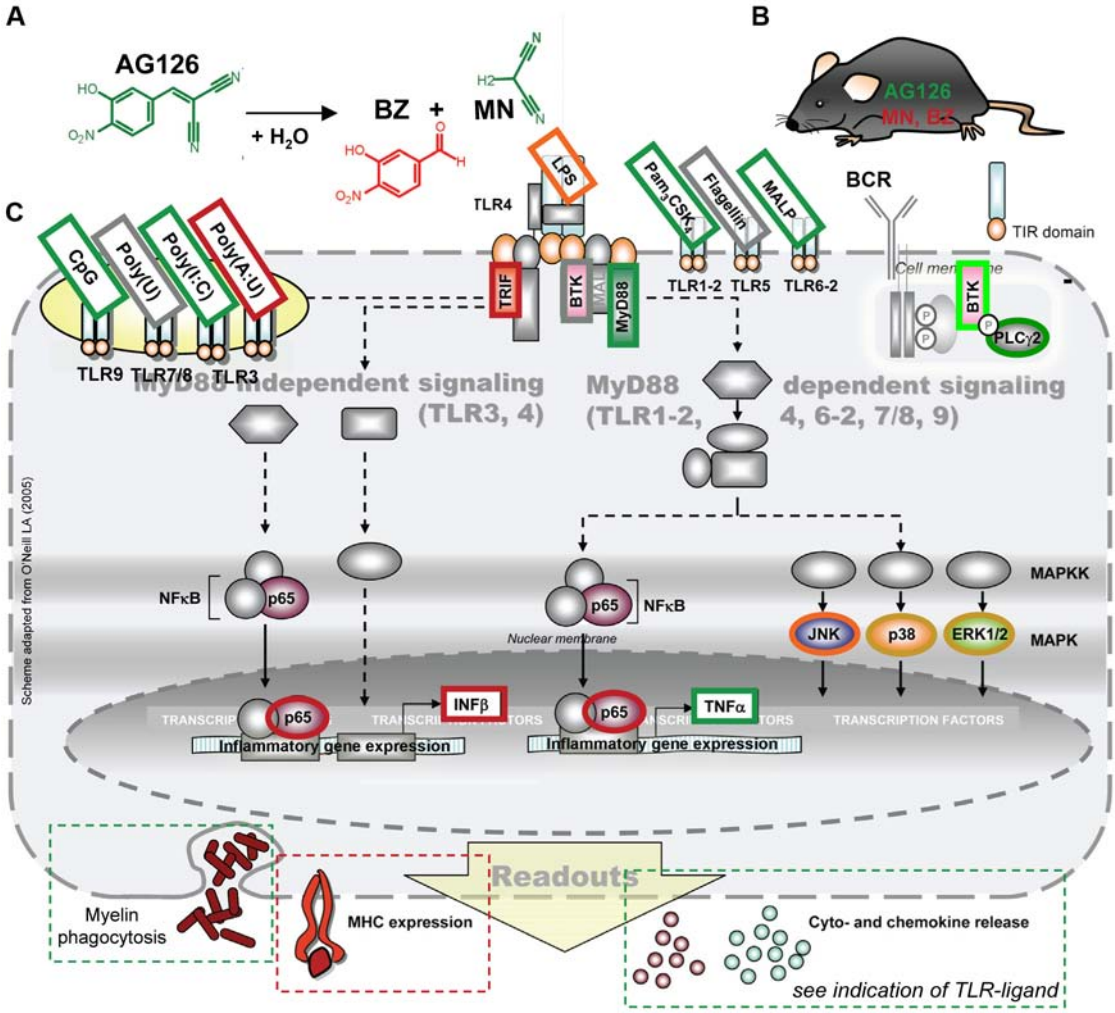

Figure 5.1.: Summary of results. ***A*** The tyrphostin AG126 decomposes in aqueous solution into at least two degradation products, MN and BZ. ***B*** AG126 revealed beneficial effects in an animal disease model for MS, while BZ and MN failed to improve disease symptoms when delivered systemically. AG126 has to be administered as the parent — and presumably CNS-penetrating — compound in order to deliver full efficacy on both clinical course and tissue protection. ***C*** The TLR signaling scheme as previously described in Fig. 1.1. depicts AG126-affected (*green*) and -unaffected (*red*) signaling elements and readouts. Green-marked TLR ligands indicate suppressive effects of AG126 on the pro-inflammatory cyto- and chemokine release upon microglial TLR stimulation. *Orange*-framed TLR ligands indicate modulatory, but no suppressive effects of AG126 on these candidates. *Gray* marked ligands failed to induce a pronounced cyto- and chemokine release on microglia and were not tested further for AG126 effects. Activation of *red*-framed signaling elements was not affected by AG126. Signaling elements framed in *brown* show AG126 acting on specific subtypes of respective MAPK. Direct interaction of AG126 on human BTK could be shown in phosphorylation assays and in BCR signaling of the human B cell line Ramos. (*bright* green). BTK is thus a likely and true PTK target of AG126, but cannot explain the full range of effects and is not affected by the breakdown products, as shown in ***A***.

6. References

Adachi, O., Kawai, T., Takeda, K., Matsumoto, M., Tsutsui, H., Sakagami, M., Nakanishi, K., and Akira, S. (1998). Targeted disruption of the myd88 gene results in loss of il-1- and il-18-mediated function. *Immunity*, 9(1):143–150.

Akira, S. and Takeda, K. (2004). Toll-like receptor signalling. *Nat Rev Immunol*, 4(7):499–511.

Akira, S., Uematsu, S., and Takeuchi, O. (2006). Pathogen recognition and innate immunity. *Cell*, 124(4):783–801.

Akiyama, T., Ishida, J., Nakagawa, S., Ogawara, H., Watanabe, S., Itoh, N., Shibuya, M., and Fukami, Y. (1987). Genistein, a specific inhibitor of tyrosine-specific protein kinases. *J Biol Chem*, 262(12):5592–5595.

Alexopoulou, L., Holt, A. C., Medzhitov, R., and Flavell, R. A. (2001). Recognition of double-stranded rna and activation of nf-kappab by toll-like receptor 3. *Nature*, 413(6857):732–738.

Amaldi, I., Reith, W., Berte, C., and Mach, B. (1989). Induction of hla class ii genes by ifn-gamma is transcriptional and requires a trans-acting protein. *J Immunol*, 142(3):999–1004.

Ananieva, O., Darragh, J., Johansen, C., Carr, J. M., McIlrath, J., Park, J. M., Wingate, A., Monk, C. E., Toth, R., Santos, S. G., Iversen, L., and Arthur, J. S. C. (2008). The kinases msk1 and msk2 act as negative regulators of toll-like receptor signaling. *Nat Immunol*, 9(9):1028–1036.

Anderson, E. and van Breemen, V. L. (1958). Electron microscopic observations on spinal ganglion cells of rana pipiens after injection of malononitrile. *J Biophys Biochem Cytol*, 4(1):83–86.

Angstwurm, K., Hanisch, U.-K., Gassemi, T., Bille, M. B., Prinz, M., Dirnagl, U., Kettenmann, H., and Weber, J. R. (2004). Tyrosine kinase inhibition reduces inflammation in the acute stage of experimental pneumococcal meningitis. *Infect Immun*, 72(6):3294–3298.

Anjum, R. and Blenis, J. (2008). The rsk family of kinases: emerging roles in cellular signalling. *Nat Rev Mol Cell Biol*, 9(10):747–758.

Aramoto, H., Breslin, J. W., Pappas, P. J., Hobson, R. W., and Durán, W. N. (2004). Vascular endothelial growth factor stimulates differential signaling pathways in in vivo microcirculation. *Am J Physiol Heart Circ Physiol*, 287(4):H1590–H1598.

Bajpai, U. D., Zhang, K., Teutsch, M., Sen, R., and Wortis, H. H. (2000). Bruton's tyrosine kinase links the b cell receptor to nuclear factor kappab activation. *J Exp Med*, 191(10):1735–1744.

Balachandra, S., Genovese, T., Mazzon, E., Di, P. R., Thiemerman, C., Siriwardena, A., and Cuzzocrea, S. (2005). Inhibition of tyrosine-kinase-mediated cellular signaling by tyrphostins ag 126 and ag556 modulates murine experimental acute pancreatitis. *Surgery*, 138(5):913–923.

Barron, K. D. (1995). The microglial cell. a historical review. *J Neurol Sci*, 134 Suppl:57–68.

Benarroch, E. E. (2009). The locus ceruleus norepinephrine system: functional organization and potential clinical significance. *Neurology*, 73(20):1699–1704.

Berridge, M. J., Bootman, M. D., and Roderick, H. L. (2003). Calcium signalling: dynamics, homeostasis and remodelling. *Nat Rev Mol Cell Biol*, 4(7):517–529.

Beutler, B., Jiang, Z., Georgel, P., Crozat, K., Croker, B., Rutschmann, S., Du, X., and Hoebe, K. (2006). Genetic analysis of host resistance: Toll-like receptor signaling and immunity at large. *Annu.Rev.Immunol.*, 24:353–389.

Beutler, B. A. (2009). Tlrs and innate immunity. *Blood*, 113(7):1399–1407.

Bowman, C. C., Rasley, A., Tranguch, S. L., and Marriott, I. (2003). Cultured astrocytes express toll-like receptors for bacterial products. *Glia*, 43(3):281–291.

Brenner, T., Poradosu, E., Soffer, D., Sicsic, C., Gazit, A., and Levitzki, A. (1998). Suppression of experimental autoimmune encephalomyelitis by tyrphostin ag-556. *Exp Neurol*, 154(2):489–498.

Brodsky, I. E. and Medzhitov, R. (2009). Targeting of immune signalling networks by bacterial pathogens. *Nat Cell Biol*, 11(5):521–526.

Brunner, C., Müller, B., and Wirth, T. (2005). Bruton's tyrosine kinase is involved in innate and adaptive immunity. *Histol Histopathol*, 20(3):945–955.

Bsibsi, M., Ravid, R., Gveric, D., and van Noort, J. M. (2002). Broad expression of toll-like receptors in the human central nervous system. *J Neuropathol Exp Neurol*, 61(11):1013–1021.

Bullard, L. E., Qi, X., and Penn, J. S. (2003). Role for extracellular signal-responsive kinase-1 and -2 in retinal angiogenesis. *Invest Ophthalmol Vis Sci*, 44(4):1722–1731.

Butovsky, O., Talpalar, A. E., Ben-Yaakov, K., and Schwartz, M. (2005). Activation of microglia by aggregated beta-amyloid or lipopolysaccharide impairs mhc-ii expression and renders them cytotoxic whereas ifn-gamma and il-4 render them protective. *Mol Cell Neurosci*, 29(3):381–393.

Cameron, B. and Landreth, G. E. (2010). Inflammation, microglia, and alzheimer's disease. *Neurobiol Dis*, 37(3):503–509.

Carpentier, P. A., Duncan, D. S., and Miller, S. D. (2008). Glial toll-like receptor signaling in central nervous system infection and autoimmunity. *Brain Behav Immun*, 22(2):140–147.

Carson, M. J., Doose, J. M., Melchior, B., Schmid, C. D., and Ploix, C. C. (2006). Cns immune privilege: hiding in plain sight. *Immunol Rev*, 213:48–65.

Chakraborty, P., Ghosh, D., and Basu, M. K. (2000). Macrophage protein kinase c: its role in modulating membrane microviscosity and superoxide in leishmanial infection. *J Biochem*, 127(2):185–190.

Chatterjee, P. K., Patel, N. S. A., Kvale, E. O., Brown, P. A. J., Stewart, K. N., Britti, D., Cuzzocrea, S., Mota-Filipe, H., and Thiemermann, C. (2003). The tyrosine kinase inhibitor tyrphostin ag126 reduces renal ischemia/reperfusion injury in the rat. *Kidney Int*, 64(5):1605–1619.

Chun, J. and Prince, A. (2006). Activation of ca2+-dependent signaling by tlr2. *J Immunol*, 177(2):1330–1337.

Colton, C. A. and Chernyshev, O. N. (1996). Inhibition of microglial superoxide anion production by isoproterenol and dexamethasone. *Neurochem Int*, 29(1):43–53.

Conforti, R., Ma, Y., Morel, Y., Paturel, C., Terme, M., Viaud, S., Ryffel, B., Ferrantini, M., Uppaluri, R., Schreiber, R., Combadière, C., Chaput, N., André, F., Kroemer, G., and Zitvogel, L. (2010). Opposing effects of toll-like receptor (tlr3) signaling in tumors can be therapeutically uncoupled to optimize the anticancer efficacy of tlr3 ligands. *Cancer Res*, 70(2):490–500.

Creagh, E. and O'Neill, L. (2006). Tlrs, nlrs and rlrs: a trinity of pathogen sensors that co-operate in innate immunity. *Trends Immunol.*, 27(8):352–357.

Cuzzocrea, S., McDonald, M., Mazzon, E., Siriwardena, D., Calabro, G., Britti, D., Mazzullo, G., de, S. A., Caputi, A., and Thiemermann, C. (2000a). The tyrosine kinase inhibitor tyrphostin ag126 reduces the development of acute and chronic inflammation. *Am.J.Pathol.*, 157(1):145–158.

Cuzzocrea, S., McDonald, M. C., Mazzon, E., Mota-Filipe, H., Lepore, V., Ciccolo, A., Terranova, M. L., Britti, D., Caputi, A. P., and Thiemermann, C. (2000b). The tyrosine kinase inhibitor tyrphostin ag 126 reduced the development of colitis in the rat. *Lab Invest*, 80(9):1439–1453.

Dabbagh, K., Dahl, M. E., Stepick-Biek, P., and Lewis, D. B. (2002). Toll-like receptor 4 is required for optimal development of th2 immune responses: role of dendritic cells. *J Immunol*, 168(9):4524–4530.

Dasgupta, D., Chakraborty, P., and Basu, M. K. (2000). fmlp receptor stimulated activation of macrophage: its effect on killing of intracellular leishmania donovani. *Biosci Rep*, 20(5):345–354.

Davis, J. B. and Maher, P. (1994). Protein kinase c activation inhibits glutamate-induced cytotoxicity in a neuronal cell line. *Brain Res*, 652(1):169–173.

Davoust, N., Vuaillat, C., Androdias, G., and Nataf, S. (2008). From bone marrow to microglia: barriers and avenues. *Trends Immunol*, 29(5):227–234.

De, B. K., Vanden, B. W., Beck, I., Van, M. W., Hennuyer, N., Hapgood, J., Libert, C., Staels, B., Louw, A., and Haegeman, G. (2005). A fully dissociated compound of plant origin for inflammatory gene repression. *Proc.Natl.Acad.Sci.U.S.A*, 102(44):15827–15832.

Denhardt, D. T. (1996). Signal-transducing protein phosphorylation cascades mediated by ras/rho proteins in the mammalian cell: the potential for multiplex signalling. *Biochem J*, 318 (Pt 3):729–747.

Dent, G., Munoz, N. M., Zhu, X., Rühlmann, E., Magnussen, H., Leff, A. R., and Rabe, K. F. (2000). Involvement of protein tyrosine kinases in activation of human eosinophils by platelet-activating factor. *Immunology*, 100(2):231–237.

Doyle, S., Jefferies, C., Feighery, C., and O'Neill, L. (2007). Signaling by toll-like receptors 8 and 9 requires bruton's tyrosine kinase. *J.Biol.Chem.*, 282(51):36953–36960.

Doyle, S., Jefferies, C., and O'Neill, L. (2005). Bruton's tyrosine kinase is involved in p65-mediated transactivation and phosphorylation of p65 on serine 536 during nfkappab activation by lipopolysaccharide. *J.Biol.Chem.*, 280(25):23496–23501.

Doyle, S., Vaidya, S., O'Connell, R., Dadgostar, H., Dempsey, P., Wu, T., Rao, G., Sun, R., Haberland, M., Modlin, R., and Cheng, G. (2002). Irf3 mediates a tlr3/tlr4-specific antiviral gene program. *Immunity*, 17(3):251–263.

Draheim, H. J., Prinz, M., Weber, J. R., Weiser, T., Kettenmann, H., and Hanisch, U. K. (1999). Induction of potassium channels in mouse brain microglia: cells acquire responsiveness to pneumococcal cell wall components during late development. *Neuroscience*, 89(4):1379–1390.

Du, H. J., Tang, N., Liu, B. C., You, B. R., Shen, F. H., Ye, M., Gao, A., and shu Huang, C. (2006). Benzo[a]pyrene-induced cell cycle progression is through erks/cyclin d1 pathway and requires the activation of jnks and p38 mapk in human diploid lung fibroblasts. *Mol Cell Biochem*, 287(1-2):79–89.

Dugo, L., Chatterjee, P., Mazzon, E., McDonald, M., Paola, R., Fulia, F., Caputi, A., Thiemermann, C., and Cuzzocrea, S. (2002). The tyrosine kinase inhibitor tyrphostin ag 126 reduces the multiple organ failure induced by zymosan in the rat. *Intensive Care Med.*, 28(6):775–788.

Feinstein, D. L., Heneka, M. T., Gavrilyuk, V., Russo, C. D., Weinberg, G., and Galea, E. (2002). Noradrenergic regulation of inflammatory gene expression in brain. *Neurochem Int*, 41(5):357–365.

Ferlito, M., Romanenko, O. G., Guyton, K., Ashton, S., Squadrito, F., Halushka, P. V., and Cook, J. A. (2002). Implication of galpha i proteins and src tyrosine kinases in endotoxin-induced signal transduction events and mediator production. *J Endotoxin Res*, 8(6):427–435.

Finotto, S., Krieglstein, K., Schober, A., Deimling, F., Lindner, K., Brühl, B., Beier, K., Metz, J., Garcia-Arraras, J. E., Roig-Lopez, J. L., Monaghan, P., Schmid, W., Cole, T. J., Kellendonk, C., Tronche, F., Schütz, G., and Unsicker, K. (1999). Analysis of mice carrying targeted mutations of the glucocorticoid receptor gene argues against an essential role of glucocorticoid signalling for generating adrenal chromaffin cells. *Development*, 126(13):2935–2944.

Fluckiger, A. C., Li, Z., Kato, R. M., Wahl, M. I., Ochs, H. D., Longnecker, R., Kinet, J. P., Witte, O. N., Scharenberg, A. M., and Rawlings, D. J. (1998). Btk/tec kinases regulate sustained increases in intracellular ca2+ following b-cell receptor activation. *EMBO J*, 17(7):1973–1985.

Färber, K., Pannasch, U., and Kettenmann, H. (2005). Dopamine and noradrenaline control distinct functions in rodent microglial cells. *Mol Cell Neurosci*, 29(1):128–138.

Furr, S. R., Chauhan, V. S., Sterka, D., Grdzelishvili, V., and Marriott, I. (2008). Characterization of retinoic acid-inducible gene-i expression in primary murine glia following exposure to vesicular stomatitis virus. *J Neurovirol*, pages 1–11.

Gal, E. M., Fung, F. H., and Greenberg, D. M. (1952). Studies on the biological action of malononitriles. ii. distribution of rhodanese (transulfurase) in the tissues of normal and tumor-bearing animals and the effect of malononitriles thereon. *Cancer Res*, 12(8):574–579.

Gal, E. M. and Greenberg, D. M. (1951). Growth retarding effect of substituted malononitriles on transplat tumors in mice. *J. Am. Chem. Soc*, 73 (1):502–503.

García, J. J., del Carmen Sáez, M., la Fuente, M. D., and Ortega, E. (2003). Regulation of phagocytic process of macrophages by noradrenaline and its end metabolite 4-hydroxy-3-metoxyphenyl-glycol. role of alpha- and beta-adrenoreceptors. *Mol Cell Biochem*, 254(1-2):299–304.

Garg, T. K. and Chang, J. Y. (2003). Oxidative stress causes erk phosphorylation and cell death in cultured retinal pigment epithelium: prevention of cell death by ag126 and 15-deoxy-delta 12, 14-pgj2. *BMC Ophthalmol*, 3:5.

Gazit, A., Osherov, N., Posner, I., Yaish, P., Poradosu, E., Gilon, C., and Levitzki, A. (1991). Tyrphostins. 2. heterocyclic and alpha-substituted benzylidenemalononitrile tyrphostins as

potent inhibitors of egf receptor and erbb2/neu tyrosine kinases. *J Med Chem*, 34(6):1896–1907.

Gazit, A., Yaish, P., Gilon, C., and Levitzki, A. (1989). Tyrphostins i: synthesis and biological activity of protein tyrosine kinase inhibitors. *J Med Chem*, 32(10):2344–2352.

Genevier, H. C. and Callard, R. E. (1997). Impaired ca2+ mobilization by x-linked agammaglobulinaemia (xla) b cells in response to ligation of the b cell receptor (bcr). *Clin Exp Immunol*, 110(3):386–391.

Gerondakis, S., Grumont, R. J., and Banerjee, A. (2007). Regulating b-cell activation and survival in response to tlr signals. *Immunol Cell Biol*, 85(6):471–475.

Gibson, F. C., Ukai, T., and Genco, C. A. (2008). Engagement of specific innate immune signaling pathways during porphyromonas gingivalis induced chronic inflammation and atherosclerosis. *Front Biosci*, 13:2041–2059.

Girardin, S. E., Boneca, I. G., Viala, J., Chamaillard, M., Labigne, A., Thomas, G., Philpott, D. J., and Sansonetti, P. J. (2003). Nod2 is a general sensor of peptidoglycan through muramyl dipeptide (mdp) detection. *J Biol Chem*, 278(11):8869–8872.

Glezer, I. and Rivest, S. (2004). Glucocorticoids: protectors of the brain during innate immune responses. *Neuroscientist*, 10(6):538–552.

Gold, R., Linington, C., and Lassmann, H. (2006). Understanding pathogenesis and therapy of multiple sclerosis via animal models: 70 years of merits and culprits in experimental autoimmune encephalomyelitis research. *Brain*, 129(Pt 8):1953–1971.

Gold, S. M. and Heesen, C. (2006). Stress and disease progression in multiple sclerosis and its animal models. *Neuroimmunomodulation*, 13(5-6):318–326.

Gorden, K. K. B., Qiu, X. X., Binsfeld, C. C. A., Vasilakos, J. P., and Alkan, S. S. (2006). Cutting edge: activation of murine tlr8 by a combination of imidazoquinoline immune response modifiers and polyt oligodeoxynucleotides. *J Immunol*, 177(10):6584–6587.

Gordon, S. (2007). Macrophage heterogeneity and tissue lipids. *J Clin Invest*, 117(1):89–93.

Gordon, S. and Taylor, P. R. (2005). Monocyte and macrophage heterogeneity. *Nat Rev Immunol*, 5(12):953–964.

Gorina, R., Sanfeliu, C., Galitó, A., Messeguer, A., and Planas, A. M. (2007). Exposure of glia to pro-oxidant agents revealed selective stat1 activation by h2o2 and jak2-independent antioxidant features of the jak2 inhibitor ag490. *Glia*, 55(13):1313–1324.

Gosain, A., Jones, S. B., Shankar, R., Gamelli, R. L., and DiPietro, L. A. (2006). Norepinephrine modulates the inflammatory and proliferative phases of wound healing. *J Trauma*, 60(4):736–744.

Gray, P., Dunne, A., Brikos, C., Jefferies, C., Doyle, S., and O'Neill, L. (2006). Myd88 adapter-like (mal) is phosphorylated by bruton's tyrosine kinase during tlr2 and tlr4 signal transduction. *J.Biol.Chem.*, 281(15):10489–10495.

Greenberg, E. M. G. D. M. (1953). Studies on the biological action of malononitriles. iii. effect of malononitrile administration on excretion of thiocyanate in normal and walker carcinoma 256-bearing rats. *Cancer Res*, 13(3):226–230.

Guillemin, G. J. and Brew, B. J. (2004). Microglia, macrophages, perivascular macrophages, and pericytes: a review of function and identification. *J Leukoc Biol*, 75(3):388–397.

Hanisch, U. (2002). Microglia as a source and target of cytokines. *Glia*, 40(2):140–155.

Hanisch, U. and Kettenmann, H. (2007). Microglia: active sensor and versatile effector cells in the normal and pathologic brain. *Nat.Neurosci.*, 10(11):1387–1394.

Hanisch, U., Prinz, M., Angstwurm, K., Hausler, K., Kann, O., Kettenmann, H., and Weber, J. (2001). The protein tyrosine kinase inhibitor ag126 prevents the massive microglial cytokine induction by pneumococcal cell walls. *Eur.J.Immunol.*, 31(7):2104–2115.

Hanisch, U., van Rossum, D., Xie, Y., Gast, K., Misselwitz, R., Auriola, S., Goldsteins, G., Koistinaho, J., Kettenmann, H., and Moller, T. (2004). The microglia-activating potential of thrombin: the protease is not involved in the induction of proinflammatory cytokines and chemokines. *J.Biol.Chem.*, 279(50):51880–51887.

Hanisch, U.-K., Johnson, T. V., and Kipnis, J. (2008). Toll-like receptors: roles in neuroprotection? *Trends Neurosci*, 31(4):176–182.

Hashimoto, C., Hudson, K. L., and Anderson, K. V. (1988). The toll gene of drosophila, required for dorsal-ventral embryonic polarity, appears to encode a transmembrane protein. *Cell*, 52(2):269–279.

Heneka, M. T., Nadrigny, F., Regen, T., Martinez-Hernandez, A., Dumitrescu-Ozimek, L., Terwel, D., Jardanhazi-Kurutz, D., Walter, J., Kirchhoff, F., Hanisch, U.-K., and Kummer, M. P. (2010). Locus ceruleus controls alzheimer's disease pathology by modulating microglial functions through norepinephrine. *Proc Natl Acad Sci U S A*, 107(13):6058–6063.

Henkel, J. S., Beers, D. R., Zhao, W., and Appel, S. H. (2009). Microglia in als: the good, the bad, and the resting. *J Neuroimmune Pharmacol*, 4(4):389–398.

Hirasawa, K., Jun, H. S., Han, H. S., Zhang, M. L., Hollenberg, M. D., and Yoon, J. W. (1999). Prevention of encephalomyocarditis virus-induced diabetes in mice by inhibition of the tyrosine kinase signalling pathway and subsequent suppression of nitric oxide production in macrophages. *J Virol*, 73(10):8541–8548.

Hoffmann, A., Kann, O., Ohlemeyer, C., Hanisch, U., and Kettenmann, H. (2003). Elevation of basal intracellular calcium as a central element in the activation of brain macrophages (microglia): suppression of receptor-evoked calcium signaling and control of release function. *J.Neurosci.*, 23(11):4410–4419.

Horwood, N., Page, T., McDaid, J., Palmer, C., Campbell, J., Mahon, T., Brennan, F., Webster, D., and Foxwell, B. (2006). Bruton's tyrosine kinase is required for tlr2 and tlr4-induced tnf, but not il-6, production. *J.Immunol.*, 176(6):3635–3641.

Hosoi, T., Hirose, R., Saegusa, S., Ametani, A., Kiuchi, K., and Kaminogawa, S. (2003). Cytokine responses of human intestinal epithelial-like caco-2 cells to the nonpathogenic bacterium bacillus subtilis (natto). *Int J Food Microbiol*, 82(3):255–264.

Hu, X. X., Goldmuntz, E. A., and Brosnan, C. F. (1991). The effect of norepinephrine on endotoxin-mediated macrophage activation. *J Neuroimmunol*, 31(1):35–42.

Jack, C., Ruffini, F., Bar-Or, A., and Antel, J. P. (2005). Microglia and multiple sclerosis. *J Neurosci Res*, 81(3):363–373.

Janeway, C. A. and Medzhitov, R. (2002). Innate immune recognition. *Annu Rev Immunol*, 20:197–216.

Jefferies, C., Doyle, S., Brunner, C., Dunne, A., Brint, E., Wietek, C., Walch, E., Wirth, T., and O'Neill, L. (2003). Bruton's tyrosine kinase is a toll/interleukin-1 receptor domain-binding protein that participates in nuclear factor kappab activation by toll-like receptor 4. *J.Biol.Chem.*, 278(28):26258–26264.

Johnson, P. and Cross, J. L. (2009). Tyrosine phosphorylation in immune cells: direct and indirect effects on toll-like receptor-induced proinflammatory cytokine production. *Crit Rev Immunol*, 29(4):347–367.

Kaisho, T. and Akira, S. (2006). Toll-like receptor function and signaling. *J Allergy Clin Immunol*, 117(5):979–87; quiz 988.

Kann, O., Hoffmann, A., Schumann, R., Weber, J., Kettenmann, H., and Hanisch, U. (2004). The tyrosine kinase inhibitor ag126 restores receptor signaling and blocks release functions in activated microglia (brain macrophages) by preventing a chronic rise in the intracellular calcium level. *J.Neurochem.*, 90(3):513–525.

Kao, S.-J., Lei, H.-C., Kuo, C.-T., Chang, M.-S., Chen, B.-C., Chang, Y.-C., Chiu, W.-T., and Lin, C.-H. (2005). Lipoteichoic acid induces nuclear factor-kappab activation and nitric oxide synthase expression via phosphatidylinositol 3-kinase, akt, and p38 mapk in raw 264.7 macrophages. *Immunology*, 115(3):366–374.

Kato, H., Takeuchi, O., Sato, S., Yoneyama, M., Yamamoto, M., Matsui, K., Uematsu, S., Jung, A., Kawai, T., Ishii, K. J., Yamaguchi, O., Otsu, K., Tsujimura, T., Koh, C.-S., e Sousa, C. R., Matsuura, Y., Fujita, T., and Akira, S. (2006). Differential roles of mda5 and rig-i helicases in the recognition of rna viruses. *Nature*, 441(7089):101–105.

Kawai, T., Adachi, O., Ogawa, T., Takeda, K., and Akira, S. (1999). Unresponsiveness of myd88-deficient mice to endotoxin. *Immunity*, 11(1):115–122.

Kerfoot, S. M., Long, E. M., Hickey, M. J., Andonegui, G., Lapointe, B. M., Zanardo, R. C. O., Bonder, C., James, W. G., Robbins, S. M., and Kubes, P. (2004). Tlr4 contributes to disease-inducing mechanisms resulting in central nervous system autoimmune disease. *J Immunol*, 173(11):7070–7077.

Kim, J. and Sharma, R. P. (2004). Calcium-mediated activation of c-jun nh2-terminal kinase (jnk) and apoptosis in response to cadmium in murine macrophages. *Toxicol Sci*, 81(2):518–527.

Kim, Y. J. and Lee, C. S. (2010). Tyrosine kinase inhibitor ag126 reduces 7-ketocholesterol-induced cell death by suppressing mitochondria-mediated apoptotic process. *Neurochem Res*, 35(4):603–612.

Kizaki, T., Shirato, K., Sakurai, T., etsu Ogasawara, J., Oh-ishi, S., Matsuoka, T., Izawa, T., Imaizumi, K., Haga, S., and Ohno, H. (2009). Beta2-adrenergic receptor regulate toll-like receptor 4-induced late-phase nf-kappab activation. *Mol Immunol*, 46(6):1195–1203.

Koistinaho, M. and Koistinaho, J. (2002). Role of p38 and p44/42 mitogen-activated protein kinases in microglia. *Glia*, 40(2):175–183.

Kono, H. and Rock, K. L. (2008). How dying cells alert the immune system to danger. *Nat Rev Immunol*, 8(4):279–289.

Koss, D. J., Riedel, G., and Platt, B. (2009). Intracellular ca2+ stores modulate soccs and nmda receptors via tyrosine kinases in rat hippocampal neurons. *Cell Calcium*, 46(1):39–48.

Kovalenko, M., Gazit, A., Böhmer, A., Rorsman, C., Rönnstrand, L., Heldin, C. H., Waltenberger, J., Böhmer, F. D., and Levitzki, A. (1994). Selective platelet-derived growth factor receptor kinase blockers reverse sis-transformation. *Cancer Res*, 54(23):6106–6114.

Kovalenko, M., Rönnstrand, L., Heldin, C. H., Loubtchenkov, M., Gazit, A., Levitzki, A., and Böhmer, F. D. (1997). Phosphorylation site-specific inhibition of platelet-derived growth factor beta-receptor autophosphorylation by the receptor blocking tyrphostin ag1296. *Biochemistry*, 36(21):6260–6269.

Krady, J. K., Basu, A., Levison, S. W., and Milner, R. J. (2002). Differential expression of protein tyrosine kinase genes during microglial activation. *Glia*, 40(1):11–24.

Kumar, N., Windisch, V., and Ammon, H. L. (1995). Photoinstability of some tyrphostin drugs: chemical consequences of crystallinity. *Pharm Res*, 12(11):1708–1715.

Lehnardt, S. (2010). Innate immunity and neuroinflammation in the cns: the role of microglia in toll-like receptor-mediated neuronal injury. *Glia*, 58(3):253–263.

Lemaitre, B., Nicolas, E., Michaut, L., Reichhart, J. M., and Hoffmann, J. A. (1996). The dorsoventral regulatory gene cassette spätzle/toll/cactus controls the potent antifungal response in drosophila adults. *Cell*, 86(6):973–983.

Levitzki, A. (1992). Tyrphostins: tyrosine kinase blockers as novel antiproliferative agents and dissectors of signal transduction. *FASEB J.*, 6(14):3275–3282.

Levitzki, A. and Mishani, E. (2006). Tyrphostins and other tyrosine kinase inhibitors. *Annu.Rev.Biochem.*, 75:93–109.

Liew, F. Y., Xu, D., Brint, E. K., and O'Neill, L. A. J. (2005). Negative regulation of toll-like receptor-mediated immune responses. *Nat Rev Immunol*, 5(6):446–458.

Linker, R. A., Mäurer, M., Gaupp, S., Martini, R., Holtmann, B., Giess, R., Rieckmann, P., Lassmann, H., Toyka, K. V., Sendtner, M., and Gold, R. (2002). Cntf is a major protective factor in demyelinating cns disease: a neurotrophic cytokine as modulator in neuroinflammation. *Nat Med*, 8(6):620–624.

Liu, J., Xu, C., Hsu, L.-C., Luo, Y., Xiang, R., and Chuang, T.-H. (2010a). A five-amino-acid motif in the undefined region of the tlr8 ectodomain is required for species-specific ligand recognition. *Mol Immunol*, 47(5):1083–1090.

Liu, X., Chauhan, V. S., Young, A. B., and Marriott, I. (2010b). Nod2 mediates inflammatory responses of primary murine glia to streptococcus pneumoniae. *Glia*.

Long-Smith, C. M., Sullivan, A. M., and Nolan, Y. M. (2009). The influence of microglia on the pathogenesis of parkinson's disease. *Prog Neurobiol*, 89(3):277–287.

Loniewski, K. J., Patial, S., and Parameswaran, N. (2007). Sensitivity of tlr4- and -7-induced nf kappa b1 p105-tpl2-erk pathway to tnf-receptor-associated-factor-6 revealed by rnai in mouse macrophages. *Mol Immunol*, 44(15):3715–3723.

Lotze, M. T., Zeh, H. J., Rubartelli, A., Sparvero, L. J., Amoscato, A. A., Washburn, N. R., Devera, M. E., Liang, X., Tör, M., and Billiar, T. (2007). The grateful dead: damage-associated molecular pattern molecules and reduction/oxidation regulate immunity. *Immunol Rev*, 220:60–81.

Lyall, R. M., Zilberstein, A., Gazit, A., Gilon, C., Levitzki, A., and Schlessinger, J. (1989). Tyrphostins inhibit epidermal growth factor (egf)-receptor tyrosine kinase activity in living cells and egf-stimulated cell proliferation. *J Biol Chem*, 264(24):14503–14509.

MacGibbon, A. K., Koerber, S. C., Pease, K., and Dunn, M. F. (1987). Characterization of a transient intermediate formed in the liver alcohol dehydrogenase catalyzed reduction of 3-hydroxy-4-nitrobenzaldehyde. *Biochemistry*, 26(11):3058–3067.

Mahajan, S., Ghosh, S., Sudbeck, E. A., Zheng, Y., Downs, S., Hupke, M., and Uckun, F. M. (1999). Rational design and synthesis of a novel anti-leukemic agent targeting bruton's tyrosine kinase (btk), lfm-a13 [alpha-cyano-beta-hydroxy-beta-methyl-n-(2, 5-dibromophenyl)propenamide]. *J Biol Chem*, 274(14):9587–9599.

Mantovani, A., Sica, A., Sozzani, S., Allavena, P., Vecchi, A., and Locati, M. (2004). The chemokine system in diverse forms of macrophage activation and polarization. *Trends Immunol*, 25(12):677–686.

Mantovani, A., Sozzani, S., Locati, M., Allavena, P., and Sica, A. (2002). Macrophage polarization: tumor-associated macrophages as a paradigm for polarized m2 mononuclear phagocytes. *Trends Immunol*, 23(11):549–555.

Martin, P. M., Horwitz, K. B., Ryan, D. S., and McGuire, W. L. (1978). Phytoestrogen interaction with estrogen receptors in human breast cancer cells. *Endocrinology*, 103(5):1860–1867.

Martinez, F. O., Helming, L., and Gordon, S. (2009). Alternative activation of macrophages: an immunologic functional perspective. *Annu Rev Immunol*, 27:451–483.

Martinon, F. and Tschopp, J. (2005). Nlrs join tlrs as innate sensors of pathogens. *Trends Immunol*, 26(8):447–454.

Marzocco, S., Mazzon, E., Pinto, A., Autore, G., and Cuzzocrea, S. (2006). Tyrphostin ag 126 reduces intestinal ischemia-reperfusion injury in the rat. *Naunyn Schmiedebergs Arch Pharmacol*, 372(5):362–373.

Matsumoto, N., Iinuma, H., Sawa, T., and Takeuchi, T. (1998). Synthesis of anti-rheumatic agent epoxyquinomicin b. *Bioorg Med Chem Lett*, 8(21):2945–2948.

Matzinger, P. (2002). The danger model: a renewed sense of self. *Science*, 296(5566):301–305.

Matzinger, P. (2007). Friendly and dangerous signals: is the tissue in control? *Nat Immunol*, 8(1):11–13.

McGeer, P. L. and McGeer, E. G. (2007). Nsaids and alzheimer disease: epidemiological, animal model and clinical studies. *Neurobiol Aging*, 28(5):639–647.

McLarnon, J. G. (2005). Purinergic mediated changes in ca2+ mobilization and functional responses in microglia: effects of low levels of atp. *J Neurosci Res*, 81(3):349–356.

Medzhitov, R. and Janeway, C. A. (2002). Decoding the patterns of self and nonself by the innate immune system. *Science*, 296(5566):298–300.

Medzhitov, R., Preston-Hurlburt, P., and Janeway, C. A. (1997). A human homologue of the drosophila toll protein signals activation of adaptive immunity. *Nature*, 388(6640):394–397.

Meydan, N., Grunberger, T., Dadi, H., Shahar, M., Arpaia, E., Lapidot, Z., Leeder, J. S., Freedman, M., Cohen, A., Gazit, A., Levitzki, A., and Roifman, C. M. (1996). Inhibition of acute lymphoblastic leukaemia by a jak-2 inhibitor. *Nature*, 379(6566):645–648.

Milanski, M., Degasperi, G., Coope, A., Morari, J., Denis, R., Cintra, D. E., Tsukumo, D. M. L., Anhe, G., Amaral, M. E., Takahashi, H. K., Curi, R., Oliveira, H. C., Carvalheira, J. B. C., Bordin, S., Saad, M. J., and Velloso, L. A. (2009). Saturated fatty acids produce an inflammatory response predominantly through the activation of tlr4 signaling in hypothalamus: implications for the pathogenesis of obesity. *J Neurosci*, 29(2):359–370.

Mori, K., Ozaki, E., Zhang, B., Yang, L., Yokoyama, A., Takeda, I., Maeda, N., Sakanaka, M., and Tanaka, J. (2002). Effects of norepinephrine on rat cultured microglial cells that express alpha1, alpha2, beta1 and beta2 adrenergic receptors. *Neuropharmacology*, 43(6):1026–1034.

Moriguchi, T., Toyoshima, F., Gotoh, Y., Iwamatsu, A., Irie, K., Mori, E., Kuroyanagi, N., Hagiwara, M., Matsumoto, K., and Nishida, E. (1996). Purification and identification of a major activator for p38 from osmotically shocked cells. activation of mitogen-activated protein kinase kinase 6 by osmotic shock, tumor necrosis factor-alpha, and h2o2. *J Biol Chem*, 271(43):26981–26988.

Mosser, D. M. and Edwards, J. P. (2008). Exploring the full spectrum of macrophage activation. *Nat Rev Immunol*, 8(12):958–969.

Nancy Ing, N. and O'Malley, B. (1995). *The steroid hormone receptor superfamily: molecular mechanisms of action. In Molecular Endocrinology: Basic Concepts and Clinical Correlations,*. New York: Raven Press, Ltd.

Napoli, I. and Neumann, H. (2009). Protective effects of microglia in multiple sclerosis. *Exp Neurol*.

Napolitani, G., Bortoletto, N., Racioppi, L., Lanzavecchia, A., and D'Oro, U. (2003). Activation of src-family tyrosine kinases by lps regulates cytokine production in dendritic cells by controlling ap-1 formation. *Eur J Immunol*, 33(10):2832–2841.

Nau, R. and Brück, W. (2002). Neuronal injury in bacterial meningitis: mechanisms and implications for therapy. *Trends Neurosci*, 25(1):38–45.

Netea, M. G., van der Graaf, C., der Meer, J. W. M. V., and Kullberg, B. J. (2004). Toll-like receptors and the host defense against microbial pathogens: bringing specificity to the innate-immune system. *J Leukoc Biol*, 75(5):749–755.

Nimmerjahn, A., Kirchhoff, F., and Helmchen, F. (2005). Resting microglial cells are highly dynamic surveillants of brain parenchyma in vivo. *Science*, 308(5726):1314–1318.

Norton, W. T. and Poduslo, S. E. (1973). Myelination in rat brain: method of myelin isolation. *J Neurochem*, 21(4):749–757.

Novogrodsky, A., Vanichkin, A., Patya, M., Gazit, A., Osherov, N., and Levitzki, A. (1994). Prevention of lipopolysaccharide-induced lethal toxicity by tyrosine kinase inhibitors. *Science*, 264(5163):1319–1322.

Ogawa, S., Lozach, J., Benner, C., Pascual, G., Tangirala, R., Westin, S., Hoffmann, A., Subramaniam, S., David, M., Rosenfeld, M., and Glass, C. (2005). Molecular determinants of crosstalk between nuclear receptors and toll-like receptors. *Cell*, 122(5):707–721.

Ohmichi, M., Pang, L., Ribon, V., Gazit, A., Levitzki, A., and Saltiel, A. R. (1993). The tyrosine kinase inhibitor tyrphostin blocks the cellular actions of nerve growth factor. *Biochemistry*, 32(17):4650–4658.

Okun, E., Griffioen, K. J., Lathia, J. D., Tang, S.-C., Mattson, M. P., and Arumugam, T. V. (2009). Toll-like receptors in neurodegeneration. *Brain Res Rev*, 59(2):278–292.

Olson, J. and Miller, S. (2004). Microglia initiate central nervous system innate and adaptive immune responses through multiple tlrs. *J.Immunol.*, 173(6):3916–3924.

O'Neill, L. A. J. (2004). Tlrs: Professor mechnikov, sit on your hat. *Trends Immunol*, 25(12):687–693.

O'Neill, L. A. J. (2008). When signaling pathways collide: positive and negative regulation of toll-like receptor signal transduction. *Immunity*, 29(1):12–20.

Orlicek, S. L., Hanke, J. H., and English, B. K. (1999). The src family-selective tyrosine kinase inhibitor pp1 blocks lps and ifn-gamma-mediated tnf and inos production in murine macrophages. *Shock*, 12(5):350–354.

Orr, C. F., Rowe, D. B., and Halliday, G. M. (2002). An inflammatory review of parkinson's disease. *Prog Neurobiol*, 68(5):325–340.

Orrenius, S., Zhivotovsky, B., and Nicotera, P. (2003). Regulation of cell death: the calcium-apoptosis link. *Nat Rev Mol Cell Biol*, 4(7):552–565.

Oshiumi, H., Matsumoto, M., Funami, K., Akazawa, T., and Seya, T. (2003a). Ticam-1, an adaptor molecule that participates in toll-like receptor 3-mediated interferon-beta induction. *Nat Immunol*, 4(2):161–167.

Oshiumi, H., Sasai, M., Shida, K., Fujita, T., Matsumoto, M., and Seya, T. (2003b). Tir-containing adapter molecule (ticam)-2, a bridging adapter recruiting to toll-like receptor 4 ticam-1 that induces interferon-beta. *J Biol Chem*, 278(50):49751–49762.

Pais, T. F., Figueiredo, C., Peixoto, R., Braz, M. H., and Chatterjee, S. (2008). Necrotic neurons enhance microglial neurotoxicity through induction of glutaminase by a myd88-dependent pathway. *J Neuroinflammation*, 5:43.

Pazmany, T., Kosa, J. P., Tomasi, T. B., Mechtler, L., Turoczi, A., and Lehotzky, A. (2000). Effect of transforming growth factor-beta1 on microglial mhc-class ii expression. *J Neuroimmunol*, 103(2):122–130.

Picard, D. and Yamamoto, K. R. (1987). Two signals mediate hormone-dependent nuclear localization of the glucocorticoid receptor. *EMBO J*, 6(11):3333–3340.

Pineau, I. and Lacroix, S. (2009). Endogenous signals initiating inflammation in the injured nervous system. *Glia*, 57(4):351–361.

Pollard, J. W. (2009). Trophic macrophages in development and disease. *Nat Rev Immunol*, 9(4):259–270.

Poltorak, A., He, X., Smirnova, I., Liu, M. Y., Huffel, C. V., Du, X., Birdwell, D., Alejos, E., Silva, M., Galanos, C., Freudenberg, M., Ricciardi-Castagnoli, P., Layton, B., and Beutler, B. (1998). Defective lps signaling in c3h/hej and c57bl/10sccr mice: mutations in tlr4 gene. *Science*, 282(5396):2085–2088.

Pratt, W. B. (1993). The role of heat shock proteins in regulating the function, folding, and trafficking of the glucocorticoid receptor. *J Biol Chem*, 268(29):21455–21458.

Prinz, M., Garbe, F., Schmidt, H., Mildner, A., Gutcher, I., Wolter, K., Piesche, M., Schroers, R., Weiss, E., Kirschning, C. J., Rochford, C. D. P., Brück, W., and Becher, B. (2006). Innate immunity mediated by tlr9 modulates pathogenicity in an animal model of multiple sclerosis. *J Clin Invest*, 116(2):456–464.

Prinz, M., Häusler, K. G., Kettenmann, H., and Hanisch, U. (2001). beta-adrenergic receptor stimulation selectively inhibits il-12p40 release in microglia. *Brain Res*, 899(1-2):264–270.

Prinz, M., Kann, O., Draheim, H., Schumann, R., Kettenmann, H., Weber, J., and Hanisch, U. (1999). Microglial activation by components of gram-positive and -negative bacteria: distinct and common routes to the induction of ion channels and cytokines. *J.Neuropathol.Exp.Neurol.*, 58(10):1078–1089.

Proud, C. G. (2007). A sharper instrument for dissecting signalling events: a specific agc kinase inhibitor. *Biochem J*, 401(1):e1–e3.

Ramdas, L., McMurray, J. S., and Budde, R. J. (1994). The degree of inhibition of protein tyrosine kinase activity by tyrphostin 23 and 25 is related to their instability. *Cancer Res*, 54(4):867–869.

Rivest, S. (2009). Regulation of innate immune responses in the brain. *Nat Rev Immunol*, 9(6):429–439.

Rock, F. L., Hardiman, G., Timans, J. C., Kastelein, R. A., and Bazan, J. F. (1998). A family of human receptors structurally related to drosophila toll. *Proc Natl Acad Sci U S A*, 95(2):588–593.

Romais, B. (1989). *Mikroskopische Technik*. Urban&Schwarzenberg.

Sagara, Y., Ishige, K., Tsai, C., and Maher, P. (2002). Tyrphostins protect neuronal cells from oxidative stress. *J Biol Chem*, 277(39):36204–36215.

Salvioli, S., Ardizzoni, A., Franceschi, C., and Cossarizza, A. (1997). Jc-1, but not dioc6(3) or rhodamine 123, is a reliable fluorescent probe to assess delta psi changes in intact cells: implications for studies on mitochondrial functionality during apoptosis. *FEBS Lett*, 411(1):77–82.

Sansonetti, P. J. (2006). The innate signaling of dangers and the dangers of innate signaling. *Nat Immunol*, 7(12):1237–1242.

Sarkar, S. N., Smith, H. L., Rowe, T. M., and Sen, G. C. (2003). Double-stranded rna signaling by toll-like receptor 3 requires specific tyrosine residues in its cytoplasmic domain. *J Biol Chem*, 278(7):4393–4396.

Schwartz, M., Butovsky, O., Brück, W., and Hanisch, U.-K. (2006). Microglial phenotype: is the commitment reversible? *Trends Neurosci*, 29(2):68–74.

Semaan, N., Alsaleh, G., Gottenberg, J.-E., Wachsmann, D., and Sibilia, J. (2008). Etk/bmx, a btk family tyrosine kinase, and mal contribute to the cross-talk between myd88 and fak pathways. *J Immunol*, 180(5):3485–3491.

Seong, S.-Y. and Matzinger, P. (2004). Hydrophobicity: an ancient damage-associated molecular pattern that initiates innate immune responses. *Nat Rev Immunol*, 4(6):469–478.

Shideman, C., Hu, S., Peterson, P., and Thayer, S. (2006). Ccl5 evokes calcium signals in microglia through a kinase-, phosphoinositide-, and nucleotide-dependent mechanism. *J.Neurosci.Res.*, 83(8):1471–1484.

Sierra, A., Gottfried-Blackmore, A., Milner, T., McEwen, B., and Bulloch, K. (2008). Steroid hormone receptor expression and function in microglia. *Glia*, 56(6):659–674.

Soltoff, S. P. (2004). Evidence that tyrphostins ag10 and ag18 are mitochondrial uncouplers that alter phosphorylation-dependent cell signaling. *J Biol Chem*, 279(12):10910–10918.

Sospedra, M. and Martin, R. (2005). Immunology of multiple sclerosis. *Annu Rev Immunol*, 23:683–747.

Spengler, R. N., Chensue, S. W., Giacherio, D. A., Blenk, N., and Kunkel, S. L. (1994). Endogenous norepinephrine regulates tumor necrosis factor-alpha production from macrophages in vitro. *J Immunol*, 152(6):3024–3031.

Stenger, S. and Modlin, R. L. (2002). Control of mycobacterium tuberculosis through mammalian toll-like receptors. *Curr Opin Immunol*, 14(4):452–457.

Stewart, C. R., Stuart, L. M., Wilkinson, K., van Gils, J. M., Deng, J., Halle, A., Rayner, K. J., Boyer, L., Zhong, R., Frazier, W. A., Lacy-Hulbert, A., Khoury, J. E., Golenbock, D. T., and Moore, K. J. (2010). Cd36 ligands promote sterile inflammation through assembly of a toll-like receptor 4 and 6 heterodimer. *Nat Immunol*, 11(2):155–161.

Sugiyama, T., Hoshino, K., Saito, M., Yano, T., Sasaki, I., Yamazaki, C., Akira, S., and Kaisho, T. (2008). Immunoadjuvant effects of polyadenylic:polyuridylic acids through tlr3 and tlr7. *Int Immunol*, 20(1):1–9.

Takata, M. and Kurosaki, T. (1996). A role for bruton's tyrosine kinase in b cell antigen receptor-mediated activation of phospholipase c-gamma 2. *J Exp Med*, 184(1):31–40.

Tan, S., Sagara, Y., Liu, Y., Maher, P., and Schubert, D. (1998). The regulation of reactive oxygen species production during programmed cell death. *J Cell Biol*, 141(6):1423–1432.

Tanaka, K. F., Kashima, H., Suzuki, H., Ono, K., and Sawada, M. (2002). Existence of functional beta1- and beta2-adrenergic receptors on microglia. *J Neurosci Res*, 70(2):232–237.

Tang, S.-C., Arumugam, T. V., Xu, X., Cheng, A., Mughal, M. R., Jo, D. G., Lathia, J. D., Siler, D. A., Chigurupati, S., Ouyang, X., Magnus, T., Camandola, S., and Mattson, M. P. (2007). Pivotal role for neuronal toll-like receptors in ischemic brain injury and functional deficits. *Proc Natl Acad Sci U S A*, 104(34):13798–13803.

Taylor, P. R., Martinez-Pomares, L., Stacey, M., Lin, H.-H., Brown, G. D., and Gordon, S. (2005). Macrophage receptors and immune recognition. *Annu Rev Immunol*, 23:901–944.

Terada, H. (1990). Uncouplers of oxidative phosphorylation. *Environ Health Perspect*, 87:213–218.

Tournier, C., Whitmarsh, A. J., Cavanagh, J., Barrett, T., and Davis, R. J. (1997). Mitogen-activated protein kinase kinase 7 is an activator of the c-jun nh2-terminal kinase. *Proc Natl Acad Sci U S A*, 94(14):7337–7342.

Triantafilou, M. and Triantafilou, K. (2002). Lipopolysaccharide recognition: Cd14, tlrs and the lps-activation cluster. *Trends Immunol*, 23(6):301–304.

Turpaev, K. and Drapier, J.-C. (2009). Stimulatory effect of benzylidenemalononitrile tyrphostins on expression of no-dependent genes in u-937 monocytic cells. *Eur J Pharmacol*, 606(1-3):1–8.

Ulrichts, P., Bovijn, C., Lievens, S., Beyaert, R., Tavernier, J., and Peelman, F. (2010). Caspase-1 targets the tlr adaptor mal at a crucial tir-domain interaction site. *J Cell Sci*, 123(Pt 2):256–265.

van Rossum, D. and Hanisch, U. (2004a). *Brain damage and repair: From molecular research to clinical therapy*. Kluwer Academic Publishers.

van Rossum, D. and Hanisch, U. (2004b). Microglia. *Metab Brain Dis.*, 19(3-4):393–411.

van Rossum, D., Hilbert, S., Strassenburg, S., Hanisch, U.-K., and Brück, W. (2008). Myelin-phagocytosing macrophages in isolated sciatic and optic nerves reveal a unique reactive phenotype. *Glia*, 56(3):271–283.

Waetzig, V., Czeloth, K., Hidding, U., Mielke, K., Kanzow, M., Brecht, S., Goetz, M., Lucius, R., Herdegen, T., and Hanisch, U. (2005). c-jun n-terminal kinases (jnks) mediate pro-inflammatory actions of microglia. *Glia*, 50(3):235–246.

Wake, H., Moorhouse, A. J., Jinno, S., Kohsaka, S., and Nabekura, J. (2009). Resting microglia directly monitor the functional state of synapses in vivo and determine the fate of ischemic terminals. *J Neurosci*, 29(13):3974–3980.

Wang, B. S., Lin, J. K., and Lin-Shiau, S. Y. (1999). Role of tyrosine kinase activity in 2,2',2"-tripyridine-induced nitricoxide generation in macrophages. *Biochem Pharmacol*, 57(12):1367–1373.

Wang, D., Müller, N., McPherson, K. G., and Reichardt, H. M. (2006). Glucocorticoids engage different signal transduction pathways to induce apoptosis in thymocytes and mature t cells. *J Immunol*, 176(3):1695–1702.

Wewers, M. D. and Sarkar, A. (2009). P2x(7) receptor and macrophage function. *Purinergic Signal*, 5(2):189–195.

Wüst, S., Tischner, D., John, M., Tuckermann, J. P., Menzfeld, C., Hanisch, U.-K., van den Brandt, J., Lühder, F., and Reichardt, H. M. (2009). Therapeutic and adverse effects of a non-steroidal glucocorticoid receptor ligand in a mouse model of multiple sclerosis. *PLoS One*, 4(12):e8202.

Wüst, S., van den Brandt, J., Tischner, D., Kleiman, A., Tuckermann, J. P., Gold, R., Lühder, F., and Reichardt, H. M. (2008). Peripheral t cells are the therapeutic targets of glucocorticoids in experimental autoimmune encephalomyelitis. *J Immunol*, 180(12):8434–8443.

Yaish, P., Gazit, A., Gilon, C., and Levitzki, A. (1988). Blocking of egf-dependent cell proliferation by egf receptor kinase inhibitors. *Science*, 242(4880):933–935.

Yamamoto, M., Sato, S., Hemmi, H., Hoshino, K., Kaisho, T., Sanjo, H., Takeuchi, O., Sugiyama, M., Okabe, M., Takeda, K., and Akira, S. (2003). Role of adaptor trif in the myd88-independent toll-like receptor signaling pathway. *Science*, 301(5633):640–643.

Young, S. W., Poole, R. C., Hudson, A. T., Halestrap, A. P., Denton, R. M., and Tavaré, J. M. (1993). Effects of tyrosine kinase inhibitors on protein kinase-independent systems. *FEBS Lett*, 316(3):278–282.

Yu, P., Hatakeyama, T., Aramoto, H., Miyata, T., Shigematsu, H., Nagawa, H., Hobson, R. W., and Durán, W. N. (2005). Mitogen-activated protein kinases regulate platelet-activating factor-induced hyperpermeability. *Microcirculation*, 12(8):637–643.

Zakar, T., Mijovic, J., Bhardwaj, D., and Olson, D. (1999). Tyrosine kinase inhibitors block the glucocorticoid stimulation of prostaglandin endoperoxide h synthase expression in amnion cells. *Can.J.Physiol Pharmacol.*, 77(2):138–142.

Zaru, R., Ronkina, N., Gaestel, M., Arthur, J., and Watts, C. (2007). The mapk-activated kinase rsk controls an acute toll-like receptor signaling response in dendritic cells and is activated through two distinct pathways. *Nat.Immunol.*, 8(11):1227–1235.

Zhang, Z. and Schluesener, H. J. (2006). Mammalian toll-like receptors: from endogenous ligands to tissue regeneration. *Cell Mol Life Sci*, 63(24):2901–2907.

A. Acknowledgments

First and foremost I would like to thank my supervisor, Professor Uwe K. Hanisch, for his excellent guidance throughout this project and I am very grateful for the chance to work in his laboratory. I am deeply thankful for his enthusiasm, patience and motivation.

I would also like to thank my thesis committee: Prof. Wolfgang Brück, Prof. Hannelore Ehrenreich and Prof. Eberhard Fuchs for their critical and supporting comments to my project.

Many thanks go to my entire working group for the great time together. Thank you, Denise, Jörg, Tommy as well as Elke, Silke, Arek, Susann and Astrid for your great technical assistance in the lab.

I would also like to thank my cooperation partners, more precisely Michael for his cookie-supported NMR analysis, Konstantin and Vanessa for the great B cell work. Many thanks also to the work of Vicki Wätzig from Kiel, Dr. Ian Greig and Dr. Peter Teismann from Aberdeen.

Furthermore I want to express my gratitude to all the other members of the Department of Neuropathology. Thank you for all the after hours meetings in pubs and at barbecues. Special thanks go to Wiebke, Chris, Tim, Johanna and Birgit for their proofreading. Thank you to Martin for his great computer support. I would also like to thank Andrea and Ulf for their gastronomical support.

Last but not least I would like to thank my parents, my grandmother and my brother for their permanent support and for keeping me grounded.